ELECTRODYNAMICS OF COLLOIDS

Promotor: dr. J. Lyklema, emeritus hoogleraar in de fysische chemie, met bijzondere aandacht voor de grensvlak- en kolloïdchemie

Co-promotor: dr. H. P. van Leeuwen, universitair hoofddocent bij het departement Biomoleculaire Wetenschappenen

NN08201, 2382

Marcel Minor

ELECTRODYNAMICS OF COLLOIDS

Proefschrift
ter verkrijging van de graad van doctor
op gezag van de rector magnificus
van de Landbouwuniversiteit Wageningen,
dr. C. M. Karssen,
in het openbaar te verdedigen
op dinsdag 20 januari 1998
des namiddags te vier uur in de Aula.

ISN 951923

CIP-DATA KONINKLIJKE BIBLIOTHEEK, DEN HAAG

Minor, Marcel

Electrodynamics of Colloids / Marcel Minor. - [S.1. : s.n.]
Proefschrift Landbouwuniversiteit Wageningen. Met lit. opg. -
Met samenvatting in het Nederlands.
ISBN 90-5485-801-X
Trefw.: kolloïdchemie

Foto omslag: Gert Buurman

NWO

Dit proefschrift is tot stand gekomen met steun van de Stichting Scheikundig Onderzoek in Nederland (SON) met een subsidie van de Nederlandse Organisatie voor Wetenschappelijk Onderzoek (NWO).

BIBLIOTHEEK
LANDBOUWUNIVERSITEIT
WAGENINGEN

NN08201, 2382

STELLINGEN

-1-

Wanneer resultaten van elektrodynamische experimenten niet voldoen aan het zogenoemde elektrodynamische standaardmodel is eerder de ζ-potentiaal dan de oppervlaktegeleiding als abnormaal te bestempelen.

Dit proefschrift, hoofdstuk 3.

-2-

Door de complementariteit van diëlektrische respons en propgeleidbaarheidsmetingen is de oppervlaktegeleiding van kolloïden in een uitzonderlijk breed gebied van elektrolytconcentraties te bepalen.

Dit proefschrift, hoofdstuk 3.

-3-

Bacteriecellen en behaarde latex bolletjes hebben voor een elektrodynamicus veel gemeen.

Dit proefschrift, hoofdstuk 4.
A. van der Wal, M. Minor, W. Norde, A. J. B. Zehnder, J. Lyklema, *J. Colloid Interface Sci.* **186,** 71 (1997).
A. van der Wal, M. Minor, W. Norde, A. J. B. Zehnder, J. Lyklema, *Langmuir* **13,** 165 (1997).

-4-

Afhankelijk van het soort experiment is "poreus silica" poreus dan wel niet poreus voor tegenionen.

Dit proefschrift, hoofdstuk 5.

-5-

Diëlektrische spectroscopie is gevoelig voor relaxatieprocessen aan kolloïdale grensvlakken, maar niet voor alle.

Dit proefschrift, hoofdstuk 7.

-6-

Biobeschikbaarheid van bioinactieve metaalcomplexen is een tweeledig begrip. Zij hangt enerzijds af van de dissociatiekinetiek in het medium en anderzijds van de snelheidsbepalende stap in het bio-opnameproces.

P.G.C. Campbell, in A. Tessier en D.R. Turner (Eds.), Metal Speciation and Bioavailability in Aquatic Systems, John Wiley, Chichester, 1995, p. 55.

-7-

Complexen van metaalionen met oppervlaktegroepen van kolloïdale deeltjes kunnen zeer wel labiel zijn.

H.B. Xue en L. Sigg, *Anal. Chim. Acta* **284,** 505 (1994).
J.H.A.M. Wonders, Ph. D. Thesis, Wageningen, 1995.

-8-

In tegenstelling tot wat in de aërodynamica algemeen wordt verondersteld heeft compressibiliteit wel degelijk invloed op grenslaagtransitie.

-9-

Koffie kan geruime tijd na het inschenken nog warm gedronken worden wanneer een grote mok wordt gebruikt en direct melk en suiker worden toegevoegd.

-10-

De door recombinanttechnieken gemaakte nutriënten zijn voor velen nog moeilijk te verteren.

-11-

Het verhandelbaar zijn van CO_2-uitstootquota, zoals op de VN-klimaatconferentie in Kyoto besloten, steekt af tegen het ideaal het broeikaseffect te verminderen.

-12-

De NS zouden kunnen overwegen een fysisch chemicus in dienst te nemen voor het nauwkeurig voorspellen van mist, ijzel en bevriezing van bovenleidingen.

-13-

Het kunnen onderdrukken van een gezonde nieuwsgierigheid naar wetenschap is noodzakelijk bij de afronding van promotieonderzoek.

Stellingen behorende bij het proefschrift "Electrodynamics of Colloids",
M. Minor, Landbouwuniversiteit Wageningen, 20 januari 1998.

Table of Contents

Chapter 1

INTRODUCTION

GENERAL BACKGROUND

Hydrophobic colloids commonly carry a charge. This charge, usually located at the surface of the particles, is compensated by ions in the solution giving rise to an electric double layer. The presence of such a microscopic electric double layer has important consequences for the macroscopic properties of the sol. For instance it determines the stability of the colloids against coagulation, their ability to adsorb substances, and their ability to coat objects. In order to understand such macroscopic properties it is of obvious importance to study the structure of the double layer in detail. A large number of investigations have been devoted to double layers in equilibrium. These studies yield thermodynamic parameters e.g. on the adsorption of molecules or (macro)ions in the dense part of the double layer (Stern layers) or in the diffuse part of the double layer.

If a double layer is perturbed by an external force, its structure tends to adjust. The corresponding relaxation processes are by no means rare phenomena. They occur during particle-particle interaction in coagulation and during all other processes referred to above. Non-equilibrium parameters determine the characteristic times of these relaxation processes and the mobilities of the ions in the various parts of the double layer are of paramount importance in this respect. These parameters as well as the ζ-potential (which is the potential at the plane of shear and also a non-equilibrium characteristic) can in principle be obtained from the response of the sol to various applied perturbations.

ELECTROKINETICS

Electrokinetic phenomena are characterised by the tangential motion of liquid with respect to an adjacent charged surface. They reflect the electric properties of the surface/solution interface, and play an important role in the stability of hydrophobic colloids. Particle electrophoresis is by far the most widely used technique to obtain the ζ-potential. Less familiar are streaming potentials of close-packed porous plugs of particles. The streaming potential is the potential difference that arises over the plug at zero net electric current caused by the flow of liquid under an applied pressure gradient. One of the great advantages of the use of plugs instead of extremely dilute suspensions, such as in microelectrophoresis, is that not only the streaming potential but also the static electric conductivity can be measured. The streaming potential is sensitive to the charge in the region of the double layer where the liquid moves, i.e., the part beyond the plane of shear, whereas all mobile charge in the double layer, including the part behind the shear plane, contributes to the plug conductivity. Hence, the combination of different types of electrokinetic experiments provides more detailed information on the (non-equilibrium) double layer.

DIELECTRIC SPECTROSCOPY

Dielectric spectroscopy is a technique to study the relaxation of the double layer by measuring the response of a dispersion to an applied alternating electric field. The observable macroscopic current can be related to the induced dipole moments of the particles, which, in turn, can be related to the transport processes in the double layer (1,2). This technique not only reveals stationary properties of the double layer, as does a static conductivity experiment, it also provides information on the relaxation times. In the appropriate frequency interval, the dynamics of the polarization of the double layer can be followed. It is also possible to follow desorption/adsorption of surface charges and to retrieve the corresponding rate constants.

COLLOID STABILITY

Since the development of the DLVO theory for colloid stability (3,4) in the 1940's, a large number of refinements and elaborations have been published concerning such items as the shapes of the particles and the chemistry of the surface (sites). In these theories the calculation of the electrostatic forces is usually done in the traditional way by equilibrium thermodynamics. However, coagulation of colloids is a dynamic process. In a particle encounter, diffuse double layers overlap and tend to adopt a new equilibrium structure. According to Overbeek (5) and Lyklema (6), the characteristic time for the adjustment of the diffuse part of the double layers is much shorter than the typical duration of an encounter. Hence, the use of equilibrium thermodynamics is justified for calculating the structure of the diffuse layer during particle encounters. However, this is not necessarily true for the surface charge density. Estimates for relaxation times of the surface charge vary over orders of magnitude and may be well comparable to the characteristic time of an encounter. With respect to the former, two extreme situations can be considered: (i) the surface charge does not adjust at all during the collision (interaction at constant charge), (ii) the surface charge is completely relaxed during the encounter (interaction at constant (electrochemical) potential). These two limiting situations can be tackled within the framework of equilibrium thermodynamics, but the intermediate situation asks for a dynamic approach. The first attempts to incorporate small disequilibration of the double layer into the theory of slow coagulation have been made by Dukhin and Lyklema (7,8). Recently, Kijlstra and Van Leeuwen (9) developed a stability model which can handle large deviations from equilibrium, likely to occur in particle-particle interactions. Still these theories are primitive in the sense that surface charge may relax only via desorption/adsorption. Shulepov et al. (10,11) applied Kijlstra's method to more sophisticated surface charge relaxation mechanisms (desorption/adsorption, and migration along the surface).

STATE OF THE ART IN THE ELECTRODYNAMICS OF COLLOIDS

It is timely to consider non-equilibrium electric properties of colloids on a higher level of integration which includes electrokinetics, dielectric relaxation, double-layer relaxation in particle-particle interaction, etc. We denote all of this by the term *electrodynamics.* In order to describe electrodynamic phenomena, a set of basic equations governing ionic and solvent transport has to be solved under the appropriate boundary conditions. These *electrodynamic equations* (also referred to as the electrokinetic equations) encompass the Poisson equation for electrostatics, the Nernst-Planck equations for ionic transport, the ionic continuity equations, and the Navier-Stokes equations for solvent transport. Numerical solutions to these equations have been put forward (12,2) in order to describe electrophoresis and the conductivity of a suspension in an alternating electric field. Long before numerical solutions were available, Dukhin (1) noted that the diffuse double layer, under the usual conditions, is practically in local equilibrium with the surrounding electrolyte. This *local quasi-equilibrium condition* is the cornerstone in many important analytical theories for electrokinetic phenomena (1,13-19) and also takes a central position in this thesis. Hinch et al. (20) extended the applicability of Dukhin's LF dielectric dispersion theory to asymmetrical suspending electrolytes. However, their results poorly agree with numerical calculations and therefore do not seem of direct practical use. O'Brien and Perrins also used the assumption of local quasi-equilibrium in the derivation of expressions for the conductivity and streaming potentials in plugs (17,18).

Electrokinetic potentials must be deduced from experiments by applying some electrokinetic model. A popular one is the "standard electrokinetic model". In this model the surface is, under dynamic conditions, characterised by a shear plane at which the potential is identified as ζ. The ions within the stagnant liquid behind the shear plane are considered to be immobile. Application of this standard model shows that generally ζ-potentials obtained from suspension conductivities in dc or ac fields are systematically larger than those obtained from particle mobilities (21,17,22-29) or from streaming potentials of porous plugs (30). The most probable cause for this inconsistency is the neglect of conduction behind the shear plane (25,26). The extent of such conduction may be expected to be related to surface roughness, surface porosity, the viscoelectric effect (27), the properties of the (occupied) Stern layer, and the presence of a macromolecular (hairy) surface layer. In a number of studies on latexes, the ζ-potentials inferred from low-frequency (LF) dielectric measurements have been compared to the theoretically predicted ζ-potentials based on mobility measurements (31,23,24,32). However, these latter ζ-potentials are also subject to the restrictions of the standard model. Exceptions are a few analyses (25,26,28,29) where conduction behind the shear plane was taken into account. These last mentioned studies were able to explain the high values of the (complex) conductivity. Still the set of experiments is minimal: there are as many variables as there are equations. More independent experiments are necessary to conclusively solve the problem.

AIM AND OUTLINE OF THIS STUDY

In the perspective of the difficulties encountered in the above mentioned studies it is in the first place highly wanted to obtain electrodynamic data for a limited number of well-defined systems by a number of different methods over a broad range of ionic strengths and frequencies. Combination of data must reveal the dynamic double-layer parameters such as the mobilities in the different regions of the double layer and the ζ-potentials. In pursuit of these aims the first purpose of this thesis was to study low-frequency dielectric spectroscopy on dilute dispersions of poly(styrene) sulphate latex. Latex particles can be made spherical, homodisperse and in large amounts. Furthermore, porous plugs of such latexes allow the measurement of streaming potentials and plug conductivities. Silica dispersions and bacterial cells were also studied (latter not in this thesis). In the second place we want to relate theoretically the low-frequency dielectric response, particle mobility, and sol stability against coagulation to more complex relaxation mechanisms that may take place in the Stern layer.

The outline of this thesis is as follows.

In **chapter 2** plug conductivities and streaming potentials of a close-packed porous plug of poly(styrene) sulphate latex will be determined for a number of indifferent electrolytes and ionic strengths. The ζ-potentials and the mobilities of the ions in the different parts of the double layer will be obtained.

Chapter 3 will give practical expressions for the low-frequency dielectric response of dilute dispersions of spherical particles in a binary electrolyte. The low-frequency dielectric response of dilute sulphate latex dispersions will be experimentally determined as a function of the ionic strength. The surface conductivities will be compared to the values obtained for plugs.

The influence of adsorption of the uncharged polymer poly(ethylene) oxide on latex will be investigated by means of low-frequency dielectric dispersion, plug conductivities and streaming potentials in plugs in **chapter 4**. It will be shown that the drag on ions in the polymer layer can be described by considering the polymer layer as an inhomogeneous Brinkman fluid. The necessary polymer and counterion distributions will be calculated from statistical self-consistent-field models.

In order to investigate the influence of the surface charge density on the streaming potential and static conductivity, plugs of monodisperse spherical silica particles will be subject of study in **chapter 5**. Contrary to latex, the surface charge density of silica can be controlled by pH.

In **chapter 6** the dynamic aspects of particle electrophoresis will be considered. It will be shown, both theoretically and experimentally, that it is possible to apply an alternating electric field with such a frequency that unwanted electroosmosis, induced by charge on the capillary wall, is suppressed, whereas particles are still able to follow the field according to their dc mobility. This shows that knowledge of the dynamics and pertinent relaxation times is not only of scientific interest, but that it is also able to offer solutions to practical problems.

In **chapter 7** the influence of polarization of the surface charge (or an occupied inner Helmholtz layer) on the particle mobility, static conductivity, and low-frequency dielectric response will be studied within the framework of the thin double-layer theory. It will be shown how the dynamic characteristics of the relaxation of surface charge are accessible by dielectric spectroscopy. Since these characteristics determine the particle-particle interaction under non-equilibrium conditions, **chapter 8** will be devoted to colloid stability. The stability will be expressed in terms of dynamic characteristics of relaxation in the surface layer (inner Helmholtz layer). The connection between the stability against coagulation and dielectric spectroscopy will be made.

REFERENCES

(1) Dukhin, S. S., Shilov, V. N., "Dielectric Phenomena and the Double Layer in Disperse Systems and Polyelectrolytes", Wiley, New York, 1974.

(2) DeLacey, E. H. B., White, L. R., *J. Chem. Soc., Faraday Trans. 2* **77,** 2007 (1981).

(3) Derjaguin, B. V., Landau, L. D., *Acta Physicochim. URRS* **14,** 663 (1941).

(4) Verwey, E. J. W., Overbeek, J. T. G., "Theory of the Stability of Lyophobic Colloids", Elsevier, Amsterdam, 1948.

(5) Overbeek, J. Th. G., *J. Colloid Interface Sci.* **58,** 408 (1977).

(6) Lyklema, J., *Pure & Appl. Chem.* **52,** 1221 (1980).

(7) Dukhin, S. S., Lyklema, J., *Langmuir* **3,** 94 (1987).

(8) Dukhin, S. S., Lyklema, J., *Faraday Discuss. Chem. Soc.* **90,** 261 (1990).

(9) Kijlstra, J., Leeuwen, H. P. van, *J. Colloid Interface Sci.* **160,** 424 (1993).

(10) Shulepov, S. Yu., Dukhin, S. S., Lyklema, J., *J. Colloid Interface Sci.* **171,** 340 (1995).

(11) Shulepov, S. Yu., *J. Colloid Interface Sci.* **189,** 199 (1997).

(12) O'Brien, R. W., White, L. R., *J. Chem. Soc., Faraday Trans. 2* **74,** 1607 (1978).

(13) Fixman, M., *J. Chem. Phys.* **72,** 5177 (1980).

(14) O'Brien, R. W., *J. Colloid Interface Sci.* **81,** 234 (1980).

(15) Fixman, M., *J. Chem. Phys.* **78,** 1483 (1983).

(16) O'Brien, R. W., *J. Colloid Interface Sci.* **92,** 204 (1983).

(17) O'Brien, R. W., Perrins, W. T., *J. Colloid Interface Sci.* **99,** 20 (1984).

(18) O'Brien, R. W., *J. Colloid Interface Sci.* **110,** 477 (1986).

(19) Kang, S. -Y., Sangani, A. S., *J. Colloid Interface Sci.* **165,** 195 (1994).

(20) Hinch, E. J., Sherwood, J. D., Chew, W. C., Sen, P. N., *J. Chem. Soc., Faraday Trans. 2* **80,** 535 (1984).

(21) Put, A. G. van der, Bijsterbosch, B. H., *J. Colloid Interface Sci.* **75,** 512 (1980).

(22) Myers, D. F., Saville, D. A., *J. Colloid Interface Sci.* **131,** 448 (1989).

(23) Rosen, L. A., Saville, D. A., *Langmuir* **7,** 36 (1991).

(24) Rosen, L. A., Saville, D. A., *J. Colloid and Interface Sci.* **149,** 542 (1992).

(25) Kijlstra, J., Leeuwen, H. P. van, Lyklema, J., *Langmuir* **9,** 1625 (1993).

(26) Rosen, L. A., Baygents, J. C., Saville, D. A., *J. Chem. Phys* **98,** 4183 (1993).

(27) Lyklema, J., "Fundamentals of Interface and Colloid Science. Solid-Liquid Interfaces", Vol. II, Academic Press, London, 1995.

(28) Wal, A. van der, Minor, M., Norde, W., Zehnder, A. J. B., Lyklema, J., *Langmuir* **13,** 165 (1997).

(29) Wal, A. van der, Minor, M., Norde, W., Zehnder, A. J. B., Lyklema, J., *J. Colloid Interface Sci.* **186,** 71 (1997).

(30) Minor, M., Linde, A. J. van der, Lyklema, J., submitted to *J. Colloid Interface Sci.* (chapter 2 of this thesis).

(31) Rosen, L. A., Saville, D. A., *J. Colloid Interface Sci.* **140,** 82 (1990).

(32) Dunstan, D. E., *J. Chem. Soc. Faraday Trans.* **89,** 521 (1993).

Chapter 2

STREAMING POTENTIALS AND CONDUCTIVITIES OF LATEX PLUGS IN INDIFFERENT ELECTROLYTES[1]

ABSTRACT. Streaming potential and conductivity measurements were performed on porous plugs in a number of indifferent electrolytes. The plugs were made of monodisperse spherical polystyrene sulphate latex with fixed surface charge density. The observed surface conductivity could be interpreted with the classical Bikerman expression corrected for conduction behind the shear plane. It was shown that electroosmosis positively, and the depletion of co-ions in the double layer negatively contribute to the surface conductivity. It was further demonstrated that a significant part of the conduction is located behind the slip plane. The ion mobility of the indifferent counterions behind as well as beyond the shear plane is close to the bulk mobility. In the correct determination of ζ-potentials in the low electrolyte concentration range, it is necessary to take surface conduction behind the plane of shear into account. By doing so, the maximum in the curve of the ζ-potential versus electrolyte concentration disappears.

---

[1] Submitted for publication in *J. Colloid Interface Sci.* in coauthorship with Linde, A. J. van der, Lyklema, J.

1. INTRODUCTION

Concentrated systems of sub micrometer-sized particles are subject of research in many fields, for instance in soil science, paper manufacturing and in membrane studies. In these investigations, usually the system in total is of interest. The electrokinetic properties of the individual particles are commonly studied in *dilute* systems (micro-electrophoresis, conductivity of dilute suspension) where the imposed field is in interaction with isolated particles only and, hence, theory is relatively simple. Exceptions are e.g. dc conductivity studies (1) and high-frequency dielectric studies (2) on concentrated latex dispersions, and electrokinetic investigations on porous plugs (3,4). The latter type of experiment is much more elaborate than micro-electrophoresis but it has the advantage that ζ-potentials of large particles can be determined. Furthermore, measurements can be performed at high electrolyte concentrations, well above the critical coagulation concentration. In micro-electrophoresis coagulation would interfere with the measurements.

From measurement of the electric conductivity of the plug, extra information can be gained with respect to micro-electrophoresis. The surface conductivity, which is calculated from the plug conductivity, is an important double layer characteristic. Knowledge of the surface conductivity is a necessity to determine ζ-potentials from streaming potentials (or particle mobilities) at low electrolyte concentrations if conduction behind the shear plane takes place. Furthermore, from the combination of conductivity and streaming potential experiments, information on the amount of conduction behind and beyond the shear plane can be evaluated.

Although interpretation of conductivity data is more difficult for plugs than for dilute dispersions, the measurements are extremely sensitive to the double layer properties. The conductivity change due to the presence of colloidal particles scales with the number of particles per unit volume. The particle density in a plug exceeds the density in common dilute dispersions experiments by at least one order of magnitude. Hence, the signal-to-noise ratio is increased by the same factor.

A more technical advantage of working with plugs is the accurate knowledge of the bulk concentration inside the plug which can be rinsed intensively with an electrolyte solution of well-known concentration prior to the measurement. In experiments on dilute suspensions, the ionic strength is usually adjusted by adding aliquots of electrolyte. This procedure is more susceptible to errors, since the latex volume fraction must be well-known and adsorption/desorption should not occur. Furthermore, in plugs the particle density is perfectly constant throughout the experiments and this allows for a better comparison between the different data.

The extreme sensitivity also allows for the determination of the surface conductivity from plug conductivities up to the relatively high ionic strength of 100 mM without any problems, as will be shown in this paper.

To calculate the current passing through the plug due to an applied electric field or pressure gradient, it is necessary to determine the distribution of ions, electric potentials, and flow fields in the pores. This involves the solution of a set of coupled partial differential equations, commonly referred to as the "electrokinetic equations". O'Brien and Perrins (5) solved these equations and determined the conductivity of a granular plug. The plug is assumed to be composed of close-packed spheres of uniform surface potential in a simple cubic (SC), body-centred cubic (BCC) or face-centred cubic (FCC) array. To simplify the problem, they restricted themselves to the situation of relatively thin double layers ($\kappa a >> 1$) which makes it possible to use the condition of quasi-equilibrium between the double layer and the adjacent electrolyte (6). The case of plugs with random structure was dealt with by interpolation between the three arrays. This procedure is not exact.

O'Brien also solved the electrokinetic equations to describe electroosmosis in plugs (7). The packing of the plug is assumed to be in one of the three lattice arrays mentioned above. More recently Kang and Sangani (8) rigorously solved the equations for the conduction as well as electroosmosis in completely random arrays.

In order to test these available theories, conductivity and streaming potential measurements were performed on plugs of monodisperse polystyrene sulphate latex with a fixed negative surface charge density, as function of the electrolyte concentration (0.1-100 mM). To investigate (the influence of) surface conduction, measurements were performed in electrolytes with four different counterion species, i.e., HCl, KCl, NaCl, and LiCl as the electrolytes. To check the influence of the co-ionic species, KOH was also used as electrolyte.

Outline of the paper. In the following section we present the theory for the conductivities and the streaming potentials of plugs. In section 3 we describe the preparation and characterization of the anionic latex and the measuring equipment. In section 4 the results are presented and compared with theory. In section 5 we formulate the conclusions and perspectives for further investigations.

2. THEORY

2.1. Currents and forces

The experimental determination of the conductivity of a plug involves the measurement of the average of the local current density $\vec{i}$. As in (5,7) we will denote averages by angular brackets. Let q be a scalar or vector function of the position. Then

$$\langle q \rangle \equiv \frac{1}{V} \int_V q dV' \qquad [1]$$

where V is a sample volume, assumed to contain many particles, but still small compared to the plug dimensions. Averages of vector fields (pressure gradient, fluid velocity, electric field) and scalar functions (e.g. concentration) are important quantities in this study. In general, q varies significantly over distances of the order of the particle radius, whereas $\langle q \rangle$ varies over distances of the order of the plug dimension.

An electric current can be induced in the plug by forces on the ions. The most common forces are generated by an electric field $\vec{E}$ or pressure gradient $\vec{\nabla} p$. For small forces the response is linear:

$$\langle \vec{i} \rangle = K^* \langle \vec{E} \rangle + K_p^* \langle -\vec{\nabla} p \rangle \qquad [2]$$

Here, K^* is the electric conductivity. O'Brien and Perrins (5) found that for a plug, composed of close-packed monodisperse spheres with thin double layers ($\kappa a >> 1$) in a symmetrical electrolyte, K^* is related to the relative surface conductivity parameter Du_i according to:

$$\frac{K^*}{K^\infty} = 1 + 3\phi \left[f(0) + \frac{e^2 z_2^2 n_2^\infty / f_2^\infty}{K^\infty} \left(f(Du_2) - f(0) \right) \right] \qquad [3]$$

where ϕ is the particle volume fraction, ez_i is the i-type ion charge, f_i is the ion friction coefficient, and n_i^∞ the equilibrium density beyond the double layer (superscript ∞). The subscript i=1 refers to the co-ion, i=2 to the counterion. In this theory only the surface conduction due to the excess of counterions in the double layer is taken into account. Or, for that matter, the (negative) contribution due to the exclusion of co-ions is considered to be insignificant. This assumption is justified in the situation of relatively high surface potentials where the double layer is non-linear. K^∞ is the electric conductivity of the equilibrium electrolyte beyond the double layer:

$$K^\infty = \sum_{i=1}^{i=2} K_i^\infty, \quad K_i^\infty = e^2 z_i^2 n_i^\infty / f_i^\infty \qquad [4]$$

and $f(Du_2)$ is a tabulated function of Du_2 and the type of lattice. Du_i is related to the absolute surface conductivity K_i^σ via:

$$Du_i = \frac{K_i^\sigma}{a K_i^\infty} \qquad [5]$$

where a is the particle radius. The surface conductivity K_i^σ can be related to the excess of i-type ions in the double layer. We allow the ions behind the shear plane to be mobile with mobility u_i^i. The conductivity in the non-stagnant double layer regime consists of two parts (5): (i) a contribution caused by the movement of charge with respect to the liquid and (ii) a contribution caused by the electroosmotic liquid flow relative to the particle surface. This electroosmotic flow makes the ions move faster relative to the surface. We can write:

$$K_i^\sigma = \tilde{u}_i^i \sigma_i^i + \left(1 + 3m_i / z_i^2 \right) \tilde{u}_i^\infty \sigma_i^d \qquad [6]$$

where m_i is the dimensionless ionic drag coefficient: $m_i = 2\varepsilon kTf_i^\infty / 3\eta e^2$, ε is the fluid dielectric permittivity, k is the Boltzmann constant, T is the temperature, η is the fluid viscosity, σ_i^i and σ_i^d are the (surface) densities of charge behind and beyond the shear plane, respectively, $\tilde{u}_i^i$ and $\tilde{u}_i^\infty$ are the ion mobilities behind the beyond the shear plane including their sign: $\tilde{u}_i = z_i e / f_i$, $u_i = |\tilde{u}_i|$. We have assumed that the ions move according to their bulk mobility beyond the shear plane. It is convenient to introduce the ratio Θ_i, which is the conduction behind the shear plane relative to the conduction due to electromigration beyond the shear plane[2]:

$$\Theta_i = \tilde{u}_i^i \sigma_i^i / \tilde{u}_i^\infty \sigma_i^d \qquad [7]$$

More common is the notation relating K_i^σ or Du_i to the ζ-potential (10,5):

$$Du_i = \frac{2}{\kappa a}\left(1 + \frac{3m_i}{z_i^2} + \Theta_i\right)\left[\exp(-z_i e\zeta/2kT) - 1\right] \qquad [8]$$

The current $\langle \vec{i}_s \rangle$ due to an imposed pressure gradient is known as the streaming current. O'Brien related K_p^* to Du_2 and the ζ-potential (7):

$$K_p^* = -\frac{\varepsilon kT}{\eta e}\left(\frac{e\zeta}{kT}[1 + 3\phi f(0)] - \left[\frac{e\zeta}{kT} - \frac{2}{z_1}\ln 2\right] g(Du_2)\right) \qquad [9]$$

where p is the pressure and $g(Du_2)$ is a function of Du_2, tabulated by O'Brien, also depending on the type of lattice.

2.2. Limiting expressions for high electrolyte concentrations

Equation [3] can be simplified and extended to cope with surface conduction due to both types of ionic species for the case where Du_2 is small ($Du_2 << 1$). Experimentally this condition is fulfilled at sufficiently high ionic strengths. Then $f(Du_2)$ can be expanded till first order in Du_2:

$$f(Du_2) \approx f(0) + \left.\frac{df(Du_2)}{d(Du_2)}\right|_{Du_2=0} Du_2 \approx f(0) - 2Du_2 f(0) \qquad [10]$$

The derivative in $Du_2 = 0$ can be estimated from numerical data (5,8) by assuming $f(Du_2)$ to be linear between $f(0) \approx -0.4$ and $f(\frac{1}{2}) = 0$. Substitution of this expression in Eq. [3] yields:

$$K^* = (1 + 3\phi f(0))K^\infty - \frac{6\phi f(0)}{a} K_2^\sigma \qquad [11]$$

The incorporation of surface conduction due to a negative excess of co-ions is straightforward in this low Du_i-limit. Since the low relative surface conduction is interpreted as a perturbation, cross-terms involving $Du_1 Du_2$ are unimportant and the surface conductivity is just the sum for the two species. Hence, K_2^σ in Eq. [11] can be replaced by K^σ:

---

[2] This Θ_i is somewhat different from $\Theta_i = \sigma_i^i / \sigma_i^d$ introduced by Kijlstra (9).

$$K^{\sigma} = \sum_{i=1}^{i=2} K_i^{\sigma} \qquad [12]$$

This is the Bikerman expression for the surface conductivity (11,12). Surface conductivity is an excess quantity. Therefore, counterions contribute positively and co-ions negatively as can be seen from Eq. [8]. In a plot of K^* versus K^{∞}, Eq. [11] describes a straight line if the surface conductivity K^{σ} does not change with the electrolyte concentration. The slope of the curve is determined by the type of array and the volume fraction but is independent of the surface conductivity. Surface conduction results in a non-zero intercept. The intercept is directly proportional to the surface conductivity and to the volume density of surface area (surface area per unit plug volume) which scales with a^{-1} in a close-packed plug. Formula [11] is very suited for a fast analysis of plug conductivity data (13). It immediately reveals the surface conductivity K^{σ}.

If $Du_2 << 1$, $g(Du_2) \approx 0$ and the second term in Eq. [9] can be neglected. Hence, in this limit, the Smoluchowski formula (7) is obtained and can be used in the interpretation of streaming potentials.

2.3. Liquid transport and plug permeability

From the liquid flow through the plug upon applying a pressure gradient, information on the consistency of the plug can be gained. To that end the average liquid velocity has to be related to the plug parameters a and ϕ. Zick and Homsy (14) and, more recently, Kang and Sangani (8) calculated the Stokes flow through a bed of spherical *uncharged* particles. If $6\pi\eta a M\langle\vec{v}\rangle$ is the average force on a particle in a fixed bed through which a fluid with average velocity $\langle\vec{v}\rangle$ is pumped, $\langle\vec{v}\rangle$ is related to $\langle\vec{\nabla}p\rangle$ according to:

$$\langle\vec{v}\rangle = -\frac{2}{9}\frac{a^2}{\eta\phi M}\langle\vec{\nabla}p\rangle \qquad [13]$$

where M is a non-dimensional number, found by solving the Stokes equations. M is determined by the type of lattice and volume fraction. For infinitely dilute suspensions, M=1. Kang and Sangani found M=105.2 for a random close-packed array ($\phi = 0.611$). Zick and Homsy determined M in SC, FCC, and BCC arrays for volume fractions between zero and the maximum value for close-packed systems. The average velocity $\langle\vec{v}\rangle$ is related to the measurable liquid flow rate J and the plug cross section A via $J = |\langle\vec{v}\rangle| A$.

3. EXPERIMENTAL SECTION

3.1. Latex preparation and characterisation

Monodisperse polystyrene latex with sulphate groups was made using the procedure of Goodwin et al. (15) with $K_2S_2O_8$ as the initiator. The polystyrene sulphate latex was cleaned by steam-

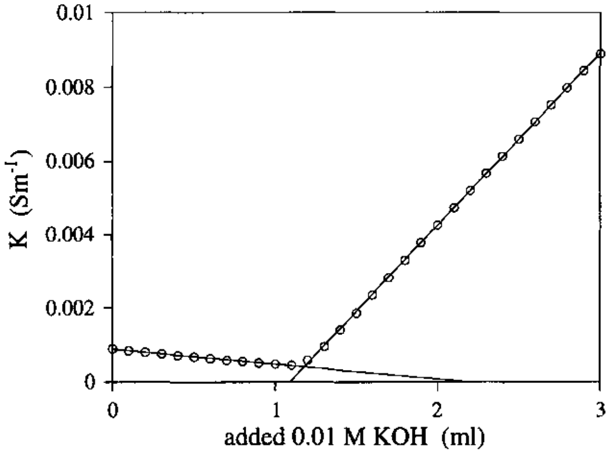

Figure 1. Conductometric titration curve of polystyrene sulphate latex.

stripping and brought in the H$^+$-form by treating it with purified Dowex ion exchange resins (mixed bed) according to the method described by Van den Hul and Vanderhoff (16). From dynamic light scattering a particle radius of 400 nm was obtained. By the Single Particle Optical Sizer (17) less than 1% of the particles was found in doublets. The polydispersity ratio $\bar{a}_w/\bar{a}_n$ from E.M. photographs is less than 1.005 for particles made via this procedure. Drying at 90 °C and 130 °C (the latter temperature well above the glass transition temperature of the polystyrene) yields dry weights within 1% which indicates that water has evaporated but no (poly)styrene.

A conductometric titration was performed to determine the surface charge density. A volume of 50 ml latex, 4.76% by volume, was titrated under stirring in a vessel at 25.0 °C in a nitrogen atmosphere. A burette (Metrohm, 655 Dosimat) dosated small aliquots (0.1 ml) of 0.01 M KOH. The conductance was monitored with a precision bridge (Wayne Kerr, Automatic Precision Bridge B905) equipped with a conductivity cell (WTW, LTA 01, cell constant 11.2 m^{-1}). The complete set-up is automated. From Fig. 1 it is concluded that there are strong acidic groups on the surface. Presumably these are sulphates, as expected from the used initiator. The surface charge density was found to be $\sigma^0 = -6.4\ \mu\text{C/cm}^2$.

3.2. Plug preparation

Close-packed plugs were made by centrifugation (at $7 \cdot 10^3 \times g$ m/s^2) of a 10 vol% latex suspension for two hours. The particles were directly centrifuged into the plug holder (cylinder with length 1.5 cm, diameter 1.0 cm). Via this wet method homogenous plugs were made and encapsulation of air bubbles was avoided. The plug is placed between two platina-blacked electrodes. Small holes in the electrodes allow for liquid transport through the plug. Membranes between the plug and electrodes preventing the plug for possible disintegration were not necessary for these plugs if handled with care. Two reservoirs filled with electrolyte solution are connected with the plug ends. Pressure is put on one of the reservoirs for rinsing purpose or for performing streaming potential experiments.

3.3. Streaming potential and conductivity equipment

The streaming potential is determined with a home-made set-up. The basic design of Van der Put (3,18) has been fully automated. The equipment can be used for plugs as well as for flat plates. The pressure difference is applied by means of nitrogen and the sensing electrodes can be connected to a voltmeter or a conductivity meter. Throughout a number of years this equipment has proved to provide accurate and reproducible results. The determination of the streaming potential at six applied pressures varying between zero and $\Delta p = 0.40 \cdot 10^5 \mathrm{N/m^2}$ takes only 15 minutes and the plots show perfectly straight lines where correlation coefficients of 0.9999 to 1 are common. Even at high ionic strengths where streaming potentials of less then 1 mV are found, correlation coefficients better then 0.999 are usual (19).

4. RESULTS AND DISCUSSION

The liquid flow rate J through the plug was measured for every electrolyte concentration in order to check the plug. Plug breaking is shown immediately by a change in the rate in contrast with the conductivity and streaming potentials which are rather insensitive to small cracks in the plug. The average fluid velocity $\langle \vec{v} \rangle$ has a tendency to decrease with decreasing electrolyte concentration, but always remains within a 15% range: $J = (0.25 \pm 0.02)$ ml/hour and $|\langle \vec{v} \rangle| = 8.8 \cdot 10^{-7}$ m/s (at $\Delta p = 0.40 \cdot 10^5 \mathrm{N/m^2}$). This indicates that the influence of the diffuse double layers on the fluid velocity is of minor importance. This is expected; even for the lowest electrolyte concentration $\kappa a \approx 13$. Hence, $\langle \vec{v} \rangle$ can be compared with calculations of Stokes flow through a bed of spherical *uncharged* particles, as performed by Zick and Homsy (14) and Kang and Sangani (8). From Eq. [13] we calculate $|\langle \vec{v} \rangle| = 16 \cdot 10^{-7}$ m/s for a random lattice. This value significantly exeeds the measured velocity. Zick and Homsy computed M as a function of the volume fraction for the three previously mentioned arrays. In their figure 1 the sensitivity in M for ϕ is shown. From three independent methods it will be shown in this section that $\phi = 0.63 \pm 0.01$ which is in line with the lower liquid rate.

Before every measurement of the liquid rate, conductivity, and streaming potential, the plug is rinsed intensively with the new electrolyte solution until the conductivity attains a stationary value. In Fig. 2, by way of illustration, the conductivity and the specific resistance, $\rho^* = 1/K^*$, are shown as a function of time after exchanging the electrolyte solution in the reservoirs from 100 to 30 mM KCl. The conductivity decreases after applying the pressure difference ($\Delta p = 0.40 \cdot 10^5 \mathrm{N/m^2}$). The time needed to attain a new stationary situation is related to the length l of the plug, the volume fraction ϕ, and the average fluid velocity $\langle \vec{v} \rangle$ (see appendix A for a full derivation) and is of the order of hours for our set-up. $\langle \vec{v} \rangle$ scales with a^2, so for larger

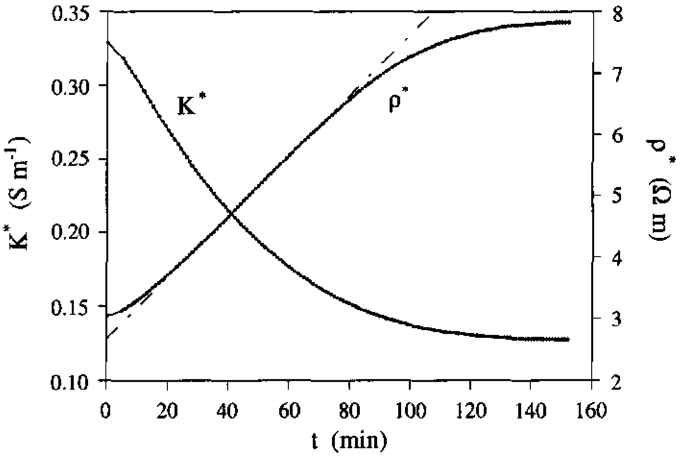

Figure 2. Plug conductivity and specific resistance versus time after changing the electrolyte in the reservoirs from 100 to 30 mM KCl and applying pressure.

particles the new situation is attained faster. On the other hand, rinsing a plug with particles of e.g. 40 nm will take days. The volume fraction can be obtained from the linear part of the $\rho^*(t)$ curve as is shown in appendix A. The value $\phi^{d\rho^*/dt} = 0.63 \pm 0.01$ is obtained from three $\rho^*(t)$ curves: 100→30, 30→10 and 10→3 mM. The error covers the three calculated values.

The plug conductivity is calculated from the plug conductance and the cell constant based on the cell geometry. In Fig. 3 the electric conductivity of the plug is presented as a function of the electric conductivity of the bulk electrolyte for the four different counterion species. The influence of the nature of the counterion on the plug conductivity is evident. For high electrolyte concentrations a linear dependence is found as is shown by the straight lines which are fits through the four points corresponding with the highest electrolyte concentrations. We note that curves of K^* versus c are less straight at high electrolyte concentrations since the linear relation between K^∞ and c is invalid due to activity effects. The measurement in 100 mM HCl is not included in the graph in order to show the information in more detail, but it perfectly lies on the straight line. This linear behaviour is expected for a surface with constant K_2^σ as predicted by Eq. [11]. The slope of the curves is given by $(1+3\phi f(0))$ and, hence, must be identical for the four electrolytes. This is confirmed by the experiments. From the intercepts the surface conductivities K_2^σ can be obtained. For a fast interpretation of the conductivity data according to Eq. [11], the reader is referred to Ref. (13). In the range $c < 3$ mM the conductivities deviate from the straight lines. This is expected from the theory since in that range double layer polarization becomes significant. Below, we will present the more elaborate interpretation based on Eq. [3] which is operational in the low electrolyte range as well.

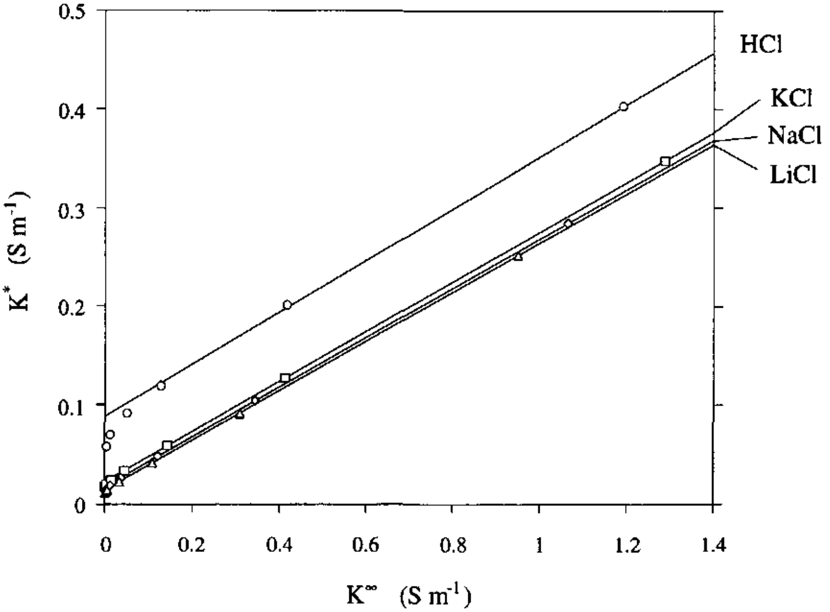

Figure 3. Conductivity of the plug as a function of the conductivity of the bulk solution for the electrolytes HCl, KCl, NaCl, and LiCl. The straight lines are fits based on the data corresponding to the four highest electrolyte concentrations.

The relative surface conductivity parameter Du_2 is obtained from the conductivity measurements. The slope of the curve at high electrolyte concentration is given by $(1+3\phi f(0))$ where we have to keep in mind that $f(0)$ is a weak function of the volume fraction ϕ. For our plug, $f(0)$ is estimated by the method of cubic interpolation between the results for the three regular arrays (5). This allows computation of the volume fraction ϕ^{con} from the limiting slopes. We determined ϕ^{con} iteratively and found $\phi^{\text{con}} = 0.633 \pm 0.008$. The error is based on the four values obtained. It is now straightforward to extract the experimental $f(Du_2)$ from the conductivity data. The theoretical relation $f(Du_2)$ is estimated for $\phi = \phi^{\text{con}}$ by cubic interpolation between the numerical results (5). By linear interpolation between the computed $f(Du_2)$ versus Du_2 values, Du_2 is found for the measured $f(Du_2)$. We were not able to calculate Du_2 for $c < 1$ mM since $f(Du_2)$ is not tabulated for $Du_2 > 5$ in (5).

From these Du_2-values the surface conductivities K_2^σ are calculated according to Eq. [5]. In Fig. 4, K_2^σ is presented as a function of the electrolyte concentration. For $c \geq 3$ mM K_2^σ is nearly independent of the electrolyte concentration and K_2^σ tends to be higher for lower c. The more mobile the counterions are, the higher is the surface conductivity K_2^σ. In Fig. 5 we have depicted the average of K_2^σ ($c \geq 3$ mM) as a function of the limiting ($c \downarrow 0$) bulk counterion

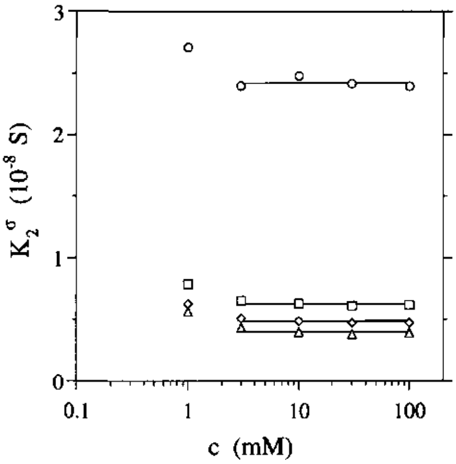

Figure 4. Dependence of the surface conductivity K_2^σ on the electrolyte concentration c for: (○) HCl, (□) KCl, (◇) NaCl, (△) LiCl.

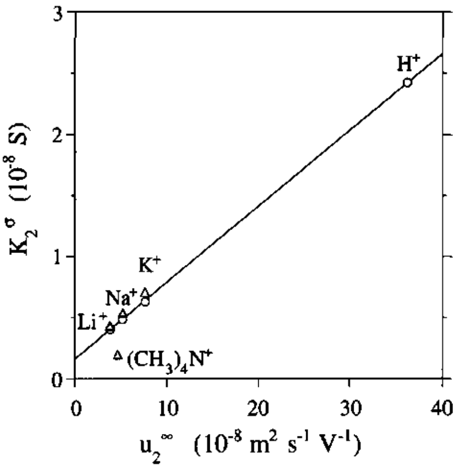

Figure 5. Dependence of the surface conductivity K_2^σ on the limiting counterion mobility u_2^∞; (○) data this study, (△) data from Midmore et al.

mobility u_2^∞ (from Ref. (20)). All the points are on a straight line which does not intersect the origin. This dependence shows that in this respect there is no counterion specifity. From Fig. 5 it follows that there is a contribution to K_2^σ which is proportional to the counterion mobility and a counterion-independent contribution. If the assumption is allowed that surface conduction due to the negative excess of co-ions is negligible, double layer characteristics can be determined from these results. According to Eq. [6] and the assumption that Θ_2 is independent of the electrolyte concentration these two contributions are due to electromigration and electroosmosis, respectively. The obtained double layer characteristics (from Eq. [6] and the assumption $\sigma^0 + \sigma_2^i + \sigma_2^d \approx 0$) are tabulated in Table 1. The absolute errors are based on the absolute errors in the slope and intercept due to scatter in K_2^σ in Fig. 5. The counterion mobility in the stagnant part of the double layer is lower than its value in the bulk, albeit of the same order of magnitude. Furthermore, a large part of the conduction is due to migration behind the plane of shear.

Table 1. Double layer characteristics obtained from conductivity experiments and σ^0.

σ_2^d (μC/cm^2)	σ_2^i(μC/cm^2)	u_2^i / u_2^∞	Θ_2	$\bar{u}_2 / u_2^\infty$
4.1 ∓ 0.9	2.2 ± 0.9	0.88 ± 0.14	0.6 ± 0.4	0.98 ± 0.03

The average ion mobility in the double layer can be calculated from the surface charge density and slope only and is therefore quite accurate. The average ion mobility in the double layer does not differ much from the bulk mobility. Midmore et al. (2,21) came to basically the same conclusion on the basis of high-frequency dielectric response experiments (MHz regime) on concentrated polystyrene sulphate latex suspensions. So did Kijlstra (9) et al. from dc conductivies of dilute sulphate latex suspensions obtained by Van der Put (3). The insensitivity of K_2^σ to the electrolyte concentration was also found in these studies.

The conductivity experiments can be compared with a study of Midmore et al. (21) who measured the high-frequency dielectric response (MHz regime) of similar latices in electrolytes of 10 mM in ionic strength. Their "latex 2" coincidentally has a surface charge density of -6.7 μC/cm^2 which is close to ours. In their table III, the relative surface conductivity λ and the bulk conductivity are presented from which we have calculated the absolute surface conductivity according to $K_2^\sigma = \lambda K^\infty a$ ($a = 339$ nm, note that $Du_2 \neq \lambda$) in the electrolytes LiCl, NaCl, KCl, and $(CH_3)_4NCl$. These surface conductivities are included in Fig. 5 as triangles. Midmore et al.'s data also show a non-zero intercept of the line through the points of LiCl, NaCl and KCl. Probably due to specific adsorption of the relatively hydrophobic $(CH_3)_4N^+$-counterions onto the hydrophobic latex, these ions are retarded in their mobility and this point is situated below the line. These results show that the dc conductivity of a latex in indifferent electrolytes can be predicted quit well if the surface charge density as well as the bulk mobility of the ions is known.

The insensitivity of the surface conductivity to the electrolyte concentration ($c \geq 3$ mM) needs commentary. It implies that no charge may move from beyond to behind the shear plane upon a change in the ionic strength. If the shear plane is situated at a *fixed position* with respect to the particle surface, the countercharge behind and beyond this plane should be rather insensitive to the electrolyte concentration in the limit of high ζ-potentials due to the cancelling of two effects. A decrease in c causes an increase in κ^{-1} and the countercharge beyond the shear plane. However, the surface potential for this surface with constant charge density will increase upon an electrolyte concentration decrease. It is well known that the surface charge is more effectively screened at higher surface potentials resulting in more charge behind the shear plane. A stagnant layer with constant thickness can be caused by the polymer hairs on the surface. Furthermore, the viscoelectric effect can also sort this effect (18). As demonstrated by Lyklema and Overbeek (22,23,18), the charge beyond the shear plane is effectively constant.

For concentrations below 3 mM, K_2^σ tends to increase with decreasing c. Unfortunately no numerical results are available to determine K_2^σ for $c < 1$ mM. This trend might continue for $c < 1$ mM and could be caused by computational problems (since $f(Du_2)$ is only known for some discrete values of Du_2) or by a limitation in the used theories. As for the latter we note that the equations have been solved for particles which are surrounded by an infinitesimally thin sheet, responsible for the surface conduction. The particles are assumed to make no direct electric contact (only in one point, the contact point) but are electrically connected via the bulk electrolyte in between them. For high c, nearly all the current travels via the bulk. For c where $Du_2 = O(1)$

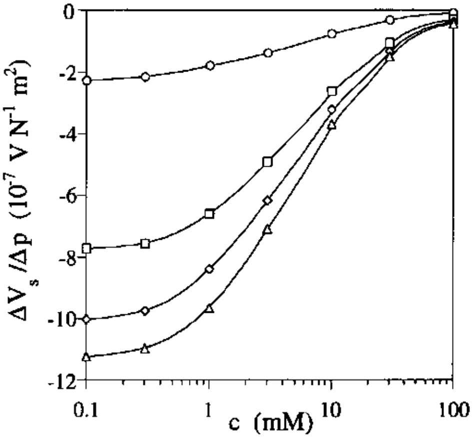

Figure 6. Streaming potentials per unit applied pressure difference as a function of the electrolyte concentration for: (○) HCl, (□) KCl, (◇) NaCl and (△) LiCl.

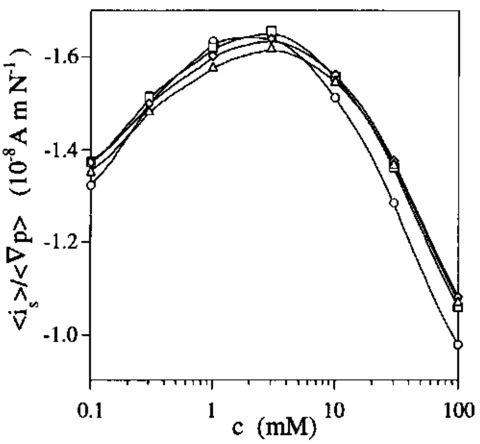

Figure 7. Streaming currents per unit applied pressure gradient as a function of the electrolyte concentration. Symbols as in figure 6.

the current in the bulk is comparable to the current which is transported in the double layer. Both situations have in common that current gradually enters the double layer over one side of the particle, and gradually leaves the double layer and enters the electrolyte solution again over the other side of the sphere. However, for low c where $Du_2 >> 1$, the major part of the current is transported via the double layer. It travels to the next particle by crossing the gap, in theory assumed to be filled with bulk electrolyte, nearby the contact points. The lower c is, the closer to these points the current will cross. Gradients in the increasing contribution of higher order moments in the electrochemical potential with increasing Du_2 (5) are the driving forces for this transport in the vicinity of the contact points. Since the process of crossing-over becomes rate-determining at low electrolyte concentrations, the plug conductivity will, with decreasing c, become increasingly sensitive to the manner by which electric contact is made between the particles. In this respect we mention double layer overlap. In appendix B we estimate the effect of double layer overlap and show its importance for low electrolyte concentrations. If particles slightly deform during centrifugation, the contact points will become flatspots and electric double layer overlap is made even more pronounced. In $c = 0.1$ mM, $Du_2 \approx 22$ estimated from the surface conductivities in $c \geq 3$ mM. The conductivity results at higher electrolyte concentrations, where $Du_2 << 1$, are of course insensitive to these effects. Therefore, it would be interesting to investigate the conductivity response upon compression of the plug at low ionic strengths.

In Fig. 6 the measured streaming potentials ΔV_s per unit applied pressure difference are depicted. The streaming potential curves are hard to compare since the plug conductivity also depends on

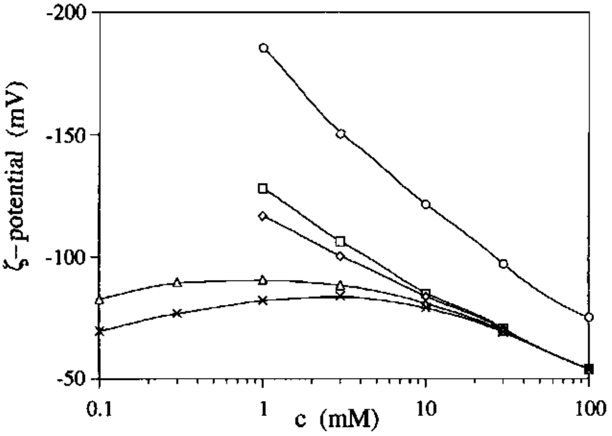

Figure 8. Comparison of ζ-potentials for polystyrene latex plugs in KCl, calculated according to different theories: (○) ζ^{con}, (□) ζ^{comb} via Kang & Sangani, (◇) ζ^{comb} via O'Brien and Perrins, (△) $\zeta^{\Theta_2=0}$, (X) ζ^{Smol}.

the type of electrolyte. Therefore we have depicted in Fig. 7 the streaming currents normalized per unit applied pressure gradient. The differences between the curves are small, which again indicates the indifferent nature of the ions. For indifferent electrolytes, theory predicts no differences at all at high electrolyte concentrations (since Du_2<<1). The experimentally found minor differences in Fig. 7 between the results for H^+ and the results for other ions at these high concentrations can be explained by a few weak acidic groups (probably carboxylic) that might be present on the latex surface. However, protons essentially behave as if they are indifferent. For $Du_2 \geq O(1)$, theory predicts some differences between indifferent electrolytes with unequal counterion mobilities. Then the electroosmotic term in Du_2 (Eq. [8]) differs.

The following analysis is based on the KCl results. By assuming immobility of ions behind the shear plane ($\Theta_2 = 0$), the ζ-potential ζ^{con} is straightforwardly obtained from Du_2 and compared in Fig. 8 with ζ-potentials obtained by a variety of other methods. ζ-potentials can be calculated from the streaming currents. As long as the double layer makes a negligible contribution to the plug conductivity (Du_2<<1), streaming potential measurements can be interpreted with Smoluchowski's formula ($g = 0$). For low electrolyte concentrations this restriction is violated and the second part of Eq. [9] becomes important in obtaining ζ-potentials from streaming potentials ($g \neq 0$).

To demonstrate the importance of surface conduction in the interpretation of streaming potentials, first the ζ-potential ζ^{Smol} is calculated from the streaming current with Smoluchowski's equation (Eq. [9], $g = 0$) and depicted in Fig. 8 as a function of c. A maximum in the ζ-potential

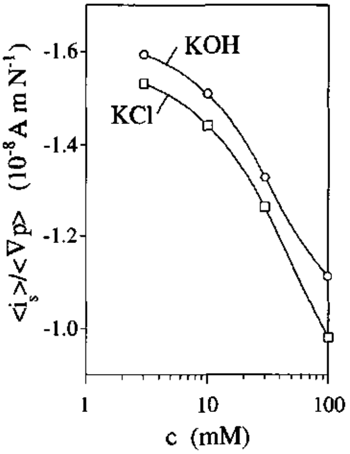

Figure 9. Streaming currents per unit applied pressure gradient as a function of the electrolyte concentration for the solutions (O) KOH and (□) KCl.

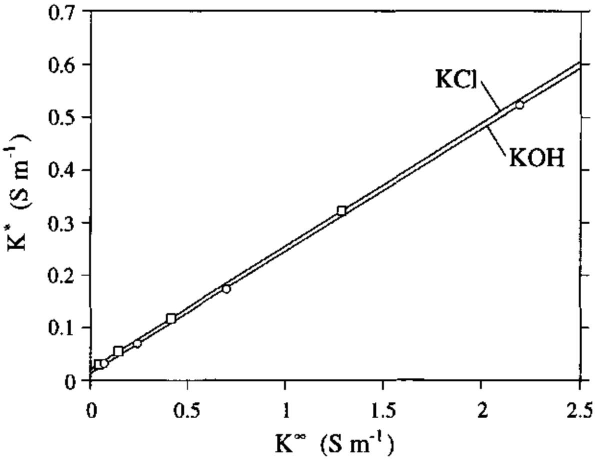

Figure 10. Conductivity of the plug as a function of the conductivity of the bulk electrolyte for the solutions (O) KOH and (□) KCl. The KOH-conductivity curve is situated below the KCl curve.

is found at $c \approx 3$ mM . The occurrence of a maximum in ζ is unlikely for a surface with constant surface charge density.

The measurements can be interpreted in a more advanced way by applying O'Brien's theory and the assumption that ions behind the shear plane are immobile. Then Du_2 is a function of the ζ-potential only and $\zeta^{\Theta_2=0}$ is calculated from the streaming currents and Eq. [9]. Therefore, $g(Du_2)$ is found from ϕ^{con} via the same cubic interpolation procedure as previously described for the determination of $f(Du_2)$. We included $\zeta^{\Theta_2=0}$ as a function of c in Fig. 8. The ζ-potentials are less underestimated in the low concentration regime, however, the maximum still exists. Moreover, the high conductivities, as shown by the discrepancy between ζ^{con} and $\zeta^{\Theta_2=0}$, are not yet explained.

We now present a further advanced method for the interpretation of the data. Therefore, $g(Du_2)$ is obtained from ϕ^{con} and Du_2 which were calculated from the conductivity data. The ζ-potentials are computed from the streaming potentials, $g(Du_2)$, and $(1+3\phi f(0))$ via Eq. [9]. In this way the *total surface conduction*, i.e., conduction beyond and behind the shear plane is taken into account for the determination of ζ^{comb} (indicated with the super index 'comb' since it is obtained from the combination of two types of electrokinetic measurements). In Fig. 8, ζ^{comb} (via O'Brien and Perrins) is also included as a function of c.

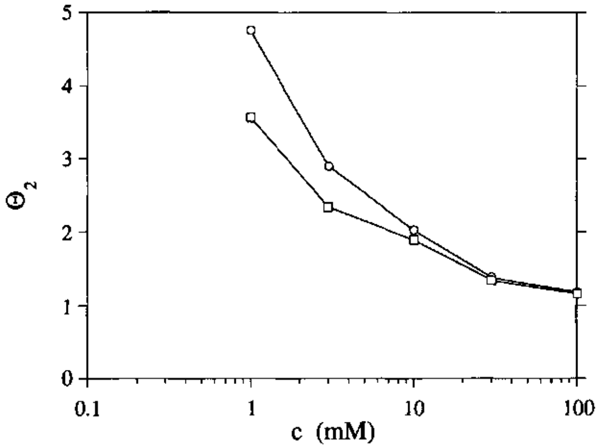

Figure 11. Θ_2 obtained from the combination of streaming currents and plug conductivities according to (O) O'Brien and Perrins and (□) according to Kang and Sangani.

By this method two discrepancies are eliminated. The maximum in the ζ-potential disappears and the conductivity and streaming current data are explained with the same surface conductivity by placing a part of the mobile countercharge behind the shear plane ($\Theta_2 \neq 0$).

Studies of the influence of the co-ions were carried out with a new plug in KCl and KOH. Figure 9 depicts the streaming currents per unit applied pressure gradient for these electrolytes ($c \geq 3$ mM). The streaming currents are nearly identical for the two different ion types which indicates absence of specificity. In KOH they are slightly higher which can be caused by dissociation of some carboxilic groups. Figure 10 shows the conductivity of the plug as a function of the conductivity of the bulk electrolyte. The KOH conductivity curve is situated below the KCl conductivity curve. Hence, the surface conductivity is lower in the electrolyte solution with the more mobile co-ions. This observation is in line with the classical Bikerman expression for the surface conductivity where the co-ions negatively contribute. In principle it must be possible to divide surface conduction into a (positive) counterion contribution and a (negative) co-ion contribution. A first rough estimation based on Eq. [11] and [12] shows that the values in table 1 can be changed significantly when we include this effect of the co-ions. However, we suggest a more rigorous study with a large number of co-ion species. In the present investigation KOH was used to show the influence of the co-ion species on the surface conductivity. Due to the relatively high mobility of the OH^--ions, the shift of the conductivity curve downwards was significant and could be detected. As a last remark we note that in an electrolyte with highly mobile co-ions, K^{σ} can even be smaller than zero. Then, the conductivity curve extrapolated from high electrolyte concentrations to the K^*-axis will have a negative intercept. The measured K^* can, of course, never be negative.

It is also possible to obtain Θ_2 from the combination of the streaming currents and the conductivities. From ζ^{comb} and Du_2, Θ_2 is calculated and the result is depicted in Fig. 11. At low electrolyte concentrations the values for Θ_2 are significantly higher than the value from the conductivity measurements only. An explanation could be found in the still rather primitive interpretation of liquid flow in the double layer. The viscosity is supposed to jump from infinite to the bulk viscosity by crossing a plane, indicated as shear plane. In reality this transition will be more gradual. More advanced hydrodynamic models for the double layer, involving a position-dependent viscosity or the incorporation of extra friction on the solvent due to the polymer hairs present on the surface might give more insight in these effects. This discrepancy seems to be severe, but we have to realize that values for Θ_2 as high as 100 are reported (24). Here Θ_2, found via two methods, appears to be of the same sign and order of magnitude.

As a last result we have calculated the ζ-potential according to Kang and Sangani who made theory for a random lattice. Since ϕ is found to be slightly higher than 0.611 for a random lattice, we again used the method of cubic interpolation, now between the SC, random, and FCC arrays. The calculated ζ-potentials ζ^{comb} according to Kang and Sangani are depicted in Fig. 8. The difference in ζ^{comb} for the two methods shows the sensitivity to the way in which particles are piled. Since in principle this is unknown, the errors in ζ^{comb} are of the order of the differences in ζ^{comb} between the two methods. However, calculations according to the method of Kang and Sangani are probably the best option to interpret the data since in reality the lattice will not be far from random. The values for Θ_2 obtained from the combined measurements according to Kang and Sangani are depicted in Fig. 11.

5. CONCLUSIONS AND PERSPECTIVES

In table 2 we summarized the volume fractions obtained via the different methods. The values are comparable within the experimental errors and significantly higher than the value 0.611 for a random close-packed lattice. This is in line with the relatively low plug permeability.

Table 2. Summary of the volume fractions determined by different methods.

ϕ^{w}	$\phi^{dp^*/dt}$	ϕ^{con}
0.635 ± 0.003	0.63 ± 0.01	0.633 ± 0.008

We were able to obtain important double layer characteristics from the plug conductivity experiments. The observed surface conductivity could be interpreted according to the classical Bikerman expression corrected for conduction behind the shear plane. It was shown that electroosmosis contributes positively and the negative excess of counterions contributes negatively to the surface conductivity. The surface conductivity is insensitive to the electrolyte concentration in the range $3 \leq c \leq 100$ mM. Although some discrepancies exist in Θ_2, obtained in different ways, a significant part of the conduction seems to take place behind the slip plane ($\Theta_2 = O(1)$). The average ion mobility of the indifferent counterions in the double layer is close to the bulk mobility. Hence, the mobility of counterions behind the shear plane must also be close to the bulk mobility.

The combination of conductivity and streaming potential measurements resolves two problems: more realistic ζ potentials are obtained and the large conductivity can be explained in terms of conduction behind the shear plane.

Options for further investigation. The advantage of plug conductivity experiments over all other conductivity experiments is the extreme sensitivity. The experiments suggest that even in concentrations much higher than 100 mM, surface conductivities can be obtained. This can be tested. Furthermore, retarded motion can be studied. Midmore showed the retardation in mobility of ions (21) specifically adsorbing in the inner Helmholtz plane. We also expect a hydrodynamically retarded motion when counterions are moving at a distance from the surface comparable to the hydrated ionic radius. For a K^+-ion, $a \approx 0.13$ nm. From the Gouy-Chapman model we have calculated that approximately 20% of the countercharge is situated behind a plane located at 0.13 nm from the surface. For a particle with surface charge density of e.g. 20 μC/cm^2 this will be nearly 50%. In the latter situation, the counterion mobility in the double layer must be lower than the bulk mobility even in the absence of specific interaction. Not finding this behaviour could indicate the presence of a rough surface with protruding surface charges. The extra adsorption of uncharged polymers might be able to impede ion motion. Furthermore, we suggest experiments with multivalent, possibly indifferent counterions. The ratio between the electroosmotic and electromigration terms is proportional to z_2^{-2}. Hence the intercept in Fig. 5 must decrease strongly.

Since the latex particles in the present study show an ideal conductivity behaviour in dc as well as high-frequency dielectric studies, low-frequency dielectric response measurements are highly recommanded for this system.

In conclusion, investigation of these high density systems is the only method to see subtle differences in the surface conductivity at high electrolyte concentration. Effects of double layer overlap, not rigorously taken into account by theory, may obscure the results at low electrolyte concentrations. Therefore, measurements in dilute suspensions (e.g. low-frequency dielectric response experiments) must be performed in order to obtain a complementary set of results. We are convinced that plugs offer interesting prospects for further electrokinetic studies.

APPENDIX A

When new electrolyte of a different concentration is pressed through the plug with length l and cross-section A, and mixing of the two electrolyte solutions inside the plug is negligible, the resistance R^* of the inhomogeneous plug can be calculated from two homogeneous plugs placed in series:

$$R^* = \frac{1}{K^*}\frac{l}{A} = \left(\frac{l_1}{lK^*_{l_1}} + \frac{l_2}{lK^*_{l_2}}\right)\frac{l}{A} \qquad [A.1]$$

where $K^*_{l_1}$ and $K^*_{l_2}$ are the conductivities of the two parts and l_1 and l_2 their lengths, respectively.

To obtain the velocity at which the electrolyte profile travels through the plug, we have to solve the conservation equation:

$$\frac{\partial n}{\partial t} = -\vec{\nabla} \cdot n\vec{v} \qquad [A.2]$$

We may neglect transport due to diffusion on the time-scales of interest. Taking the volume average over a small (compared to the plug-dimension) cylindrical volume element V (cross section O much larger than a^2, length ∂x much larger than a, cylinder axis parallel to the pressure gradient), containing a large number of particles, and applying the divergence theorem yields:

$$\frac{\partial\langle n\rangle}{\partial t} = -\frac{1}{O\partial x}\int_V \vec{\nabla} \cdot n\vec{v}\,dV = -\frac{1}{O\partial x}\int_A \vec{n} \cdot n\vec{v}\,dA \qquad [A.3]$$

where $\vec{n}$ is the unit vector normal to the surface of the volume element. The contribution from the curved surface is zero because the integrand will be as often positive as negative (no net transport of ions through this surface). For not too low electrolyte concentrations, the major contribution to the surface integral stems from the area situated beyond the double layers in the two flat surfaces O_1 and O_2 enclosing the cylinder. Since the density n in such a surface is approximately constant beyond the double layers, we may take the densities out of the integration:

$$\frac{\partial\langle n\rangle}{\partial t} = -\frac{1}{O\partial x}\int_{O_1+O_2} \vec{n} \cdot n\vec{v}\,dA = -\frac{\partial n}{\partial x}\frac{1}{O}\int_{O_2} \vec{n} \cdot \vec{v}\,dA = -\frac{\partial n}{\partial x}\left|\langle\vec{v}\rangle\right| \qquad [A.4]$$

The bulk density n can be related to $\langle n\rangle$ via the particle volume fraction; $\langle n\rangle = (1-\phi)n$, hence:

$$\frac{\partial\langle c\rangle}{\partial t} = -\frac{\left|\langle\vec{v}\rangle\right|}{(1-\phi)}\frac{\partial\langle c\rangle}{\partial x} \qquad [A.5]$$

The solution to this equation is well known: a profile that travels with velocity $\bar{v} = \left|\langle\vec{v}\rangle\right|/(1-\phi)$. Then,

$$l_1 = \bar{v}t, \quad l_2 = l - \bar{v}t \qquad \text{[A.6]}$$

Combining these equations yields the specific resistance ρ^* of the inhomogeneous plug as a function of time:

$$\rho^* \equiv \frac{1}{K^*} = \begin{cases} \dfrac{1}{K^*_{l_2}} + \left(\dfrac{1}{K^*_{l_1}} - \dfrac{1}{K^*_{l_2}}\right)\dfrac{|\langle\bar{v}\rangle|}{(1-\phi)l}t & 0 \le t \le l/\bar{v} \\ \dfrac{1}{K^*_{l_1}} & l/\bar{v} \le t \end{cases} \qquad \text{[A.7]}$$

The average velocity $|\langle\bar{v}\rangle|$ is simply calculated from the liquid rate J via $J = |\langle\bar{v}\rangle|A$. The volume fraction $\phi^{d\rho^*/dt}$ is obtained from the slope of the $\rho^*(t)$ curve.

APPENDIX B

We will consider the electric conductivity in a SC array in the situation of a high relative surface conductivity. The total current flowing through the double layer of a single particle (*sp*) is

$$I_{sp} = E_t K^\sigma 2\pi a \sin\theta \qquad \text{[B.1]}$$

where E_t is the component of the electric field along the surface and θ is the appropriate angle in spherical co-ordinates. The angle where double layers of neighbouring particles just overlap is approximately $\theta \approx (\kappa a)^{-\frac{1}{2}}$ in the situation of thin double layers. When we assume that the overlapping double layers short-circuit the touching particles, the potential jump over a particle between the two contact points is found by integration along the particle surface:

$$V_{sp} = \frac{I_p}{2\pi K^\sigma} \int_{(\kappa a)^{-1/2}}^{\pi-(\kappa a)^{-1/2}} \frac{d\theta}{\sin\theta} = -\frac{I_{sp}}{\pi K^\sigma} \ln\left(\tan((4\kappa a)^{-1/2})\right) \approx \frac{I_{sp}}{2\pi K^\sigma} \ln(4\kappa a) \qquad \text{[B.2]}$$

Note that not only the integrand diverges for $\theta = 0$ and $\theta = \pi$, also the integral is non-existing. This shows the sensitivity to the manner in which contact is made between the particles.
The potential difference ΔV over the plug of length l equals the sum of the individual particle contributions, i.e., $\Delta V = V_{sp} l/(2a)$, and the current through the plug with cross section A is equal to $I = I_{sp} A/(4a^2)$. Combination of these results yields:

$$K^* = \frac{K^\sigma}{a} \frac{\pi}{\ln(4\kappa a)} \qquad \text{[B.3]}$$

For example, in 0.1 mM electrolyte, Eq. [B.3] gives $K^* = 0.8\, K^\sigma / a$ while the double layer contribution to the conductivity in high ionic strengths is equal to $-6\phi f(0) K^\sigma / a \approx 1.2\, K^\sigma / a$. These values are comparable.

REFERENCES

(1) Midmore, B. R., O'Brien, R. W., *J. Colloid Interface Sci* **123,** 486 (1988).

(2) Midmore, B. R., Hunter, R. J., O'Brien, R. W., *J. Colloid Interface Sci.* **120,** 210 (1987).

(3) Put, A. G. van der, Ph. D. Thesis, Wageningen Agricultural University, 1980.

(4) Hoven, Th. J. J. van den, Ph. D. Thesis, Wageningen Agricultural University, 1984.

(5) O'Brien, R. W., Perrins, W. T., *J. Colloid Interface Sci.* **99,** 20 (1984).

(6) Dukhin, S. S., Derjaguin, B. V., *in* "Surface and Colloid Science", Vol. 7 (E. Matijevic, Ed.), Wiley, New York, 1974.

(7) O'Brien, R. W., *J. Colloid Interface Sci.* **110,** 477 (1986).

(8) Kang, S. -Y., Sangani, A. S., *J. Colloid Interface Sci.* **165,** 195 (1994).

(9) Kijlstra, J., Leeuwen, H. P. van, Lyklema, J., *J. Chem. Soc., Faraday Trans. 2* **88,** 3441 (1992).

(10) O'Brien, R. W., *J. Colloid Interface Sci.* **92,** 204 (1983).

(11) Bikerman, J. J., *Z. Phys. Chem. Ab. A* **136,** 378 (1933).

(12) Bikerman, J. J., *Kolloid-Z.* **72,** 100 (1935).

(13) Lyklema, J., Minor, M., *Colloids Surfaces A*, in press.

(14) Zick, A. A., Homsy, G. M., *J. Fluid Mech.* **115,** 13 (1982).

(15) Goodwin, J. W., Hearn, J., Ho, C. C., Ottewill, R. H., *Colloid and Polymer Sci.* **252,** 464 (1974).

(16) Hul, H. J. van den, Vanderhoff, J. W., *J. Colloid Interface Sci.* **28,** 336 (1968).

(17) Pelssers, E. G. M., Ph. D. Thesis, Wageningen Agricultural University, 1988.

(18) Lyklema, J., "Fundamentals of Interface and Colloid Science. Solid-Liquid Interfaces", Vol. II, Academic Press, London, 1995.

(19) A detailed description of the apparatus is available on request at the department.

(20) Lyklema, J., "Fundamentals of Interface and Colloid Science. Fundamentals", Vol. I, Academic Press, London, 1991.

(21) Midmore, B. R., Diggins, D., Hunter, R. J., *J. Colloid Interface Sci.* **129,** 153 (1989).

(22) Lyklema, J., Overbeek, J. Th. G., *J. Colloid Interface Sci.* **16,** 507 (1961).

(23) Lyklema, J., *Colloids Surfaces A* **92,** 41 (1994).

(24) Wal, A. van der, Minor, M., Norde, W., Zehnder, A. J. B., Lyklema, J., *J. Colloid Interface Sci.* **186,** 71 (1997).

Chapter 3

LOW-FREQUENCY DIELECTRIC RESPONSE OF POLYSTYRENE LATEX DISPERSIONS[1]

ABSTRACT. The low-frequency permittivity and the conductivity increments of a well-characterised polystyrene sulphate latex with constant surface charge density were measured in KCl electrolyte solutions. The ionic strength was varied in the range 0.4-6 mM. The data could be explained with one absolute surface-conductivity parameter over the complete concentration range. The titratable surface charge density correlates well with the surface conductivity, with the ions in the double layer having the bulk mobility. The results are in good agreement with static conductivities of plugs composed of the same particles obtained in a previous study (1). The electrokinetic charge obtained from streaming potentials (1) in that study is significantly lower, confirming the presence of conduction behind the shear plane.

In order to interpret the conductivity data, simple analytical expressions have been derived for the frequency-dependent complex conductivity of a dilute dispersion of spherical particles with relatively thin double layers ($\kappa a >> 1$ where a is the particle radius and κ^{-1} the double layer thickness). The expressions are restricted to binary suspending electrolytes. However, no restrictions on the ion mobilities and ion valences are made. Our results agree well with the numerical results of the dielectric model of Mangelsdorf and White (2,3) and reduce to O'Brien's static conductivity results (4) in the limit of low frequencies.

---

[1] Submitted for publication in *J. Colloid Interface Sci.* in coauthorship with Leeuwen, H. P. van, Lyklema, J.

1. INTRODUCTION

The electrokinetic potential is one of the most common characteristics of charged surfaces. Electrokinetic potentials however cannot be measured directly but must be deduced from experiments by applying some electrokinetic model. A popular one is the "standard electrokinetic model". In this model the surface is characterised by a shear plane at which the potential is ζ. The ions within the stagnant liquid behind the slip plane are considered to be immobile. Application of this standard model shows that generally ζ-potentials obtained from suspension conductivities in dc or ac fields are systematically larger than those obtained from particle mobilities (5-15) or streaming potentials on porous plugs (1). The most probable cause for this inconsistency can be found in the neglect of conduction behind the shear plane by the standard model (11,12). The extend of this conduction will be related to surface roughness, porosity, the viscoelectric effect (13), the properties of a Stern layer or the presence of a macro-molecular (hairy) surface layer. Such a hairy layer may be found on latex surfaces. Latex dispersions are interesting systems for the investigation of this phenomena since they can be made as spherical particles with a fixed surface charge density, monodisperse, and in large amounts. In a number of studies on latexes, the ζ-potentials inferred from low-frequency (LF) dielectric measurements have been compared to the "theoretically predicted ζ-potentials" based on mobility measurements (16,8-10). However, these latter ζ-potentials also contain the restrictions of the standard model. In the present article LF dielectric data of latex dispersions will be given and related to the surface charge density obtained from titrations to see in how far the conductivity data are anomalous in themselves. It will be shown that one single absolute surface-conductivity parameter is able to explain the dielectric spectra in the electrolyte concentration range 0.4-6 mM. This surface conductivity does relate well to the countercharge, which is accessible via a titration, if the ions in the complete double layer are assumed to have mobilities close to the bulk value.

The experiments will be interpreted for the case of relatively thin double layers ($\kappa a >> 1$, where a is the particle radius and κ^{-1} the double layer thickness). Although the observation of local quasi-equilibrium in such an electric double layer is already more than 20 years old (17), no simple analytical expressions for the permittivity and conductivity of a dilute dispersion of spherical particles with relatively thin double layers in an arbitrary binary suspending electrolyte has been reported so far. The expressions obtained in previous theoretical studies are intricate, restricted to symmetrical electrolytes (17-19), or incomplete (20). This considerably limits the practical use of these expressions.

Outline of the paper. Because of the lack of simple analytical expressions we outline in section 2 the derivation of tractable equations for the real and imaginary parts of the complex LF conductivity of a dilute suspension of spherical particles in an arbitrary binary electrolyte. In the experimental section 3, the characteristics of the home-made polystyrene sulphate latex are given, the LF dielectric spectrometer is described and the experimental conditions are indicated. Results will be presented and discussed in section 4.

2. THEORY

2.1. Governing electrokinetic equations

We consider a spherical particle with radius a in a suspending electrolyte where the ion charge, ion friction coefficient and number density of the ith type of ionic species ($i = 1,2,\ldots,N$) are $z_i e$, f_i and n_i, respectively. The origin of our spherical co-ordinate system is located at the centre of the particle. We will identify the position just inside the particle with a^-, the position in the inner part of the diffuse layer, adjacent to the surface, with a, the position of the shear plane with a^ζ and the position just beyond the thin diffuse double layer with a^+. An oscillating electric field with magnitude E_0 and (angular) frequency ω is imposed:

$$\vec{E} = \vec{E}_0 \exp(i\omega t), \quad E_0 = \left|\vec{E}_0\right| \qquad [1]$$

The electric potential ψ, the space charge density ρ and the dielectric permittivity $\varepsilon = \varepsilon_0\varepsilon_r$ are related via Poisson's equation:

$$\vec{\nabla} \cdot \varepsilon \vec{\nabla} \psi = -\rho = -\sum_{i=1}^{N} z_i e n_i \qquad [2]$$

where $\varepsilon = \varepsilon_0\varepsilon_r$ is the permittivity of the medium. The boundary condition at the particle surface is given by Gauss's law:

$$\left(\varepsilon \frac{\partial \psi}{\partial r}\right)\Bigg|_{a^-}^{a} = -\sigma^0 \qquad [3]$$

where σ^0 is the surface charge density. Far away from the particle the electric field approaches the applied electric field and the ion density approaches its bulk value (superscript "∞"):

$$\vec{\nabla}\psi = -\vec{E} \quad \text{as} \quad r \to \infty \qquad [4]$$

$$n_i \to n_i^\infty \quad \text{as} \quad r \to \infty \qquad [5]$$

The ions are convectively transported by the fluid with velocity $\vec{v}$ and are able to move relative to the solvent under the influence of electric and thermodynamical forces. The ionic flux density $\vec{J}_i$ is given by the Nernst-Planck equation:

$$\vec{J}_i = n_i \vec{v} - \frac{kT}{f_i}\left(n_i \frac{z_i e}{kT} \vec{\nabla}\psi + \vec{\nabla} n_i\right) \qquad [6]$$

Ions are supposed to be unable to be transferred through the particle surface:

$$\vec{J}_i \cdot \vec{e}_r = 0 \quad \text{at} \quad r = a \qquad [7]$$

where $\vec{e}_r$ is the unit vector, normal to the particle surface.

The motion of the fluid is described by the Navier-Stokes equations restricted to incompressible fluid flow and low Reynolds numbers, with extra included an electrostatic force term. In the LF domain of interest, the time-derivative term may be neglected (21):

$$\eta\vec{\nabla}^2\vec{v} - \vec{\nabla}p - \rho\vec{\nabla}\psi = \vec{0} \qquad [8]$$

$$\vec{\nabla}\cdot\vec{v} = 0 \qquad [9]$$

where η is the liquid viscosity and p is the pressure. These equations must be solved subject to the boundary conditions

$$\begin{aligned} &\vec{v} = \vec{0} \quad \text{at} \quad r \le a^{\zeta} \\ &\vec{v} = -\vec{v}_{ef} \quad \text{as} \quad r \to \infty \end{aligned} \qquad [10]$$

The liquid between $r = a$ and $r = a^{\zeta}$ is supposed to be stagnant. Here, $\vec{v}_{ef}$ denotes the electrophoretic velocity.

Conservation of ions implies:

$$\frac{\partial n_i}{\partial t} + \vec{\nabla}\cdot\vec{J}_i = 0 \qquad [11]$$

If the applied electric field strength is low, the equations can be linearized around the equilibrium values in absence of the imposed field (subscript *eq*). To that end we write:

$$\begin{aligned} \psi &= \psi_{eq} + \delta\psi + \mathrm{O}(E_0^2) \\ n_i &= n_{i,eq} + \delta n_i + \mathrm{O}(E_0^2) \\ &\text{etc.} \end{aligned} \qquad [12]$$

The liquid velocity $\vec{v}$ is first-order in E_0. Substituting these expressions in Poisson's equation and omitting the small non-linear $\mathrm{O}(E_0^2)$ terms yields:

$$\vec{\nabla}\cdot\varepsilon\vec{\nabla}\delta\psi = -\delta\rho = -\sum_i z_i e\delta n_i \qquad [13]$$

Substituting Eqs. [12] in the conservation equation, subtracting the zero-flux equilibrium situation and omitting the small non-linear terms gives us the linearized Nernst-Planck equation:

$$\begin{aligned} \vec{J}_i &= n_{i,eq}\vec{v} - \frac{kT}{f_i}\left(\frac{z_i e}{kT}\left(n_{i,eq}\vec{\nabla}\delta\psi + \delta n_i\vec{\nabla}\psi_{eq}\right) + \vec{\nabla}\delta n_i\right) \\ &= n_{i,eq}\vec{v} - n_{i,eq}\frac{kT}{f_i}\vec{\nabla}\left[\frac{z_i e}{kT}\delta\psi + \frac{\delta n_i}{n_{i,eq}}\right] \end{aligned} \qquad [14]$$

The term between square brackets is just the first-order perturbation in the non-dimensional electrochemical potential $\delta\mu_i$.

The linearized Navier-Stokes equation becomes:

$$\eta\vec{\nabla}^2\vec{v} - \vec{\nabla}\delta p - \rho_{eq}\vec{\nabla}\delta\psi - \delta\rho\vec{\nabla}\psi_{eq} = \vec{0} \tag{15}$$

For the linearized conservation equation we obtain:

$$\frac{\partial \delta n_i}{\partial t} + \vec{\nabla}\cdot\vec{J}_i = 0 \tag{16}$$

2.2. Equations and fields outside the double layer

Beyond the relatively thin diffuse double layer with thickness:

$$\kappa^{-1} = \sqrt{\varepsilon^\infty kT \Big/ \sum_i z_i^2 e^2 n_i^\infty} \tag{17}$$

the electrolyte is unperturbed by the equilibrium double layer

$$\psi_{eq} = 0, \quad n_{i,eq} = n_i^\infty \tag{18}$$

and the set of governing equations simplifies. The solutions to these simplified equations define the so called "far fields" and are labelled with the superscript "*f*".
Beyond the double layer the Poisson equation reads:

$$\nabla^2\delta\psi^f = -\frac{1}{\varepsilon^\infty}\sum_i z_i e\,\delta n_i^f \tag{19}$$

Using Nernst-Planck, the conservation equation for each species turns into:

$$\frac{f_i^\infty}{kT}\frac{\partial \delta n_i^f}{\partial t} = \nabla^2\left(n_i^\infty \frac{z_i e}{kT}\delta\psi^f + \delta n_i^f\right) \tag{20}$$

The convective term cancelled because of incompressibility. From hereon we will consider the far less complex but common situation of a binary, nut not necessarily symmetrical suspending electrolyte. Addition of the conservation equations for the two ionic species results in:

$$\nabla^2\delta n_i^f = \mathrm{i}\omega\frac{\overline{f^\infty}}{kT}\delta n_i^f, \quad \overline{f^\infty} \equiv \frac{z_2 f_1^\infty - z_1 f_2^\infty}{z_2 - z_1} \tag{21}$$

Multiplication of the conservation equations by z_i and addition yields:

$$\nabla^2\delta\psi^f = \mathrm{i}\omega\frac{1}{e}\left(\frac{f_1^\infty - f_2^\infty}{n_1^\infty z_1^2 + n_2^\infty z_2^2}\right)z_1\delta n_1^f \tag{22}$$

In obtaining [21] and [22] we used the electroneutrality condition $z_1\delta n_1^f = -z_2\delta n_2^f$. This condition is exact if the ions have equal diffusion coefficients, and is a good approximation if $f_1^\infty \neq f_2^\infty$ as long as the frequency is much smaller than the Maxwell-Wagner frequency $(= \mathrm{O}(K^\infty/\varepsilon))$. This was shown by Dukhin and Shilov (17) and Hinch et al. (20) by including Poisson's equation. We have to note here that the electroneutrality condition only cancels insignificant terms. To a very good approximation, Eq. [22] still accounts for space charge arising beyond the electric double layer if $f_1^\infty \neq f_2^\infty$. Its right-hand-side is directly proportional to the space charge density via Poisson's equation. Laplace's equation for the potential is operative everywhere beyond the double layer if $f_1^\infty = f_2^\infty$. Then charge generation beyond the double layer is absent and there are no associated diffusion potentials.

The unique solution of Eq. [21] for δn_i^f, which tends to zero far away from the particle, and able to obey the boundary conditions just beyond the double layer, is:

$$\delta n_i^f = \frac{d_{i,n} a^3 E_0}{r^2}(1+\lambda r)\exp(-\lambda r)\cos(\theta)\exp(\mathrm{i}\omega t) \qquad [23]$$

where

$$\lambda a \equiv (1+\mathrm{i})\sqrt{\omega\tau}, \quad \tau \equiv \frac{\overline{f^\infty} a^2}{2kT} \qquad [24]$$

The concentration polarization parameters $d_{i,n}$ are related by the electroneutrality condition: $z_1 d_{1,n} = -z_2 d_{2,n}$.

The potential beyond the double layer is given by:

$$\delta\psi^f = \left(-E_0 r + \frac{d_\psi a^3 E_0}{r^2}\right)\cos(\theta)\exp(\mathrm{i}\omega t) - \frac{kT}{e}\left(\frac{f_1^\infty - f_2^\infty}{z_2 f_1^\infty - z_1 f_2^\infty}\right)\frac{1}{n_1^\infty}\delta n_1^f \qquad [25]$$

where d_ψ is the polarization parameter for the electric potential. For non-zero frequencies, δn_i^f has an exponential decay with position r. Hence, the asymptotic form of $\delta\psi^f$ is given by

$$\delta\psi^f\Big|_{r >> a/(\omega\tau)^2} = -E_0 r + \frac{C(\omega) a^3 E_0}{r^2}\cos(\theta)\exp(\mathrm{i}\omega t) \qquad [26]$$

where

$$C(\omega) = d_\psi \quad \text{for} \quad \omega > 0 \qquad [27]$$

For *zero frequency* however, δn_i^f has an r^{-2}-decay. Then the asymptotic behaviour of $\delta\psi^f$ is given by Eq. [26] where now

$$C(0) = d_\psi - \frac{kT}{e}\left(\frac{f_1^\infty - f_2^\infty}{z_2 f_1^\infty - z_1 f_2^\infty}\right)\frac{1}{n_1^\infty} d_{1,n} \qquad [28]$$

This means that usually there is a discontinuity in the electric polarization parameter $C(\omega)$ in $\omega = 0$. Only in the situation where $f_1^\infty = f_2^\infty$ this discontinuity is absent (see also Refs. (21,22)).

The polarization characteristics $d_{i,n}$ and d_ψ are determined by two additional boundary conditions applied just beyond the electric double layer. These "inner" boundary conditions are well known. Dukhin noticed that for frequencies well below the Maxwell-Wagner frequency, and not too extreme relative surface conductivities, the double layer is in local quasi-equilibrium with the adjacent electrolyte (17). Then, at not too low relative surface potentials, the tangential flux of co-ions along the surface is negligible due to the relatively low number density of these ions in this region. Hence, to a reasonable approximation, co-ions (subscript "1") are not allowed to enter the double layer regime (23):

$$\frac{\partial}{\partial r}\left[n_1^{\infty}\frac{z_1 e}{kT}\delta\psi^f + \delta n_1^f\right]\Bigg|_{r=a^+} = 0 \qquad [29]$$

The change in tangential flux of counterions (subscript "2") in the double layer regime is balanced by the flux entering this regime radially from the neighbouring electrolyte:

$$\frac{\partial}{\partial r}\left[n_2^{\infty}\frac{z_2 e}{kT}\delta\psi^f + \delta n_2^f\right]\Bigg|_{r=a^+} + Du_2\ a\ \nabla_t^2\left[n_2^{\infty}\frac{z_2 e}{kT}\delta\psi^f + \delta n_2^f\right]\Bigg|_{r=a^+} = 0 \qquad [30]$$

where ∇_t^2 is the usual Laplacian operator in spherical co-ordinates, but without the $\partial/\partial r$-term. Du_2 is the dimensionless relative surface conductivity parameter due to the excess of counterions in the double layer. Physically, Du_2 can be interpreted as the comparison between surface conduction and bulk conduction. Du_2 is related to the absolute surface conductivity K_2^{σ} via (6):

$$Du_2 = \frac{K_2^{\sigma}}{aK_2^{\infty}} \qquad [31]$$

where $K_2^{\infty} = e^2 z_2^2 n_2^{\infty} / f_2^{\infty}$ is the part of the bulk conductivity due to counterions. Since the far fields change significantly only over distances of the order of the particle radius a, the boundary conditions [29] and [30] may be imposed at the particle surface. The time derivatives, reflecting accumulation of ions in the double layer, are not important in the frequency regime of interest for a surface with constant surface charge density. However, this term can be of great importance in modern theories involving a dynamic Stern layer (24).

We allow the ions behind the shear plane to be mobile with mobility u_i^i. Conductivity in the non-stagnant double layer regime consists of two parts (6): (i) a contribution caused by the movement of charge with respect to the liquid and (ii) a contribution caused by the electroosmotic liquid flow relative to the particle surface. This electroosmotic flow make the ions move faster with respect to the surface. We can write:

$$K_2^{\sigma} = \tilde{u}_2^i \sigma_2^i + \left(1 + 3m_2/z_2^2\right)\tilde{u}_2^{\infty}\sigma_2^d \qquad [32]$$

Here, σ_i^i and σ_i^d are the (surface) densities of charge behind and beyond the shear plane, respectively, $\tilde{u}_i^i$ and $\tilde{u}_i^{\infty}$ are the ion mobilities behind the beyond the shear plane, respectively, including their sign: $\tilde{u}_i = z_i e / f_i$, $u_i = |\tilde{u}_i|$. We have assumed that the ions move according to their bulk mobility beyond the shear plane. The non-dimensional ionic drag coefficient m_i is given by:

$$m_i \equiv \frac{2\varepsilon^{\infty} kT f_i^{\infty}}{3\eta e^2} \qquad [33]$$

It is convenient to introduce the ratio Θ_i reflecting the relative contribution of conduction behind the shear plane to the surface conductivity[2]:

$$\Theta_i = \tilde{u}_i^i \sigma_i^i / \tilde{u}_i^{\infty} \sigma_i^d \qquad [34]$$

Combination of Eqs. [32]-[34] relates the surface conduction to the total counterion countercharge in the double layer ($\sigma_2^{dl} = \sigma_2^d + \sigma_2^i$):

$$K_2^{\sigma} = \left(\frac{\Theta_2}{1 + (\tilde{u}_2^{\infty}/\tilde{u}_2^i)\Theta_2} + \frac{1}{1 + (\tilde{u}_2^{\infty}/\tilde{u}_2^i)\Theta_2} \left[1 + 3m_2/z_2^2\right] \right) \tilde{u}_2^{\infty} \sigma_2^{dl} \qquad [35]$$

In principle, all countercharge can be situated beyond the shear plane ($\Theta_2 = 0$) or behind it ($\Theta_2 = \infty$) and hence Θ_2 may have a value between $0 \le \Theta_2 \le \infty$. For the common situation of not too weakly charged particles, the counterions are responsible for the most of the countercharge. Then, to a good approximation, $\sigma_2^{dl} \approx -\sigma^0$. Therefore K_2^{σ} is restricted to:

$$-\tilde{u}_2^i \sigma^0 \le K_2^{\sigma} \le -\left[1 + 3m_2/z_2^2\right] \tilde{u}_2^{\infty} \sigma^0 \qquad [36]$$

The values for u_2^i found in a number of investigations (26,27,1) are smaller than the bulk value, albeit of the same order of magnitude. Under the assumption $u_2^i \approx u_2^{\infty}$ it is possible to estimate K_2^{σ} from titration data within the range specified above.

It is also possible to relate Du_2 to the double-layer characteristics ζ and Θ_2 (28,6):

$$Du_2 = \left(\frac{1 + |z_1/z_2|}{2} \right)^{1/2} \frac{2}{\kappa a} \left(1 + 3m_2/z_2^2 + \Theta_2\right) \left[\exp\left(\frac{-z_2 e \zeta}{2kT} \right) - 1 \right] \qquad [37]$$

The current entering the double layer region (normally) from the adjacent electrolyte is more or less equally carried by co- and counterions. This current is balanced by an increase or decrease in the tangential current in the double layer region. However, this latter current is mainly carried by counterions. Hence the individual ion fluxes are not balanced and the double layer will act as a source of neutral electrolyte on one side of the particle and as a sink on the other side. These excesses/depletions will diffuse into the neighbouring electrolyte and spread out over distances of the order of the particle radius. After switching on a constant external field at t=0, a few times the characteristic time τ is needed to establish a stationary state. In an alternating field the surface is alternatingly acting as a sink or as a source, resulting in the concentration profile given by [23]. Application of the inner boundary conditions [29] and [30] to [23] and [25] yields the relations between the polarization parameters and the relative surface conductivity. For d_{ψ} we find:

---

[2] This Θ_i is somewhat different from $\Theta_i = \sigma_i^i / \sigma_i^d$ introduced by Kijlstra (25).

$$d_\psi = -\frac{1}{2} + \frac{3}{2}\,\frac{Du_2(1+h)}{2 + Du_2\left[2 - \gamma(1-h)\right]} \tag{38}$$

where

$$\gamma \equiv 1 - \frac{1+\lambda a}{1+\lambda a+\frac{1}{2}(\lambda a)^2} = \frac{\omega\tau\sqrt{\omega\tau}+\mathrm{i}\,\omega\tau}{(1+\sqrt{\omega\tau})(1+\omega\tau)} \tag{39}$$

and

$$h \equiv \frac{z_2/f_2^\infty + z_1/f_1^\infty}{z_2/f_2^\infty - z_1/f_1^\infty} = \frac{\tilde{u}_2^\infty + \tilde{u}_1^\infty}{\tilde{u}_2^\infty - \tilde{u}_1^\infty} \tag{40}$$

Notice that $-1 \le h \le 1$ and d_ψ is real if one of the ion mobilities dominates ($h \rightarrow \pm 1$). This expression for the dipole strength has also been found by Hinch et al. (20) for a particle with constant surface charge density.

In the determination of the complex conductivity of the suspension in the next section, the decomposition of d_ψ into its real and imaginary parts is wanted. The expression for this is easily found from equation [38] but is rather extended. Therefore, we notice that the real part of the denominator is much larger than its imaginary part for all frequencies and Du_2 values. Thus, the real part of d_ψ can be approximated by omitting the imaginary part in the denominator. The imaginary part of d_ψ is well approximated by linearization around $\gamma = 0$. Then we find:

$$\begin{aligned} d_\psi = {} & -\frac{1}{2} + \frac{3}{4}\,\frac{Du_2(1+h)}{1+Du_2} + \frac{3}{8}(1-h^2)\left(\frac{Du_2}{1+Du_2}\right)^2 \cdot \\ & \cdot\left(\frac{\omega\tau\sqrt{\omega\tau}}{(1+\sqrt{\omega\tau})(1+\omega\tau) - (1-h)Du_2\,\omega\tau\sqrt{\omega\tau}/(2+2Du_2)} + \frac{\mathrm{i}\,\omega\tau}{(1+\sqrt{\omega\tau})(1+\omega\tau)}\right) \end{aligned} \tag{41}$$

2.3. Conductivity in an alternating electric field

The complex conductivity $\hat{K}$ of a system is defined by

$$\vec{i} = \hat{K}\vec{E} \tag{42}$$

where $\vec{i}$ is the electric current density. Formally $\hat{K}$ can be decomposed into its real and imaginary components:

$$\hat{K}(\phi,\omega) \equiv K(\phi,\omega) + \mathrm{i}\,\omega\varepsilon_0\varepsilon_r(\phi,\omega) \tag{43}$$

Here, ϕ denotes the particle volume fraction. In the absence of particles, $\hat{K}$ simply reduces to:

$$\hat{K}(0,\omega) = K^\infty + \mathrm{i}\,\omega\varepsilon_0\varepsilon_r^\infty \equiv \hat{K}^\infty(\omega) \tag{44}$$

where K^∞ is the dc conductivity of the electrolyte solution and ε_r^∞ the relative dielectric permittivity of the electrolyte solution (≈80 for aqueous solutions) which both are independent of the frequency in the regime of interest ($\omega << K^\infty / \varepsilon_0 \varepsilon_r^\infty$). For dilute dispersions, $\hat{K}$ for *non-zero* frequencies is related to the asymptotic polarization parameter C (17,21) via

$$\hat{K}(\phi,\omega) = \hat{K}^\infty + 3\phi\, C\hat{K}^\infty \qquad [45]$$

As shown by Teubner (22), also the static conductivity can be found with Eq. [45] where the limiting polarization parameter $C(\omega \downarrow 0)$ and not $C(0)$ must be used. Since d_ψ is continuous in $\omega = 0$, the conductivity over the complete frequency range is found after replacing C by d_ψ in Eq. [45]. We have to note, however, that in principle this static conductivity cannot be measured due to the finiteness of the measurement volume. Even if one would be able to get around natural convection in the system, one would come to a frequency as low as $\omega = O(kT / l^2 \overline{f^\infty})$ where the diffusion layer thickness becomes comparable to the characteristic cell dimension l (as low as 10^{-5} Hz for a 1 cm cell). Then, the assumption in theory of an infinitely extended volume is violated. Since d_ψ calculated above is nearly real and nearly constant in the range $\omega << kT / a^2 \overline{f^\infty}$, the static conductivity can be experimentally obtained in the frequency range $kT / l^2 \overline{f^\infty} << \omega << kT / a^2 \overline{f^\infty}$. For practical reasons, e.g. of avoiding electrode-polarization effects, the static conductivity is measured at frequencies sufficiently high (many orders above $kT / l^2 \overline{f^\infty}$) and sufficiently below $kT / a^2 \overline{f^\infty}$, i.e., usually in the kHz regime.

We can draw the conclusion that O'Brien's expression for the static conductivity is also applicable for frequencies in the above specified range. In this respect, Dukhin's critical note in Ref. (29), stating that O'Brien's static conductivity results are only applicable for nonpractical frequencies $\omega << kT / l^2 \overline{f^\infty}$ is incorrect.

Substituting Eq. [41] in [45] we find to a good approximation:

$$\begin{aligned} K(\phi,\omega) = K^\infty + 3\phi K^\infty \Bigg[& -\frac{1}{2} + \frac{3}{4}\frac{Du_2(1+h)}{1+Du_2} \\ & + \frac{3}{8}(1-h^2)\left(\frac{Du_2}{1+Du_2}\right)^2 \frac{\omega\tau\sqrt{\omega\tau}}{(1+\sqrt{\omega\tau})(1+\omega\tau) - (1-h)Du_2\,\omega\tau\sqrt{\omega\tau}/(2+2Du_2)} \Bigg] \end{aligned} \qquad [46]$$

where the term $-3\phi\,\mathrm{Im}(d_\psi)\mathrm{Im}(\hat{K}^\infty)$ could be neglected. Upon placing a non-conducting, uncharged particle in an electrolyte solution, the overall static conductivity will decrease. This is reflected in the first contribution between square brackets. In general however, particles are charged and exhibit surface conduction. This results in a positive contribution to the overall static conductivity as expressed via the second term between square brackets. The two effects cancel if the suspension is in its iso-conductance point, i.e., if $Du_2 = 2/(1+3h)$. Iso-conductivity can only be observed for $-1/3 < h \leq 1$. If $-1 \leq h \leq -1/3$ the static conductivity increment is negative even for particles which exhibit an infinitely high surface conductivity. We have to note however that the condition $-1/3 < h \leq 1$ applies for commonly used suspending electrolytes. This static conductivity contribution is, as expected, identical to the static conductivity expression for a binary electrolyte found by O'Brien (Ref. (4), Eq. [6.13]).

The third term between the square brackets in Eq. [46] reflects the contribution of the relaxation process of the electrolyte cloud beyond the double layer. The oscillations in the electrolyte concentrations just beyond the double layer are significantly out-of-phase with the applied electric field for frequencies around $\omega = \tau^{-1}$. The corresponding (out-of-phase) tangential gradients in the electrolyte concentration just beyond the double layer induce tangential gradients in the electrochemical potential inside the double layer and, consequently, out-of-phase electric currents in the double layer. These currents must be balanced by the currents in the bulk. Hence, the suspension conductivity is complex around $\omega = \tau^{-1}$. Since these induced concentration-driven currents in the double layer oppose the currents driven by the electric field, the suspension conductivity is higher for frequencies $\omega >> \tau^{-1}$ (where concentration polarization is absent) than for frequencies $\omega << \tau^{-1}$.

The out-of-phase currents introduced by the relaxation of the electrolyte cloud can be interpreted as a change in the dielectric permittivity. We find to a good approximation

$$\varepsilon_r(\phi,\omega) = \varepsilon_r^\infty + \varepsilon_r^\infty \frac{9}{16}\phi(\kappa a)^2(1-h^2)\left(\frac{Du_2}{1+Du_2}\right)^2 \frac{1}{(1+\sqrt{\omega\tau})(1+\omega\tau)} \qquad [47]$$

where the term $3\phi\,\mathrm{Re}(d_\psi)\mathrm{Im}(\hat{K}^\infty)$ could be neglected. At frequencies $\omega > \tau^{-1}$ the electrolyte cloud cannot fully develop. This gives rise to dispersion around $\omega = \tau^{-1}$. The deviations in $K(\phi,\omega)$ and $\varepsilon_r(\phi,\omega)$ from their bulk values K^∞ and ε_r^∞ are usually called conductivity and permittivity increment, respectively.

In dielectric and conductivity studies increments due to changes in frequency are also considered. The conductivity is usually presented relative to the conductivity at a reference frequency $\omega_{ref,K}$ much smaller than τ^{-1}:

$$\begin{aligned}\Delta_\omega K(\phi,\omega) &\equiv K(\phi,\omega) - K(\phi,\omega_{ref,K}) \\ &= K^\infty \frac{9}{8}\phi(1-h^2)\left(\frac{Du_2}{1+Du_2}\right)^2 \frac{\omega\tau\sqrt{\omega\tau}}{(1+\sqrt{\omega\tau})(1+\omega\tau) - (1-h)Du_2\,\omega\tau\sqrt{\omega\tau}/(2+2Du_2)}\end{aligned} \qquad [48]$$

and the permittivity increment[3] relative to the permittivity at a reference frequency $\omega_{ref,\varepsilon}$ much larger than τ^{-1}:

$$\begin{aligned}\Delta_\omega \varepsilon_r(\phi,\omega) &\equiv \varepsilon_r(\phi,\omega) - \varepsilon_r(\phi,\omega_{ref,\varepsilon}) \\ &= \varepsilon_r^\infty \frac{9}{16}\phi(\kappa a)^2(1-h^2)\left(\frac{Du_2}{1+Du_2}\right)^2 \frac{1}{(1+\sqrt{\omega\tau})(1+\omega\tau)}\end{aligned} \qquad [49]$$

---

[3] The equation for the limiting increment $\Delta_\omega \varepsilon_r\big|_{\omega\tau\downarrow 0}$ is essentially identical to the expression given by Hinch et al. (Ref. (20), Eq. 110). Their mentioned lack of agreement with numerical calculations seems to be due to erroneously filling in the numbers in Eq. 110, and not due to limitations of the thin double layer theory.

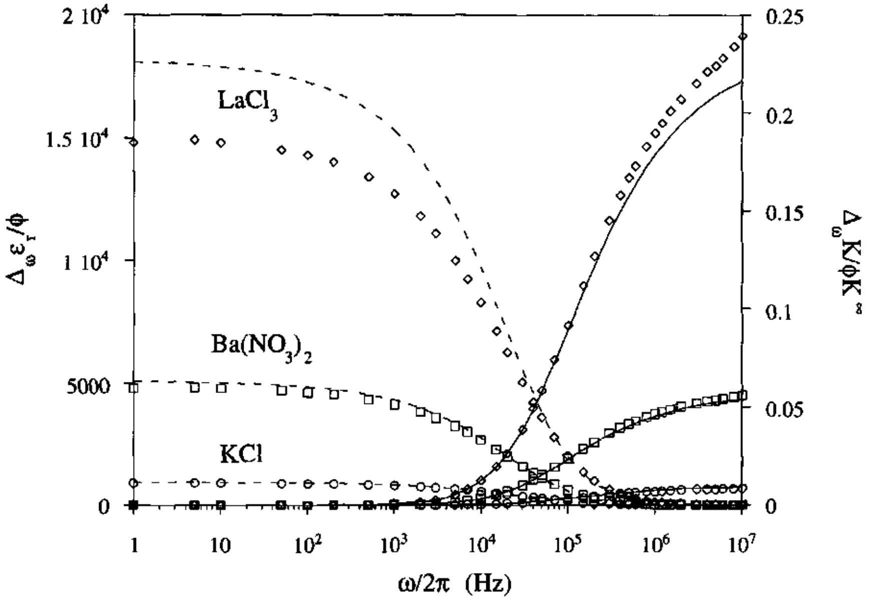

Figure 1. Conductivity increments (full curves) and dielectric permittivity increments (dashed curves) according to the analytical expressions [48], [49] and according to numerical calculations (indicated by symbols) for a particle with $a = 100$ nm, $\zeta = -50$ mV, $\Theta_2 = 0$ in KCl (○), $Ba(NO_3)_2$ (□), $LaCl_3$ (◇).

In Fig. 1 we show a comparison of the approximate formulas [48] and [49], indicated by the full and dashed curves, with the numerical solutions of the exact electrokinetic equations (2,3). The Du_2 values are calculated according to Eq. [37] with $\Theta_2 = 0$ and $\zeta = -50$ mV for relatively thin double layers ($\kappa a = 50$). The agreement is good for the symmetrical electrolyte KCl and the asymmetrical electrolyte with divalent counterions $Ba(NO_3)_2$ and still reasonable for the asymmetrical electrolyte with trivalent counterions $LaCl_3$.

The static conductivity increments and some pertinent parameters are shown in Tab. 1. The numerical static conductivity increments $(K^{num}_{\omega\tau<<1} - K^{\infty})/\phi K^{\infty}$ (2,3) agree well with the approximated increments $(K_{\omega\tau<<1} - K^{\infty})/\phi K^{\infty}$ from this study. The values of h for these electrolytes are close to zero and consequently $1 - h^2$ is even more close to unity, as shown in Table 1. This means that the effects of asymmetry of the electrolytes are only shown (via κ and Du_2) in the magnitude of the dispersion curves in the examples $Ba(NO_3)_2$ and $LaCl_3$. For HCl however, h=0.64 and the increments should have been affected significantly by the large difference in ion mobilities. The shapes of the dispersion curves will remain virtually unaffected as long as $Du_2 << 1$. However, for higher Du_2, the term involving h in the denominator of the frequency conductivity increment (Eq. [48]) will be significantly affected, resulting in a change of the shape of the curve.

Table 1. Summary of the most relevant parameters and the static conductivity increments, calculated numerically and via expression [46].

	Du_2	h	$1-h^2$	$\tau\,(10^{-6}\text{s})$	$\frac{K^{num}_{\omega\tau<<1}-K^{\infty}}{\phi K^{\infty}}$	$\frac{K_{\omega\tau<<1}-K^{\infty}}{\phi K^{\infty}}$
KCl	0.102	-0.019	0.9996	2.600	-1.380	-1.296
$Ba(NO_3)_2$	0.274	-0.058	0.9967	3.589	-1.095	-1.044
$LaCl_3$	0.683	-0.046	0.9979	4.008	-0.6421	-0.6284

3. EXPERIMENTAL METHODS

Monodisperse polystyrene latex was made using the procedure of Goodwin et al. (30) with $K_2S_2O_8$ as the initiator. The sulphate latex was cleaned by steam-stripping and brought in the H^+-form by ion exchange (1). From dynamic light scattering a particle radius of 400 nm was obtained. By the Single Particle Optical Sizer (31) less than 1% of the particles was found in doublets. The polydispersity ratio $\bar{a}_w/\bar{a}_n$ from E.M. photographs is usually less than 1.005 for particles made via this procedure. The particle volume fraction ϕ of latex was obtained from the dry mass fractions, using a particle density of 1.05 g/cm^3 (32). Conductometric titrations were performed to determine the surface charge density (1). From these it is concluded that strong acidic sulphate groups are covering the surface. The surface charge density is $\sigma^0 = -6.4\ \mu\text{C/cm}^2$.

The dielectric and conductivity spectra were determined in the frequency range 90 Hz-500 kHz using the four-electrode dielectric spectrometer of Kijlstra et al. (33). The four-electrode technique suppresses complications due to electrode polarization. The time needed for a complete frequency scan is less than 20 seconds. The cell can be filled alternatingly with suspension and a blank electrolyte solution as a reference. The temperature of the cell and storage bottles was maintained at 25.00 ± 0.05 °C by a temperature-controlled air stream. For more details concerning the apparatus we refer to Ref. (33).

The latex stock dispersion, 10% by volume, was changed into the K^+-form by titration with a 0.01 M KOH solution to the equivalence point. The dispersion was diluted with a KCl solution to a volume fraction of $\phi = 0.040$ and a (bulk) electrolyte concentration of 0.4 mM. Low-frequency dielectric measurements were performed in the electrolyte concentration range 0.4-6 mM. Before each experiment the ionic strength was increased to the new value by adding small amounts of 0.01 or 0.1 M KCl solution to the dispersion. Double layers are relatively thin in this concentration range ($26 \le \kappa a \le 102$) so that interpretation according to this theory is allowed. In 6 mM, ϕ has reduced to $\phi = 0.036$.

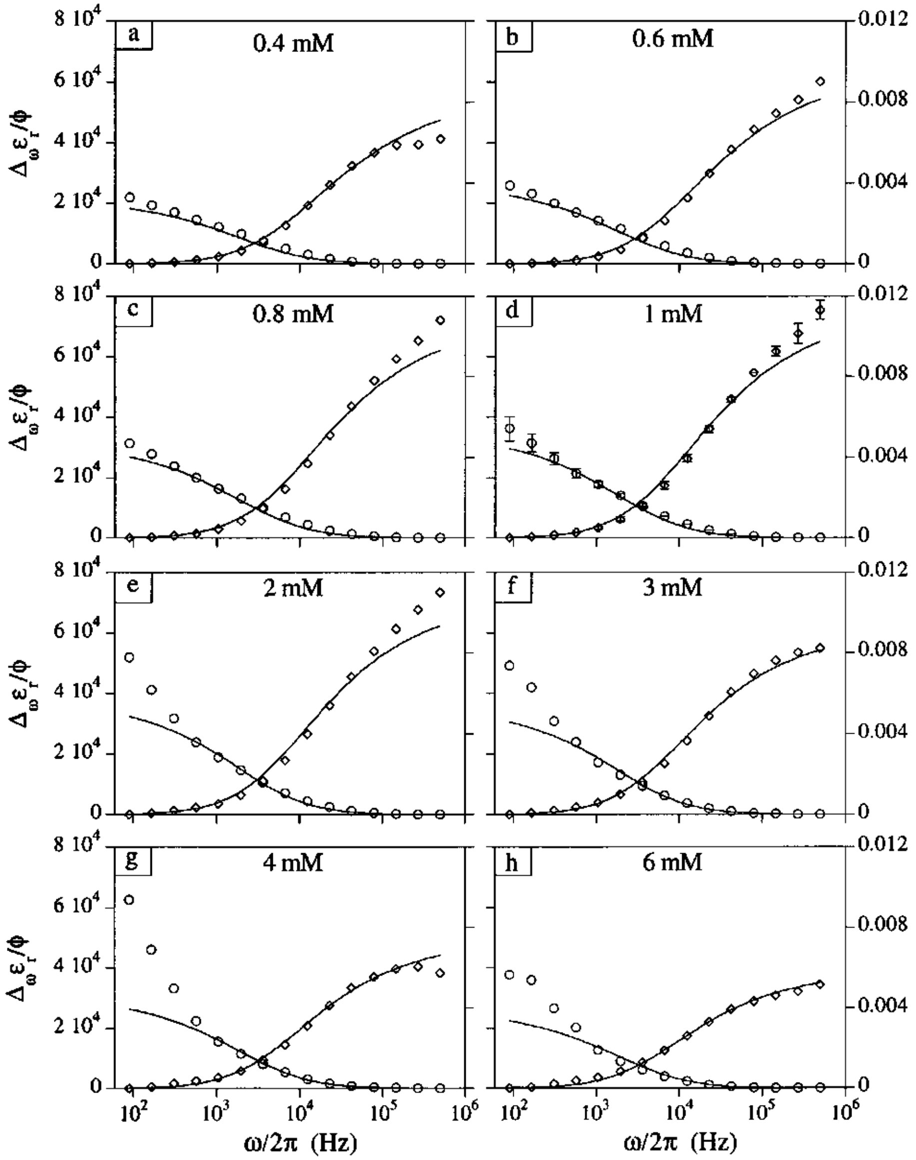

Figure 2a-h. Dielectric permittivity and conductivity increments in suspending KCl of different ionic strengths (indicated). Experimental permittivity and conductivity increments are given by the symbols (O) and (◇), respectively. Theory is depicted by full curves.

4. RESULTS AND DISCUSSION

Figures 2a-h show the normalized dielectric permittivity and conductivity increments for the different ionic strengths. The measurements are indicated by symbols. From the theoretical expressions [48] and [49] it is seen that only one adjustable parameter should suffice to explain the experiments, i.e., the relative surface conductivity Du_2. Values for Du_2 were obtained from the conductivity increment data by a least-squares fit. Theoretical results are shown by the solid lines in the figures 2a-h. Since deviations from the experimental data occurred at frequencies above 10^5 Hz, these were left out of the fitting procedure. The theoretical permittivity increments were calculated from the Du_2-values and are indicated by solid lines in the same figures. The measured permittivity increments are well explained with these Du_2-values for frequencies $\omega / 2\pi > 500$ Hz. Hence, Du_2-values calculated directly from the permittivity spectra ($\omega / 2\pi > 500$ Hz) will not differ much from these. Systematically too high increments are observed below 500 Hz.

To investigate the linear dependence on the volume fraction, we repeated the measurements in 1 mM KCl for a $\phi = 0.04$ and $\phi = 0.02$ dispersion. The differences in the normalised increments are indicated by error bars in Fig. 2d. The linearity with ϕ is indeed observed. At low frequency the out-of-phase currents decrease as $\propto \omega$ while the in-phase currents attain the limiting dc value. This results in a decreasing signal-to-noise ratio with frequency ($\propto \omega$) and relatively larger random errors in the permittivity increments at lower frequencies. However, inspection of the permittivity increments at frequencies $\omega / 2\pi \leq 500$ Hz shows a systematic deviation from theory, increasing with electrolyte concentration. The nature of this discrepancy is unknown.

In Fig. 3 we present Du_2 and K_2^σ versus the electrolyte concentration. No significant trend in K_2^σ is observed. The surface conductivity is found to be constant over the complete electrolyte concentration range. On the average, $K_2^\sigma = 0.57 \cdot 10^{-8}$ S. With this constant K_2^σ, the experimental Du_2 values are well explained as shown by the full curve. From Eq. [36], K_2^σ is restricted to $0.49 \cdot 10^{-8} \leq K_2^\sigma \leq 0.73 \cdot 10^{-8}$ S ($3m_2/z_2^2 = 0.53$ for K^+ as counterion). The experimentally found surface conductivity is within this range.

While with increasing electrolyte concentration Du_2 decreases by more than one order of magnitude, $\Delta_\omega \varepsilon_r / \phi$ and $\Delta_\omega K / \phi$ show a small increase followed by a small decrease. This non-monotonic behaviour is characteristic for a surface with constant K_2^σ. From Eq. [49] it follows that $\Delta_\omega \varepsilon_r / \phi \propto c$ for small electrolyte concentration c and that $\Delta_\omega \varepsilon_r / \phi \propto c^{-1}$ as $c \to \infty$ (note that $(\kappa a)^2 \propto c$ and $Du_2 \propto c^{-1}$). Hence, $\Delta_\omega \varepsilon_r / \phi$ as function of c should show a maximum. This maximum occurs at the electrolyte concentration for which $Du_2 = 1$. For the conductivity increments, the situation is slightly different. Du_2 appears in the denominator of the frequency-dependent part in Eq. [48]. Hence, the value of c where the maximum in $\Delta_\omega K / \phi$ appears depends on the frequency. At relatively low frequencies ($\omega\tau << 1$), $\Delta_\omega K / \phi$ attains its maximum at that concentration where $Du_2 = 1$. At relatively high frequencies ($\omega\tau >> 1$) it

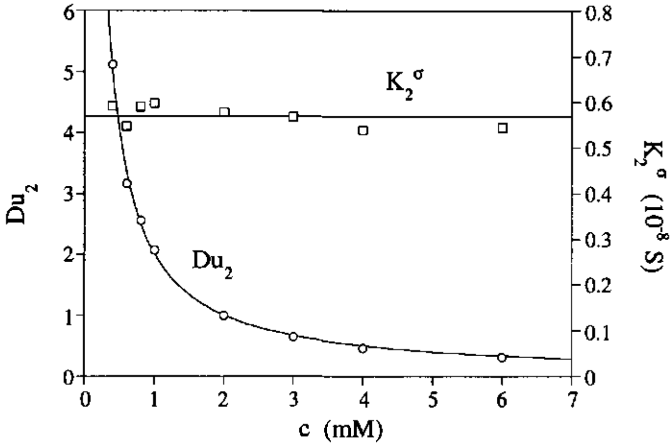

Figure 3. Relative surface conductivity Du_2 (O) and absolute surface conductivity K_2^σ (□) as functions of the ionic strength of suspending KCl. The full curves are based on the average surface conductivity $K_2^\sigma = 0.57 \cdot 10^{-8}$ S.

appears at the concentration c where $Du_2 = \sqrt{2/(1+h)} \approx 1.4$. To demonstrate this, we have plotted in Fig. 4 the asymptotic conductivity increments

$$\Delta_\omega K(\phi, \omega\tau >> 1)/\phi = K^\infty \frac{9}{8}(1-h^2)\left(\frac{Du_2}{1+Du_2}\right)^2 \frac{1+Du_2}{1+(1+h)Du_2/2} \qquad [50]$$

using the experimentally obtained Du_2, and Du_2 calculated from a constant surface conductivity $K_2^\sigma = 0.57 \cdot 10^{-8}$ S. As shown by this graph, the experimental maximum is well explained by the theory for particles with a nearly constant surface conductivity.

In a previous study (1) we have obtained the absolute surface conductivity from dc conductivity experiments on close-packed plugs composed of these latex particles in a number of indifferent electrolytes. In Fig. 5 we compare K_2^σ obtained from these plug conductivities with those from the LF dielectric experiments. The latter values for K_2^σ are only 10% lower than the values obtained independently from the plug conductivities in KCl. Hence, also from the LF dielectric spectroscopy experiments we may conclude that counterions in the double layer have a mobility close to the mobility in the bulk. We note that these data are complementary. LFDD experiments could not be performed in KCl solutions beyond 6 mM due to a too high background conductivity. However, for high electrolyte concentrations conductivities can be accurately measured and interpreted in plug. On the other hand, the theories for the plug conductivity fail at low electrolyte concentrations due to double layer overlap (1).

From these combined results we draw the interesting conclusion that the absolute surface conductivity is constant (within 10%) over a relatively large concentration range 0.4-100 mM.

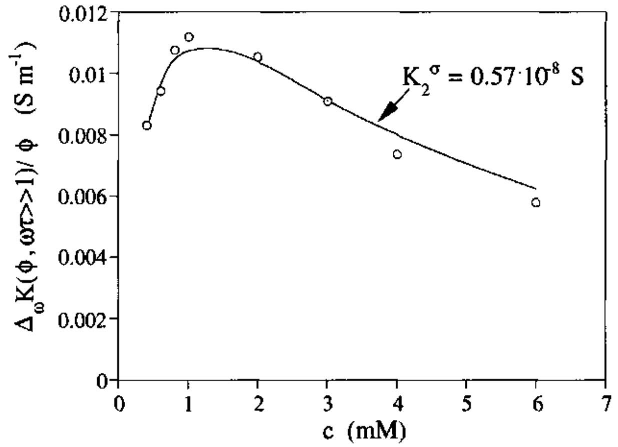

Figure 4. Asymptotic conductivity increment $\Delta_\omega K(\phi,\omega\tau >> 1)/\phi$ obtained from experiments (○) and according to theory with $K_2^\sigma = 0.57 \cdot 10^{-8}$ S (full curve) versus the ionic strength of suspending electrolyte KCl.

This result is not trivial. K_2^σ is constant if (i) not a significant part of the countercharge does move from behind to beyond the shear plane (or vice versa) and (ii) the average ion mobility in the double layer remains constant upon a change in the ionic strength (see also Ref. (1)). The explanation for these behaviours can be given by the Poisson-Boltzmann equation for a purely diffuse double layer in the situation of relatively high potentials ($|e\psi / kT| >> 1$). As shown in Ref. (1) the ζ-potential in a 100 mM KCl solution is −50 mV and higher (absolutely) for lower *c*. The potentials behind the shear plane exceed ζ. A consequence of the Gouy-Chapman double layer model is the *insensitivity* of the distribution of counterions in the high potential regime to a change in the bulk ion density. This means that, if the position of the shear plane is unaltered by the concentration change, also the amount of charge beyond and behind the slip plane stays unaltered. Furthermore, the counterions which *dominate* the surface conductivity are situated in the high potential regime of the electric double layer behind the slip plane, close to the surface. Since the ion distribution is unaltered the average ion mobility remains constant. We note that even if the distribution would be altered by some extend, its effect on the surface conductivity is negligible small since the ions within the double layer have the bulk mobility and are not significantly obstructed by the hairy surface. In the situation where ions in the double layer have a significant lower mobility than in the bulk, a change in the counterion distribution will have effect on the surface conductivity.

Springer et al. (34,35) and Dunstan (10) previously performed LF dielectric response measurements on dispersions of constant-charge sulphate latex. Springer et al. observed dielectric increments exceeding the theoretical maximum. Furthermore, their permittivity

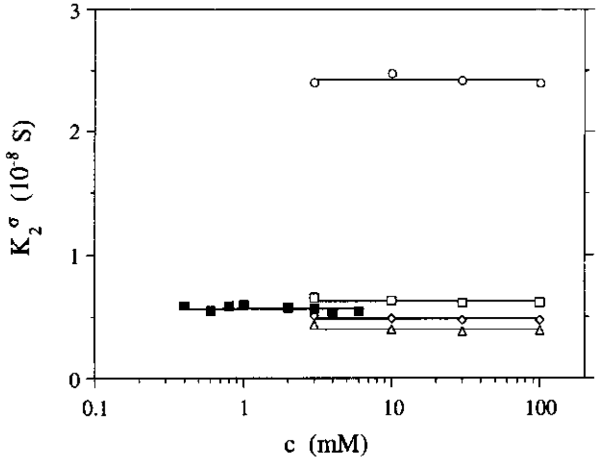

Figure 5. Absolute surface conductivity K_2^σ obtained from plug conductivities in HCl (○), KCl (□), NaCl (◇), LiCl (△), and obtained from the LF dielectric response in KCl (■).

increments increased with increasing KCl concentration. Based on their particle characteristics, $a = 222$ nm and $\sigma^0 = -1.61\ \mu\text{C/cm}^2$, and the assumptions $u_i = u_i^\infty$ and $0 \leq \Theta_2 \leq \infty$, a maximum may be expected in the range $0.8 \leq c \leq 1.2$ mM. They measured till the concentration 1.5 mM without finding a maximum. As indicated by the trend in their data, this maximum could have been found in higher electrolyte concentrations. These anomalies are serious and not resolved easily within the present theory without fundamental changes.

Dunstan (10) compared the permittivity and conductivity increments of latex dispersions, ($a = 300$ nm, $\sigma^0 = -1.2\ \mu\text{C/cm}^2$, suspended in KCl) with the spectra calculated via the "standard" theory using ζ-potentials obtained from mobility experiments by application of the "standard" theory. The experimental increments exceed the calculated ones by far due to the neglect of conduction behind the shear plane. By estimating Du_2 (from a and σ^0) we have calculated increments much closer to the experimental values in 1 mM KCl as well as in 0.1 mM KCl.

5. CONCLUSIONS AND PERSPECTIVES

Our analytical thin double layer expressions for the complex conductivity derived in (13,36) and applied to bacterial cell suspensions in (15) were extended to cope with asymmetrical electrolytes. Comparison with numerical calculations shows a good agreement. We were able to apply the thin double layer theory successfully to experiments on home-made constant-charge polystyrene latex dispersions. The observed permittivity and conductivity increments could be explained well with one constant absolute surface conductivity K_2^σ in the electrolyte concentration range 0.4-6 mM.

From the combination of LF dielectric experiments and complementary plug conductivities we concluded that the surface conductivity K_2^σ is constant (within 10%) over the large electrolyte concentration range 0.4-100 mM. It appears that K_2^σ correlates well with the surface charge density obtained from conductometric titration data. On the other hand, the electrokinetic charge obtained via ζ-potentials in (1) is much smaller than σ^0, especially at lower electrolyte concentrations. Hence, ions behind the shear plane must have a mobility not significantly smaller than their bulk value. For the particles under consideration it is more appropriate to compare conductivities directly with σ^0 instead of with electrokinetic charge obtained from mobilities or streaming potentials. In some studies the conduction behind the plane of shear is designated as "anomalous surface conduction". In this study the ζ-potential turns out to be more "anomalous" than the surface conductivity.

ACKNOWLEDGEMENT

We would like to thank Dr. Christine Mangelsdorf of the Department of Applied Mathematics at the University of Melbourne for making available the numerical results.

REFERENCES

(1) Minor, M., Linde, A. J. van der, Lyklema, J., submitted to *J. Colloid Interface Sci.* (chapter 2 of this thesis).

(2) Mangelsdorf, C. S., White, L. R., submitted to *J. Chem. Soc. Faraday Trans.*

(3) Mangelsdorf, C. S., White, L. R., *J. Chem. Soc. Faraday Trans.* **88,** 3567 (1992).

(4) O'Brien, R. W., *J. Colloid Interface Sci.* **81,** 234 (1980).

(5) Put, A. G. van der, Bijsterbosch, B. H., *J. Colloid Interface Sci.* **75,** 512 (1980).

(6) O'Brien, R. W., Perrins, W. T., *J. Colloid Interface Sci.* **99,** 20 (1984).

(7) Myers, D. F., Saville, D. A., *J. Colloid Interface Sci.* **131,** 448 (1989).

(8) Rosen, L. A., Saville, D. A., *Langmuir* **7,** 36 (1991).

(9) Rosen, L. A., Saville, D. A., *J. Colloid and Interface Sci.* **149,** 542 (1992).

(10) Dunstan, D. E., *J. Chem. Soc. Faraday Trans.* **89,** 521 (1993).

(11) Kijlstra, J., Leeuwen, H. P. van, Lyklema, J., *Langmuir* **9,** 1625 (1993).

(12) Rosen, L. A., Baygents, J. C., Saville, D. A., *J. Chem. Phys* **98,** 4183 (1993).

(13) Lyklema, J., "Fundamentals of Interface and Colloid Science. Solid-Liquid Interfaces", Vol. II, Academic Press, London, 1995.

(14) Wal, A. van der, Minor, M., Norde, W., Zehnder, A. J. B., Lyklema, J., *Langmuir* **13,** 165 (1997).

(15) Wal, A. van der, Minor, M., Norde, W., Zehnder, A. J. B., Lyklema, J., *J. Colloid Interface Sci.* **186,** 71 (1997).

(16) Rosen, L. A., Saville, D. A., *J. Colloid Interface Sci.* **140,** 82 (1990).

(17) Dukhin, S. S., Shilov, V. N., "Dielectric Phenomena and the Double Layer in Disperse Systems and Polyelectrolytes", Wiley, New York, 1974.

(18) Fixman, M., *J. Chem. Phys.* **72,** 5177 (1980).

(19) Fixman, M., *J. Chem. Phys.* **78,** 1483 (1983).

(20) Hinch, E. J., Sherwood, J. D., Chew, W. C., Sen, P. N., *J. Chem. Soc., Faraday Trans. 2* **80,** 535 (1984).

(21) DeLacey, E. H. B., White, L. R., *J. Chem. Soc., Faraday Trans. 2* **77,** 2007 (1981).

(22) Teubner, M., *J. Colloid Interface Sci.* **92,** 284 (1983).

(23) Hunter, R. J., "Foundations of Colloid Science", Vol II, Oxford University Press, New York, 1989.

(24) Minor, M., Leeuwen, H. P. van, Lyklema, J., submitted to *J. Chem. Soc. Faraday Trans.* (chapter 7 of this thesis).

(25) Kijlstra, J., Leeuwen, H. P. van, Lyklema, J., *J. Chem. Soc., Faraday Trans. 2* **88,** 3441 (1992).

(26) Lyklema, J., Minor, M., *Colloids Surfaces A* , in press.

(27) Midmore, B. R., Diggins, D., Hunter, R. J., *J. Colloid Interface Sci.* **129,** 153 (1989).

(28) O'Brien, R. W., *J. Colloid Interface Sci.* **92,** 204 (1983).

(29) Dukhin, S. S., *Adv. Colloid Interface Sci.* **44,** 1 (1993).

(30) Goodwin, J. W., Hearn, J., Ho, C. C., Ottewill, R. H., *Colloid and Polymer Sci.* **252,** 464 (1974).

(31) Pelssers, E. G. M., Ph. D. Thesis, Wageningen Agricultural University, 1988.

(32) Norde, W., Ph. D. Thesis, Wageningen Agricultural University, 1976.

(33) Kijlstra, J., Wegh, R. A. J., Leeuwen, H. P. van, *J. Electroanal. Chem.* **366,** 37 (1994).

(34) Springer, M. M., Ph. D. Thesis, Wageningen Agricultural University, 1979.

(35) Springer, M. M., Korteweg, A., Lyklema, J., *J. Electroanal. Chem.* **153,** 55 (1989).

(36) Minor, M., Wal, A. van der, Lyklema, J., *in* "Fine Particles Science and Technology", (E. Pelizzetti, Ed.), 225, Kluwer Academic Publishers, 1996.

Chapter 4

LOW-FREQUENCY DIELECTRIC RESPONSE, STATIC CONDUCTIVITIES, AND STREAMING POTENTIALS OF POLYMER-COATED LATEX DISPERSIONS AND POROUS PLUGS[1]

ABSTRACT. The low-frequency permittivity and conductivity increments, and the static conductivity of well-characterised latex dispersions and plugs have been measured over a wide range of ionic strengths. We have investigated the effects of adsorption of the neutral polymer poly(ethylene) oxide on these electrokinetic phenomena. It is shown that the counterion mobility in the double layer is significantly reduced by adsorbed polymer. A model is developed to describe the retarded motion of ions in the gel-like polymer layer, which is considered as a Brinkman fluid. The required ionic and polymer distribution functions are obtained from a self-consistent-field model.

Furthermore, ζ-potentials were inferred from streaming potentials of close-packed latex plugs. Since a significant part of the conduction is due to ions behind the shear plane, is was necessary to make use of the plug conductivity data in obtaining the correct ζ-potentials, especially at low ionic strengths. The ζ-potentials of the polymer-coated surface are lower than those of the bare surface which indicates the shear plane to be shifted outwards. The reduction in counterion mobility and the shift of the shear plane is also shown by the plug conductivity data.

---

[1] Submitted for publication in *Langmuir* in coauthorship with Leeuwen, H. P. van, Lyklema, J.

1. INTRODUCTION

The electrokinetic potential is one of the most common characteristics of charged surfaces. Electrokinetic potentials are not directly experimentally accessible but must be inferred from experiments with the help of some electrokinetic model. A popular model is the so called "standard electrokinetic model" which characterizes the interface by a shear plane at which the potential is ζ. Ions behind this plane are considered to be immobile. Application of this model generally shows that ζ-potentials inferred from conductivity experiments are systematically larger than ζ-potentials from particle mobility experiments or streaming potentials of plugs composed of these particles (1-12). The cause of this inconsistency is found in the neglect of conduction behind the shear plane.

In our previous studies, the interface of constant-charge polystyrene sulphate latex was thoroughly investigated (12,13) by means of conductometric titrations, low-frequency dielectric dispersion, streaming potentials and dc conductivities measured for close-packed porous plugs composed of these latex particles. These experiments showed that ions behind the shear plane are highly mobile. The mobility of counterions within the stagnant layer is usually not much lower than the mobility in the bulk (14,12,13).

For these "non-ideal" surfaces at least two electrokinetic parameters are needed to characterise the surface, i.e., the ζ-potential and the surface conductivity. It is likely that these characteristics are related to the surface roughness, the surface porosity, the viscoelectric effect (9), the presence of a Stern layer or the presence of a macromolecular, so called hairy surface layer. An option to study the latter influence is by adsorption of neutral polymers onto the surface. Since the bare sulphate latex surface was well characterised previously (12,13), we have used these latex particles to study the effect of adsorption of the polymer poly(ethhylene) oxide (PEO) on a variety of electrokinetic phenomena. For PEO adsorbed on latex, we measured the low-frequency (LF) dielectric permittivity and conductivity of dilute dispersions. Close-packed porous plugs were composed from the polymer-coated latex particles and the static conductivities and streaming potentials were measured.

Outline of the paper. Before describing the electrokinetic experiments, a simple model for retarded motion of counterions through adsorbed polymer films is presented. In this model the local ion mobility depends on the local polymer volume fraction. Self-consistent-field models (15-17), used for the determination of the polymer volume fraction profile and counterion profile, are discussed. An integral expression relating the surface conductivity to these profiles is given. In the experimental section the characteristics of the PEO and the polystyrene sulphate latex are given followed by section 4 in which the results are presented and discussed.

2. THEORY

2.1. Plug conductivity

O'Brien and Perrins (2) found that for a plug, composed of close-packed monodisperse spheres with relatively thin double layers ($\kappa a >> 1$) in a symmetrical electrolyte, the conductivity K^* is related to the relative surface conductivity parameter Du_2 according to:

$$\frac{K^*}{K^\infty} = 1 + 3\phi\left[f(0) + \frac{e^2 z_2^2 n_2^\infty / f_2^\infty}{K^\infty}\left(f(Du_2) - f(0)\right)\right] \tag{1}$$

where ϕ is the particle volume fraction, ez_i is the i-type ion charge, f_i is the ion friction constant and n_i^∞ the equilibrium number density beyond the electric double layer. Values beyond the double layer are indicated with the superscript "∞". The subscript i=1 refers to the co-ion, i=2 to the counterion. In this theory only the surface conduction due to the excess of counterions in the double layer is taken into account. The (negative) contribution due to the exclusion of co-ions is considered to be negligible. K^∞ is the electric conductivity of the equilibrium electrolyte beyond the double layer:

$$K^\infty = \sum_{i=1}^{i=2} K_i^\infty, \quad K_i^\infty = e^2 z_i^2 n_i^\infty / f_i^\infty \tag{2}$$

and $f(Du_2)$ is a function of Du_2 and the type of lattice, tabulated by O'Brien and Perrins (2). Du_2 is related to the absolute surface conductivity K_2^σ via:

$$Du_2 = \frac{K_2^\sigma}{aK_2^\infty} \tag{3}$$

where a is the particle radius. For a purely diffuse double layer the surface conductivity K_2^σ can be related to the excess of counterions in the double layer (or the ζ-potential) and the ion mobility in the double layer straightforwardly (2). The expressions [1]-[3] stay valid for the description of the plug conductivity in terms of the surface conductivity when the surface is more complex, e.g., in the situation of polymer adsorption. Then the question arises how to relate surface conduction to the characteristics of the coated surface. The most simple way to model this is by means of a slip plane located at a certain distance from the surface. We allow the ions behind this shear plane to be mobile with mobility u_i^i and assume that ions move according to their bulk mobility beyond the shear plane. Then we can write (12,13):

$$K_2^\sigma = \tilde{u}_2^i \sigma_2^i + \left(1 + 3m_2/z_2^2\right)\tilde{u}_2^\infty \sigma_2^d \tag{4}$$

where σ_i^i and σ_i^d are the (surface) densities of charge behind and beyond the shear plane, respectively, $\tilde{u}_i^i$ and $\tilde{u}_i^\infty$ are the ion mobilities behind and beyond the shear plane including their sign: $\tilde{u}_i = z_i e / f_i$, $u_i = |\tilde{u}_i|$. We have assumed that the ions move according to their bulk mobility beyond the shear plane. m_i is the dimensionless ionic drag coefficient: $m_i = 2\varepsilon kTf_i^\infty / 3\eta e^2$

where ε is the liquid dielectric permittivity, k is the Boltzmann constant, T is the temperature, and η the liquid viscosity. K_2^σ and Du_2 can also be related to the ζ-potential(18,2):

$$Du_2 = \frac{2}{\kappa a}\left(1 + \frac{3m_2}{z_2^2} + \Theta_2\right)\left[\exp(-z_2 e\zeta/2kT) - 1\right] \qquad [5]$$

where $\Theta_i = \tilde{u}_i^i \sigma_i^i / \tilde{u}_i^\infty \sigma_i^d$ reflects the ratio between surface conduction behind and beyond the shear plane due to electromigration.

Equation [1] can be reduced to a more simple expression if Du_2 is small ($Du_2 \ll 1$) (12):

$$K^* = (1 + 3\phi f(0))K^\infty - \frac{6\phi f(0)}{a} K_2^\sigma \qquad [6]$$

In a plot of K^* versus K^∞, Eq. [6] describes a straight line when the surface conductivity K_2^σ does not change with the electrolyte concentration. The slope of the curve is determined by the particle volume fraction and (to a lesser extent) by the type of array. The intercept is proportional to the surface conductivity and to the total of particle surface area in the *close-packed* plug which scales with a^{-1}. This expression enables a fast analysis of plug conductivity data (14).

2.2. Streaming currents in plugs

The current density $\langle \vec{i}_s \rangle$ in the plug due to an imposed pressure gradient is known as the streaming current. O'Brien related $\langle \vec{i}_s \rangle$ to Du_2 and the ζ-potential for a close packed plug of monodisperse spherical particles (19):

$$\langle \vec{i}_s \rangle = -\frac{\varepsilon kT}{\eta e}\left(\frac{e\zeta}{kT}[1 + 3\phi f(0)] - \left[\frac{e\zeta}{kT} - \frac{2}{z_1}\ln 2\right] g(Du_2)\right)\langle -\vec{\nabla} p \rangle \qquad [7]$$

where p is the pressure and $g(Du_2)$ is a tabulated function of Du_2 and the type of lattice (19).

2.3. Low-frequency dielectric spectroscopy

In a previous study (13) we have formulated practical equations for the LF dielectric increment $\Delta_\omega \varepsilon_r$ and the LF conductivity increment $\Delta_\omega K$ of spherical particles with relatively thin double layers ($\kappa a \gg 1$), dispersed in a binary electrolyte:

$$\begin{aligned} \Delta_\omega \varepsilon_r(\phi,\omega) &\equiv \varepsilon_r(\phi,\omega) - \varepsilon_r(\phi,\omega_{ref,\varepsilon}) \\ &= \varepsilon_r^\infty \frac{9}{16}\phi(\kappa a)^2(1 - h^2)\left(\frac{Du_2}{1 + Du_2}\right)^2 \frac{1}{(1 + \sqrt{\omega\tau})(1 + \omega\tau)} \end{aligned} \qquad [8]$$

and

$$\begin{aligned} \Delta_\omega K(\phi,\omega) &\equiv K(\phi,\omega) - K(\phi,\omega_{ref,K}) \\ &= K^\infty \frac{9}{8}\phi(1 - h^2)\left(\frac{Du_2}{1 + Du_2}\right)^2 \frac{\omega\tau\sqrt{\omega\tau}}{(1 + \sqrt{\omega\tau})(1 + \omega\tau) - (1 - h)\frac{Du_2}{2 + 2Du_2}\omega\tau\sqrt{\omega\tau}} \end{aligned} \qquad [9]$$

where $\omega_{ref,\varepsilon}$ and $\omega_{ref,K}$ are reference frequencies much larger than τ^{-1} and much smaller than τ^{-1}, respectively. For a symmetrical electrolyte the Du_2's in these equations are simply given by Eq. [5], the relaxation time τ is given by $\tau = \overline{f^\infty} a^2 (2kT)^{-1}$ where $\overline{f^\infty} = (f_1^\infty + f_2^\infty)/2$ and $h = (z_2 / f_2^\infty + z_1 / f_1^\infty)/(z_2 / f_2^\infty - z_1 / f_1^\infty) = (\tilde{u}_2^\infty + \tilde{u}_1^\infty)/(\tilde{u}_2^\infty - \tilde{u}_1^\infty)$. For electrolytes like KCl for which $f_1^\infty \approx f_2^\infty = f^\infty$, $\tau \approx f^\infty a^2 (2kT)^{-1}$ and $h \approx 0$.

2.4. Ion movement through polymer gels

In the previous paragraphs we introduced conduction behind the shear plane. The question which will keep us busy in the following two paragraphs is how to relate the average counterion mobility to the characteristics of the polymer film. Retardation of motion of uncharged molecules and ions through neutral polymer gels has been studied intensively (20-22). These investigations form a good starting point for the description of retarded ionic motion through adsorbed polymer layers. The basic distinction between polymer gels and adsorbed polymer layers is the inhomogeneity in the polymer density. Whereas in polymer gels the polymer density is considered constant over macroscopic distances, the polymer density in adsorbed films may vary strongly over distances of the order of the double layer thickness. In the situation of incomplete surface coverage, lateral inhomogeneities must be considered as well since covered areas will alternate with uncovered ones. The latter inhomogeneities are hard to model. Therefore, we start with the (one-dimensional) situation of high coverage were only variations in polymer density normal to the surface are present.

Ions moving in the inner part of the diffuse double layer, where the polymer coil is more dense, will experience a larger drag than those moving in the outer part of double layer where the polymer volume fraction is lower. Hence, the relation between the local ion mobility and the local polymer density is wanted. The friction coefficient within polymer gels has been modelled in various ways. The simplest is to consider the gel as a Brinkman fluid (23). The Stokes ionic friction coefficient f_i of an ion with Stokes-radius a_i translating through a Brinkman fluid is related to the bulk friction coefficient f_i^∞ according to (24):

$$f_i^\infty / f_i = u_i / u_i^\infty = \left(1 + a_i / \sqrt{k_D} + \tfrac{1}{9} a_i^2 / k_D\right)^{-1} \qquad [10]$$

where k_D is the Darcy-permeability. A number of empirical relations between the Darcy-permeability and the polymer volume fractions ϕ_{pol} have been reported. We will use a relation derived by de Gennes (25) for entangled polymers which has only one adjustable parameter α:

$$k_D = \alpha \phi_{\text{pol}}^{-3/2} \qquad [11]$$

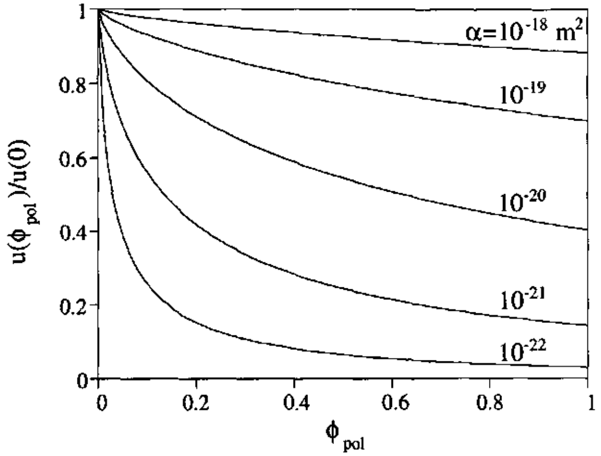

Figure 1. Relative ionic mobility $u(\phi_{\text{pol}})/u(0)$ of a potassium ion ($a = 0.13$ nm) as function of the polymer volume fraction ϕ_{pol} for values of the proportionality constant α between 10^{-22} and 10^{-18} m^2.

By way of illustration, we have plotted in Fig. 1 the relative ionic mobility as a function of the polymer volume fraction for some values of α, calculated according to Eqs. [10] and [11] for a K^+-ion ($a_i = 0.13$ nm). The ionic mobility decreases with ϕ_{pol}. We note that it might appear erroneous that $u_i \neq 0$ when $\phi_{pol} = 1$. However, since $\phi_{pol} = 1$ implies that the ion densities are zero, the contribution to conduction will be zero likewise. For the derivation of the surface conductivity K_2^σ we need to know the polymer distribution as well as the counterion distribution throughout the complete double layer. These can be obtained from a self-consistent-field lattice model as will be shown in the next paragraph.

The surface conductivity consists of an electromigration term and an electroosmotic term. The determination of the latter is straightforward in double layers with little detail, i.e., for the Gouy-Chapman (part of the) double layer situated in a region where the viscosity is constant (see Eq. [4]). In such a diffuse non-stagnant layer the minor contribution to the surface conductivity stems from electroosmosis, e.g., 30 % in suspending KCl and 5% in HCl. It is expected that the contribution to K_2^σ is even less for a coated surface since electroosmosis is commonly more retarded by polymers than electromigration is. In this respect we mention polymer gels which behave as highly viscous or even stagnant whereas self-diffusion of ions is hardly impaired. Therefore, we will only consider the polymers effect on the electromigrative term of the surface conductivity and neglect electroosmosis. We however note that, if α and, hence, k_D are known, it is possible to calculate the liquid flow profile inside the film. From this, the electroosmotic contribution to K_2^σ as well as, e.g., the electrophoretic mobility of this coated particle can be found (see Donath and Voigt (26,27)).

Following Fixman (28,29), the surface conductivity is an excess quantity:

$$K_2^\sigma = z_2 e \int_{dl} (n_{2,eq}\,\bar{u}_2 - n_2^\infty \bar{u}_2^\infty)dr \qquad [12]$$

where we have neglected electroosmosis. The subscript "eq" refers to equilibrium values (in absence of the electric field). The integration is performed over the double layer (*dl*). This expression can be approximated by:

$$K_2^\sigma = \int_{dl} \rho_{2,eq}\,\bar{u}_2 dr \qquad [13]$$

if the potentials in the double layers are not too low. Hence, the surface conductivity can be calculated according to this equation from the polymer and counterion distribution functions.

2.5. Self-consistent-field lattice modelling of homopolymers near a charged interface

Polymers at interfaces have been studied in great detail by Scheutjens and coworkers using a lattice-based numerical self-consistent-field technique (15-17). In cases where the polymer density profile is weakly varying in space it is possible to map the discrete equations onto a diffusion equation put forward by Edwards (30). Typically, a flat homogeneous surface is considered and density fluctuations parallel to the surface are ignored. In essence, one uses the analogy between the movement of a diffusing particle in the presence of the field, and the trajectory of a polymer chain in the field. Of interest are so-called chain-end distribution functions $G_i(z,s\,|\,1)$ which represent the combined statistical weight of all possible and allowed configurations for a chain fragment (of molecule *i*) of *s*–1 bonds with the end segment *s* at coordinate *z* and segment 1 being unrestricted in an external (dimensionless) potential field $U_i(z)$. The chain-end distribution functions are Green's functions that satisfy Edwards diffusion equation

$$\frac{\partial G_i(z,s\,|\,1)}{\partial s} = \left(\tfrac{1}{6}\nabla^2 - U_i(z)\right) G_i(z,s\,|\,1) \qquad [14]$$

or feature the corresponding recurrence relation given by Scheutjens and coworkers where *z* is a discrete variable indicating the dimensionless distance from the wall:

$$G_i(z,s\,|\,1) = e^{-U_i(z)}\left(\tfrac{1}{6}G_i(z-1,s-1\,|\,1) + \tfrac{4}{6}G_i(z,s-1\,|\,1) + \tfrac{1}{6}G_i(z+1,s-1\,|\,1)\right) \qquad [15]$$

A chain fragment of zero segments does not feel the potential field and therefore the natural condition $G_i(z,0\,|\,1) = 0$ applies. For chains with a degree of polymerisation N_i the corresponding complementary chain-end distribution functions $G_i(z,s\,|\,N_i)$ for chain fragments with $N_i - s$ bonds is found by a similar diffusion equation. The experimentally observable segment density profile for a segment *s* is found by the composition law:

$$\phi_i(z,s) = C_i \frac{G_i(z,s \mid 1) G_i(z,s \mid N)}{G_i(z)} \qquad [16]$$

where C_i is a normalization constant, which either conserves the number of segments in the system (canonical ensemble) or forces the density to become the bulk density if the potentials are zero (grand canonical ensemble). Obviously, the full density profile is found by summation over all the segments in the chain $\phi_{\text{pol}} = \overline{\phi}_i(z) = \sum_{s=1}^{N_i} \phi_i(z,s)$. For monomeric components (e.g. component m) Eq. [16] reduces to a Boltzmann equation:

$$\phi_m(z) = C_m G_m(z,1 \mid 1) = C_m e^{-U_m(z)} \qquad [17]$$

In our system there is a wall with fixed charges in contact with a solution containing ions and neutral homopolymer. As the thickness of the polymer film is small as compared to the particle radius the surface may be considered as flat. We choose to treat both the chain statistics and the electrostatics on the same footing within the discrete version of the SCF theory (i.e. in the Scheutjens-Fleer lattice version). In this approach all segments, solvent molecules, and ions can only be positioned on specified z-coordinates. This allows one to account for the finite size of the ions and facilitates the calculation of the electrostatic potential (31) (which needs to be done numerically anyway). The dimensionless potential felt at distance z from the surface by a segment of type x (e.g. a polymer segment, a solvent molecule, an ion), $U_x(z)$ is given by:

$$U_x(z) = U'(z) + \frac{e z_x \psi(z)}{kT} - \chi_x^{ads} \delta(1,z) \qquad [18]$$

where $\delta(1,z) = 1$ if $z = 1$ and 0 otherwise. The first term on the right-hand side is a Lagrange field coupled to the packing constraint $\sum_x \phi_x(z) = 1$, which implies the assumption of incompressibility ($\phi_x(z)$ is the fraction of layer z filled with segments of type x). The electrostatic term in the segment potential (ez_x is the charge of units of type x, $\psi(z)$ the local electrostatic potential and kT the thermal energy) is of course only operational for segments with non-zero charge. The last contribution to the right-hand-side of Eq. [18] accounts for the short-range specific adsorption energy of a segment of type x (only present in our case for the polymer units). $U_i(z)$ in Eqs. [14] and [15] is related to $U_x(z)$ according to $U_i(z,s) = \sum_x U_x(z) \delta_{i,s}^x$ where $\delta_{i,s}^x = 1$ if segment s of molecule i is of type x, and 0 otherwise.

The equations [15]-[18] are solved numerically (32) with the condition that the polymer chains, the solvent molecules and the ions can only sample the half-space $z > 0$. At $z = 0$ an impenetrable (charged) wall is positioned. The electrostatic potential (and also the $U_x(z)$) is taken zero for $z = \infty$.

3. EXPERIMENTAL METHODS

3.1. Latex characteristics

Monodisperse polystyrene sulphate latex was made according to the procedure of Goodwin et al. (33) with $K_2S_2O_8$ as the initiator. The preparation, cleaning and characterisation have been described previously (12). The latex is kept in the H^+-form. The particle radius is 400 nm. The surface charge density σ^0, obtained from conductometric titration, is $-6.4\ \mu C/cm^2$.

3.2. Low-frequency dielectric dispersion

Low-frequency permittivity and conductivity spectra were measured in the frequency range 90 Hz-500 kHz using the four-electrode spectrometer of Kijlstra et al. (34). A complete frequency sweep is performed in less than 20 s. The cell can be filled alternatingly with suspension and blank electrolyte solution as reference. The temperature of the cell is maintained at $25.00 \pm 0.05\ ^\circ C$.

Latex stock dispersion, 10% by volume, was changed into the K^+-form by titration with a 0.01 M KOH solution to the equivalence point. The dispersion was diluted by more than a factor of 2 with a PEO-solution ($\overline{M}_{PEO} = 2.3 \cdot 10^4$ g/mol, $\overline{M}_w / \overline{M}_n = 1.08$, Polymer laboratories LTD, U.K.). The total amount of PEO added per unit particle surface area present in the dispersion is 1 mg/m^2 which is well above the reported adsorption-plateau value of approximately 0.5 mg/m^2 (determined by Pelssers in Ref. (35) with $\overline{M}_{PEO} = 2 \cdot 10^4$ g/mol, $a = 348$ nm and $\sigma^0 = -4.7\ \mu C/cm^2$, which are close to our characteristics). Hence, half of the added PEO covers the particle surface fully, the other half is dissolved in the continuous phase. The ionic strength was adjusted to 0.4 mM KCl with a 0.01 M KCl solution. After these treatments the volume fraction latex has reduced to approximately 0.040. The suspension was stored overnight under continuous shaking. Dielectric experiments were performed as a function of the ionic strength in the span 0.4-6 mM KCl. Double layers are relatively thin in this range ($26 \le \kappa a \le 102$). Hence, interpretation according to the thin double layer theory is possible. Between the measurements the electrolyte concentration was increased to the new concentration by adding small amounts of 0.01 or 0.1 M KCl. Eventually, in 6 mM KCl, the particle volume fraction has reduced to 0.036.

Dielectric dispersion experiments were also performed in 1 mM KCl as a function of the amount of PEO added. For these, again an amount of the latex stock suspension was changed into the K^+-form and diluted with a KCl solution to a particle volume fraction of $\phi = 0.040$ and bulk electrolyte concentration of 1 mM KCl. PEO was dissolved in 1 mM KCl to obtain a 2.86 g/l PEO solution. Small amounts of this solution were added slowly to the dispersion under stirring prior to every dielectric experiment. The spectra were measured approximately 2 minutes after PEO addition. The added amount of PEO was varied between 0 and 2 mg/m^2 (equivalent). After the last PEO addition, ϕ has reduced to 0.031.

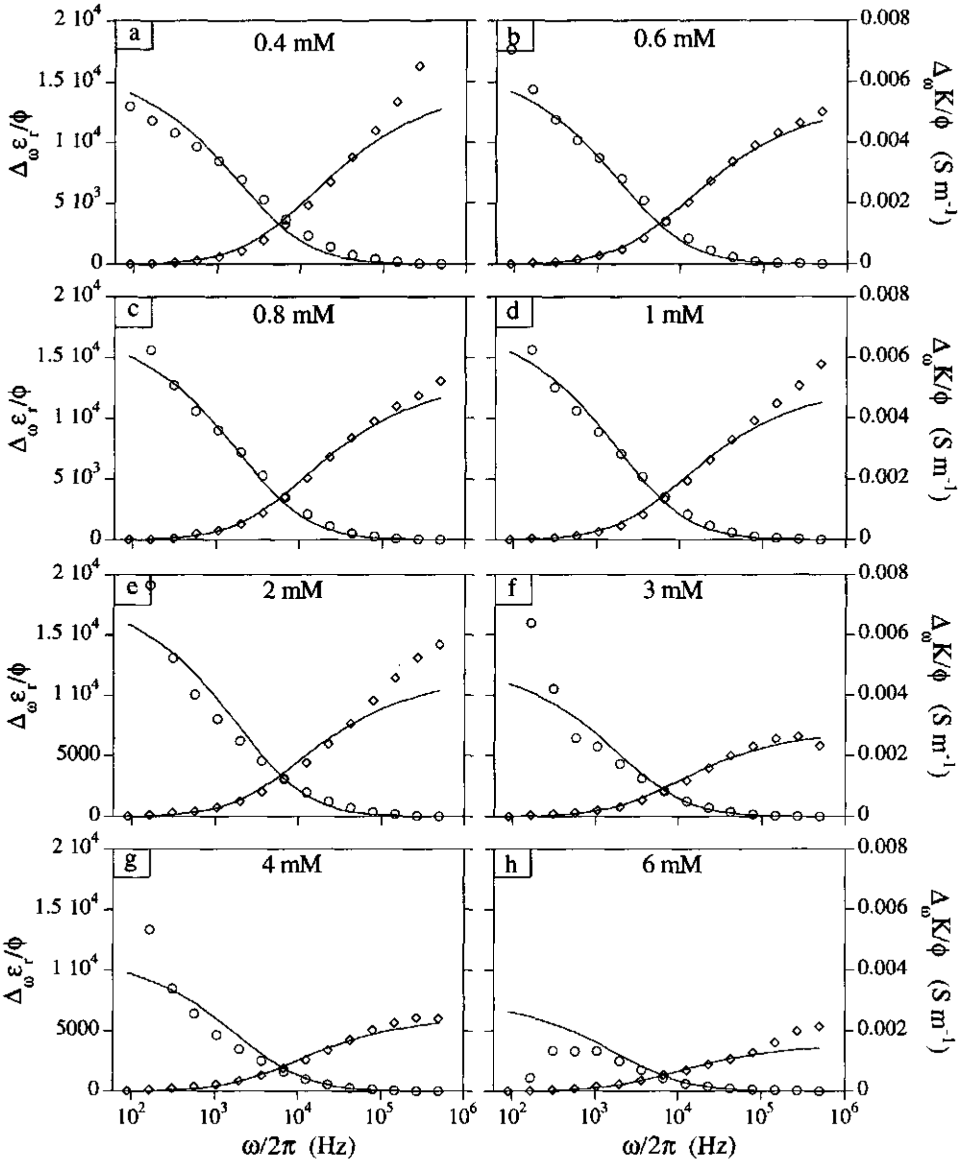

Figure 2a-h. Permittivity and conductivity increments of PEO-coated latex suspended in KCl of various ionic strengths (indicated). Experimental permittivity and conductivity increments are given by the symbols (○) and (◇), respectively. Theory is depicted by full curves.

3.3. Plug conductivity and streaming potentials

A PEO solution was added to an amount of the latex stock solution (1 mg/m^2 equivalent). The suspension was stored overnight under continuous shaking. A latex plug was made from this dispersion by centrifugation as described previously (12). The plug conductivity is measured with a commercial conductivity meter (Knick Konductometer 702). The streaming potential is determined with a home-made setup (36,12) in the concentration range 0.1-100 mM for four different counterions, i.e., in HCl, KCl, NaCl, and LiCl.

4. RESULTS AND DISCUSSION

Figures 2a-h show the normalized permittivity and conductivity increments of the PEO-coated suspension as a function of the KCl bulk ionic strength. Symbols indicate the experimental values. The spectra were interpreted according to the procedure described in a previous study (13). Values for Du_2 were obtained from the conductivity increment data via a least-squares fit. The theoretical results are depicted as solid lines. Since significant deviations also occurred for the coated particles above 10^5 Hz, these where not taken into account in the fitting procedure. Theoretical permittivity increments were calculated from Du_2-values and shown by the solid lines. Experimental permittivity increments are explained well with these Du_2's for frequencies

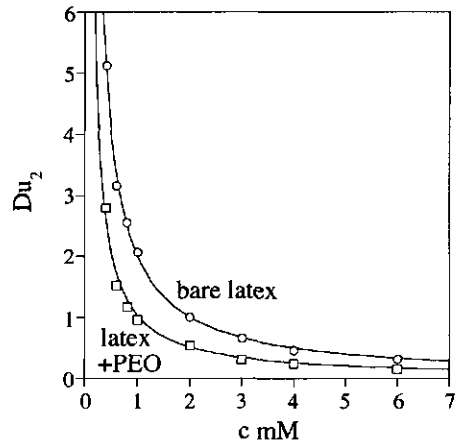

Figure 3. Relative surface conductivity Du_2 as a function of the ionic strength of suspending KCl for bare latex (O) and PEO-coated latex (□). The full curves are based on $K_2^{\sigma} = 0.57 \cdot 10^{-8}$ S and $K_2^{\sigma} = 0.28 \cdot 10^{-8}$ S for bare and coated latex, respectively.

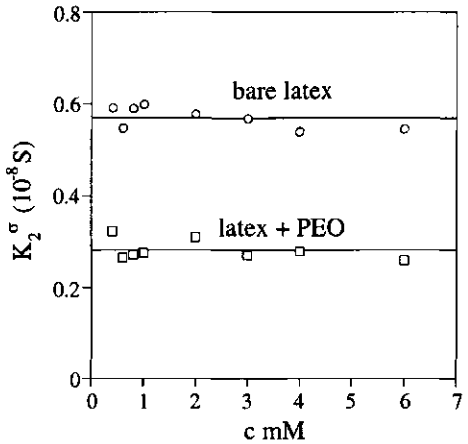

Figure 4. Absolute surface conductivity K_2^{σ} as a function of the ionic strength of suspending KCl for bare latex (O) and PEO-coated latex (□). The full curves are the average values: $K_2^{\sigma} = 0.57 \cdot 10^{-8}$ S and $K_2^{\sigma} = 0.28 \cdot 10^{-8}$ S for bare and coated latex, respectively.

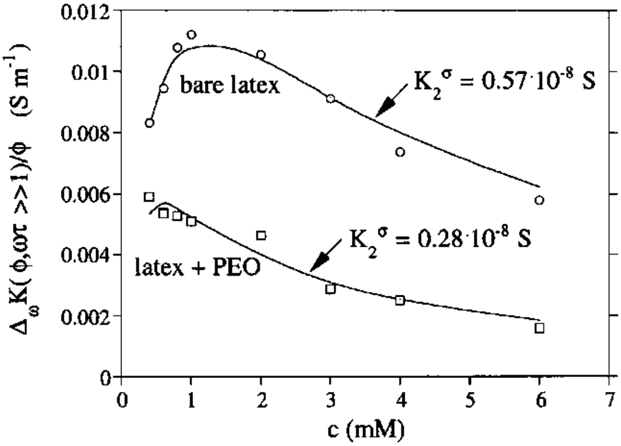

Figure 5. Asymptotic conductivity increment $\Delta_\omega K(\phi,\omega\tau >> 1)/\phi$ obtained from experiments (O) and according to theory with $K_2^\sigma = 0.57\cdot10^{-8}$ S and $K_2^\sigma = 0.28\cdot10^{-8}$ S (full curves) versus the ionic strength of the suspending electrolyte KCl.

above ≈ 500 Hz.

In Fig. 3 we present Du_2 against the bulk electrolyte concentration c. Bare-latex Du_2-values are included for comparison. The relative surface conductivity is reduced by the PEO-film. In Fig. 4 the absolute surface conductivity K_2^σ versus c is presented. As well as for the bare surface, K_2^σ is insensitive to the ionic strength. The origin for this, at first sight unexpected qualitative feature, can be found in the high potentials in the double layer and will be discussed later. The (average) surface conductivity of the coated surface is $K_2^\sigma = 0.28\cdot10^{-8}$ S which is approximately half the value of the bare surface for which $K_2^\sigma = 0.57\cdot10^{-8}$ S.

In Fig. 5 we have plotted the asymptotic conductivity increments

$$\Delta_\omega K(\phi,\omega\tau >> 1)/\phi = K^\infty \frac{9}{8}(1-h^2)\left(\frac{Du_2}{1+Du_2}\right)^2 \frac{1+Du_2}{1+(1+h)Du_2/2} \qquad [19]$$

using the experimentally obtained Du_2's, and the Du_2-values calculated from the constant surface conductivity $K_2^\sigma = 0.28\cdot10^{-8}$ S. Since the polymer film reduces the surface conductivity by a factor of two, the position of the maximum (13), located at c for which $Du_2 \approx 1.4$, shifts towards a concentration half of its original value and cannot be detected within the experimental error. The observed monotonous decrease is well described by theory for particles with a constant surface conductivity $K_2^\sigma = 0.28\cdot10^{-8}$ S. Bare-latex data (13) are also included.

In Fig. 6 the normalized permittivity and conductivity increments in 1 mM KCl solution as a function of the amount of added PEO per unit particle surface area are presented. A reduction in

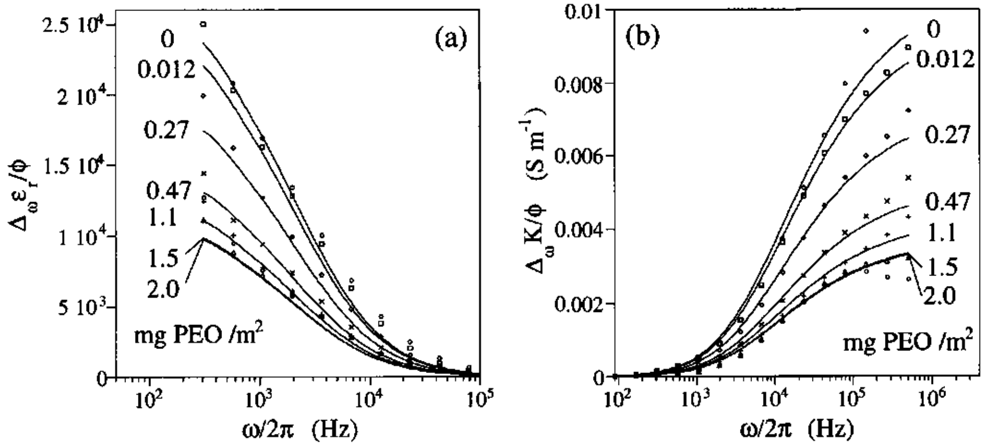

Figure 6. Permittivity (a) and conductivity increments (b) of latex dispersions in 1 mM KCl for various amounts of added PEO (indicated). Experimental increments are given by the symbols. Theory is depicted by full curves.

magnitude of the increments due to addition of PEO is observed. For clarity, not all measured spectra are included. From the conductivity spectra we obtained Du_2 by the method described before.

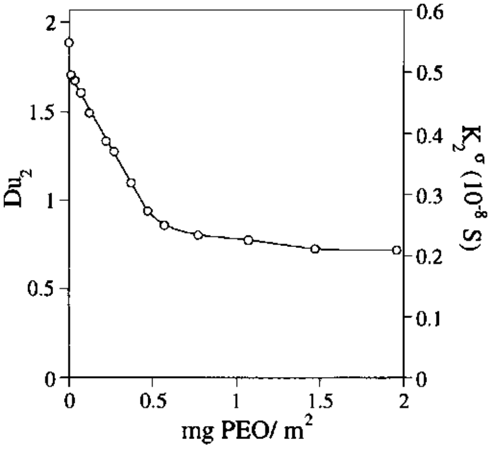

Figure 7. Du_2 and K_2^σ versus the added amount PEO for a latex dispersion in 1 mM KCl.

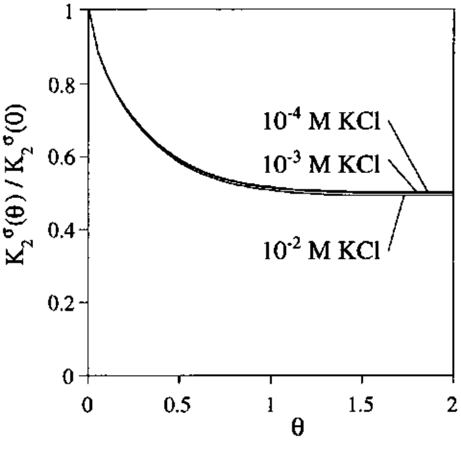

Figure 8. Surface conductivity $K_2^\sigma(\theta)$ relative to the value for the bare surface as a function of θ for three electrolyte concentrations (indicated).

In Fig. 7, Du_2 and K_2^σ are presented as a function of the amount of added PEO. A strong reduction of nearly 10% in K_2^σ is shown after the initial addition of just 0.012 mg/m^2 PEO. However, inspection of the spectra for 0 and 0.012 mg/m^2 added PEO shows that this reduction is due to the disappearance of the shoulder at higher frequencies. Till 20 kHz the spectra are nearly identical. Only above 20 kHz the spectra diverge strongly. Since the fits cover the frequency range till 50 kHz, the shoulder has some effect on the outcome for K_2^σ. The cause of the shoulder is unknown, but the initial reduction in K_2^σ does not seem to be real. After this probable artefact there is a regime where K_2^σ decreases linearly with the added amount of PEO. After addition of 0.5 mg/m^2 PEO we enter a second regime where K_2^σ is rather insensitive to further PEO-addition and K_2^σ only slightly decreases. Nearly all PEO added in excess of 0.5 mg/m^2 remains in the bulk solution and therefore has little effect on the surface conductivity. This is in line with the adsorption-plateau value found by Pelssers (35). The surface conductivity read from Fig. 7 at 1 mg/m^2 PEO should come to $K_2^\sigma = 0.28 \cdot 10^{-8}$ S as found in Fig. 4, but is a bit smaller. This little but significant difference might be caused by some slow steps in the adsorption of polymer. The latter experiments were performed on a dispersion with PEO which was shaken for more than 12 hours in contrast to the former experiments which were performed only minutes after PEO-addition.

The reduction in K_2^σ due to PEO adsorption can be explained by two mechanisms: (i) surface charge is expelled from the surface by the PEO polymer or (ii) counterion movement is hindered by PEO. Mechanism (i) is unlikely for this surface, since the charge is covalently bound to the polystyrene core. Retarded motion in uncharged gels has been observed in other studies and is the most likely. We have adopted a simple model based on a Brinkman fluid for the hairy surface layer.

The numerical self-consistent-field lattice theory is applied to a well-characterised system of polyethylene oxide (PEO) on polystyrene (PS) particles with a fixed surface charge density. The system is significantly idealised. (i) We have assumed that water is a very good solvent for PEO (the PEO-water χ parameter is set to zero). (ii) It is also assumed that the ions are ideal: all short-range excess interactions of the ions with the water, polymer, and surface are set to zero. (iii) The adsorption energy for the polymer was set to 1 kT per polymer-surface contact ($\chi^{\text{ads}} = 1$). This value is well above the critical adsorption energy (17) for the polymer-solvent system. Therefore we ensure that the polymers have a high affinity adsorption isotherm which is only very little influenced by the presence of the ions that compete for the surface sites. (iv) The surface charge was fixed to a value of 0.04 charges per lattice site. From the characteristic length of a lattice site of 0.3 nm, this value corresponds to a surface charge density of -7 μC/cm^2 which is close to the real surface charge density. (v) The number of repeating units in the PEO chain was set to $N = 1000$. (vi) The permittivity in each layer is found by a density average of the segment relative dielectric constants. We use $\varepsilon_{r,\text{water}} = \varepsilon_{r,\text{ions}} = 80$, $\varepsilon_{r,\text{EO}} = 5$ and

$\varepsilon_{r,\text{surface}} = 2$. (vii) As the film thickness is small as compared to the particle radius the surface may be treated as flat. Calculations were performed in a broad range of ionic strengths, i.e., 10^{-4}, 10^{-3}, and 10^{-2} M KCl. The surface conductivity is calculated according to Eq. [13] from the polymer and counterion distribution functions.

In Fig. 8 we have plotted the surface conductivity $K_2^{\sigma}(\theta)$ relative to the value for the bare surface as a function of θ. Here, θ represents the amount of polymer segments in the system (total of 100 layers) relative to the number of lattice adsorption positions on the surface. The proportionality constant α was set to 10^{-20} m^2 in order to give a reduction of approximately 50% in the surface conductivity for a fully covered surface ($\theta >> 1$) as was observed experimentally. Now, let us compare the results of these calculations with the experimentally observed reduction in the surface conductivity. These well-adsorbing polymers adsorb relatively flat until the first lattice layer is practically filled ($\theta \approx 1$) resulting in a decreasing surface conductivity till $\theta \approx 1$. Polymers added after $\theta \approx 1$ mainly remain in the bulk and, hence, have little effect on the surface conductivity. The two regimes observed in Fig. 7 are shown by theory, however not as distinct. The transformation is rather gradually. We however note that the theory is less applicable in the dilute regime $\theta < 1$ since the polymer density as well as the surface conductivity will then be heterogeneous (will fluctuate along the surface). The surface conductivity of polymer-covered surface is lower than that of the surrounding bare surface. Rigorously derivation of the electrokinetic equations to describe ionic transport along these inhomogeneous surfaces is cumbersome. Still, we can get some quantitative insight into this problem by an order analysis. Let us assume that the polymers adsorb rather dispersed (so not fully cover a part of the particle surface). The typical dimension of an adsorbed polymer molecule will be somewhat larger than in the bulk, but still of the same order of magnitude, say the radius of gyration. This dimension is typically much smaller than the particle radius *a*, but usually of the order of the double layer thickness. Due to a locally smaller conductivity, the field lines corresponding to the electrochemical potential will, to some extent, bend around the polymer. The lower the conductivity is in such a polymer patch, the stronger the field lines will try to avoid it. These perturbations in the field will not be noticeable anymore at a distance from the particle surface of a few times the typical dimension of the polymer molecule, which is still much smaller than a. Hence, in the used thin double layer theories only the boundary conditions for the far fields evaluated at the particle surface are affected (see also Ref. (13)). This means that the thin double layer theory (Eqs. [1], [6]-[9]) is also *applicable to such inhomogeneous surfaces*. The K_2^{σ} appearing in these equations is of course not related to surface characteristics according to Eqs. [4] and [5] but must be a (weighted) average of the surface conductivities of bare and covered surface. To obtain this relation it is sufficient to solve the electrokinetic equations for a flat inhomogeneous surface where a gradient in the electrochemical potential is applied sufficiently far from the surface (much further than the typical (largest) dimension of an adsorbed

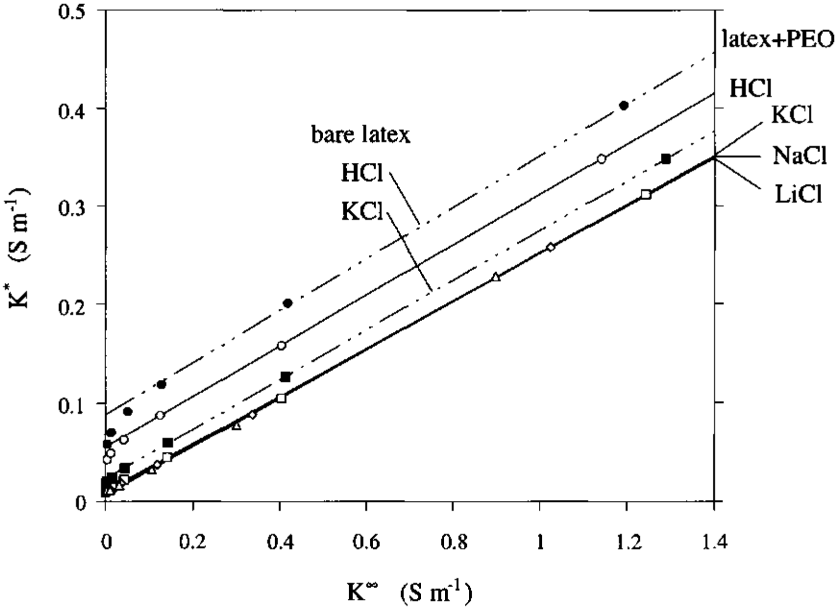

Figure 9. Conductivity of the coated plug as a function of the conductivity of the bulk for the electrolytes HCl (○), KCl (□), NaCl (◇) and LiCl (△). The straight lines are fits based on the data corresponding to the four highest electrolyte concentrations. Data for bare latex plugs in HCl (●) and KCl (■) are included.

polymer). This complex problem probably must be solved numerically, which is beyond the scope of this study. Local perturbations in the fields generated by the polymer patches do not overlap as long as the polymers are much further apart than their typical dimension. In this regime the decrease in K_2^σ must be linear with the added (= adsorbed) amount of PEO. For the conductivity of a suspension as a function of the particle volume fraction similar arguments hold, i.e., changes are linear in the volume fraction as long as the distance between particles is typically much larger than the particle radius. However, linearities up to $\phi = 0.35$ have been observed (11). This indicates that in practice these rules probably do not have to be interpreted that strictly and could explain the initial long linear dependence and the sudden transition in Fig. 7. Of course, only thorough calculations can supply support for this idea.

Also a more practical argument able to explain the linear behaviour is thinkable. Since relatively small volumes of concentrated PEO-soluton are added to a large volume of dispersion, the particles close to the location where PEO is added will be covered completely. Intensive stirring and slow addition may oppress this effects slightly, but in the most extreme situation imaginable, part of the dispersion is fully covered and part of the dispersion consists of bare latex. We note

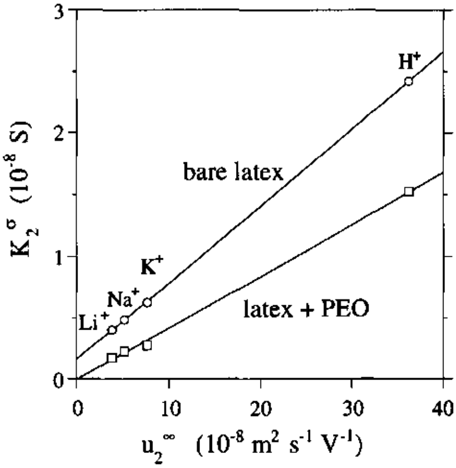

Figure 10. Dependence of the surface conductivity K_2^σ on the limiting counterion mobility u_2^∞. (○) bare latex and (□) coated latex.

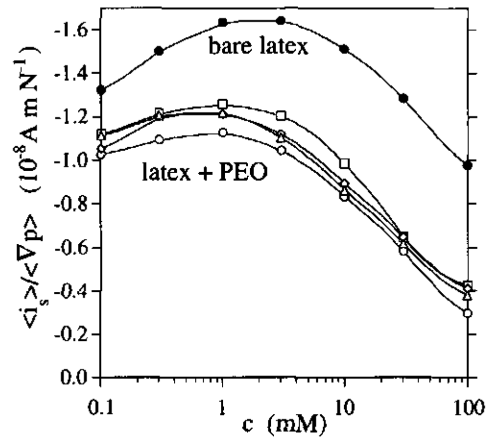

Figure 11. Streaming currents per unit applied pressure gradient as a function of the electrolyte concentration for coated latex in: (○) HCl, (□) KCl, (◇) NaCl and (△) LiCl, and bare latex in (●) HCl.

that the adsorption of this polymer is virtually irreversible so that this situation remains for longer times. Hence, the determined surface conductivity will decrease linearly upon addition of PEO to the value for which all particles are covered completely, and remains constant hereafter. This can explain the experiments.

A feature found experimentally as well as theoretically is the insensitivity of the surface conductivity to changes in the ionic strength. A property of the Poisson-Boltzmann equation for a diffuse double layer is the insensitivity of the distribution of countercharge in the high potential regime of the double layer to changes in the bulk electrolyte concentration (12,13). Since the distribution of the uncharged polymer is also insensitive to the ionic strength, the surface conductivity will be so likewise (see Eq. [13]).

In Fig. 9 the plug conductivity, calculated from the plug conductance and the geometrical cell constant (12), is presented as a function of the conductivity of the bulk electrolyte for the four different counterionic species. To show the influence of adsorbed PEO, the experiments in HCl and KCl for bare latex (12) are included. For higher electrolyte concentrations, a linear dependence is found. The straight lines are fits through the four points corresponding with the highest ionic strengths. The data points for 100 mM HCl are not included but are situated perfectly on the straight lines. The slopes of the four lines for the coated plug are nearly identical and only slightly lower than those for the other bare plug which means that the particle volume fractions in the two plugs are nearly identical.

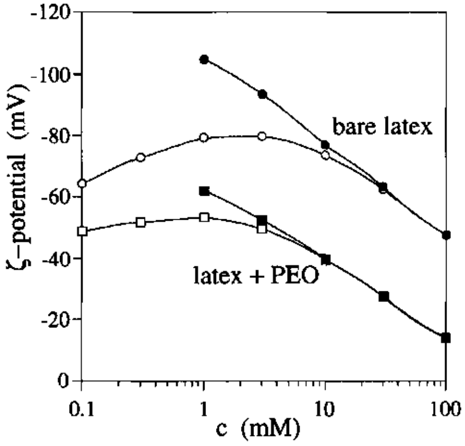

Figure 12. ζ-potentials in HCl for bare latex (spheres) and coated latex (squares), calculated according to available theories: (open symbols) ζ^{Smol}, (bold symbols) ζ^{comb}.

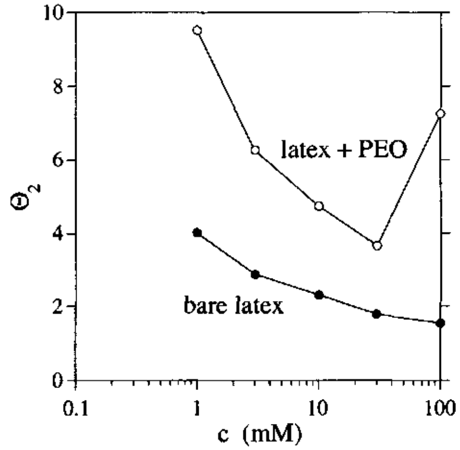

Figure 13. Θ_2 for bare (●) and coated (○) latex obtained from the combination of streaming currents and plug conductivities for plugs in HCl.

In Fig. 10 we have depicted the absolute surface conductivity K_2^{σ} ($c \geq 3$ mM), calculated from the intercepts and Eq. [6], as a function of the limiting ($c \downarrow 0$) bulk counterion mobility u_2^{∞} (from Ref. (37)). Results for bare latex (12) are included. For KCl, the surface conductivity is lowered by 55% due to the polymer coating. This reduction is comparable with the one found from low-frequency dielectric spectroscopy in KCl. Also for PEO-covered latex, K_2^{σ} is linearly related to u_2^{∞}. Two main distinctions between the curves are shown. (i) The slope of curve for PEO-coated latex is smaller. From this slope the average counterion mobility inside the double layer is determined: $\bar{u}_2 / u_2^{\infty} = 0.66$ which is lower than $\bar{u}_2 / u_2^{\infty} = 0.98$ for bare latex (12,13). (ii) The PEO-curve has a zero intercept which suggests that no significant electroosmotic contribution to the surface conductivity is present due to the polymer film.

The streaming currents per unit of applied pressure gradient for the coated plug in the four electrolytes are given in Fig. 11. For comparison purposes, the data for bare latex in HCl are included. Differences between the four curves for coated particles are larger than those for the bare particles (12). These can be caused by some specific ion interaction with PEO or adaptation of the polymer layer throughout the experiments which took nearly one month. Still these differences are relatively small compared to the absolute values which means that the ions behave as virtually indifferent. The shear plane is shifted outwards by the PEO coating as follows from the reduction in the streaming current compared to bare latex. A maximum in the curves caused by double layer polarization is also present for the coated plugs. It is situated near 1 mM which is a little lower than the 3 mM for bare particles.

In Fig. 12 we have shown the ζ-potentials as a function of the ionic strength for bare and coated latex, calculated from streaming currents according to Smoluchowski's theory (ζ^{Smol}), and from the combination of streaming potentials and plug conductivities according to the modified O'Brien theory (ζ^{comb}). The latter method rigorously accounts for double layer polarization and for conduction behind the plane of shear. For the complete computational procedure we refer to our previous article (12). Since no numerical values for $f(Du_2)$ and $g(Du_2)$ are available for $Du_2 > 5$, ζ^{comb} could not be calculated for $c < 1$ mM. Also for the coated latex the unrealistic maximum in ζ-potential disappears if surface conduction behind the slip plane is taken into account . The (nearly linear) trend in the ζ-potential versus $\log(c)$ in the range 100-10 mM HCl, where double layer polarization is still essentially absent ($Du_2 << 1$), is continued till 1 mM if double layer polarization is taken into account. This is a good indication that the procedure yields a reliable outcome since ζ-potentials, of course, may not depend on whether or not double layer polarization occurs.

As a last result we have obtained Θ_2 from the combination of the streaming currents and the conductivity measurement. From ζ^{comb} and Du_2, Θ_2 is calculated and the result is depicted in Fig. 13. The Θ_2-values for coated latex are larger than those for bare surfaces which is expected. The sudden increase for coated surfaces can be caused by charge exchange from beyond to behind the slip plane. Since ζ-potentials are low for the coated surface in high electrolyte concentrations, the insensitivity of the counterion distribution beyond the slip plane to changes of the bulk electrolyte concentration does not hold any longer.

5. CONCLUSIONS AND PERSPECTIVES

We were able to successfully analyze dielectric relaxation spectra of polymer-coated latex dispersions. The surface conductivity of a completely coated surface is approximately half the value of a bare surface and independent of the ionic strength in the range 0.4-6 mM KCl. We were able to follow polymer adsorption from the change of the surface conductivity with the amount of polymer added. As long as the adsorption plateau has not been reached, the surface conductivity reduces linearly with the added amount PEO. Extra addition after 0.5 mg/m^2, the plateau value, has nearly no effect on the surface conductivity since polymers accumulate in the bulk solution. We successfully developed a simple model for the description of retardation of ions in the polymer layer by considering it as an inhomogeneous Brinkman fluid. The ion and polymer distributions necessary in this model were obtained from self-consistent-field calculations. At least semi-quantitatively this model confirms the experimental features.

From plug conductivity measurements a reduction to 45% of the bare surface conductivity value was found for KCl as electrolyte. This value is comparable to the reduction seen by dielectric spectroscopy in KCl. The counterion mobility in the double layer of bare particles is close to the bulk mobility ($\bar{u}_2 / u_2^\infty = 0.98$) (12,13). The average counterion mobility in the double layer due to the polymer film has reduced to $\bar{u}_2 / u_2^\infty = 0.66$. Furthermore, no electroosmotic contribution to the surface conduction is shown by coated particles.

The ζ-potentials obtained from streaming potentials are lower for the coated surface than for the bare one. Due to conduction behind the shear plane, it was necessary to use plug conductivity data in the calculation of ζ. Only then the maximum in the plot of the ζ-potential against the electrolyte concentration disappears, and realistic values are obtained in low electrolyte concentrations.

It is perhaps interesting to compare the outcome of this investigation with the results of our previous electrokinetic studies on bacterial cells (11,10). For these cells, a major part of the countercharge is situated in the polyelectrolyte-gel-like walls enclosing these cells. From static conductivity and titration experiments we obtained the mobility of the counterions in the cell walls of four different bacterial species. Values were found within the interval $0.2 < u_2^i / u_2^\infty < 0.8$ which is comparable to the values around 0.5 which were found for the fully covered polymer-coated latex particles. This suggest that, quite generally, indifferent ions moving within a polymer layer or polyelectrolyte layer have mobilities (significantly) lower than their bulk values, albeit of the same order of magnitude. Results like those presented here could also help to further the understanding of partially drainable coils.

ACKNOWLEDGEMENT

We are indebted to Dr. F. A. M. Leermakers at our department for his expert help with the self-consistent-field lattice calculations.

REFERENCES

(1) Put, A. G. van der, Bijsterbosch, B. H., *J. Colloid Interface Sci.* **75,** 512 (1980).

(2) O'Brien, R. W., Perrins, W. T., *J. Colloid Interface Sci.* **99,** 20 (1984).

(3) Myers, D. F., Saville, D. A., *J. Colloid Interface Sci.* **131,** 448 (1989).

(4) Rosen, L. A., Saville, D. A., *Langmuir* **7,** 36 (1991).

(5) Rosen, L. A., Saville, D. A., *J. Colloid and Interface Sci.* **149,** 542 (1992).

(6) Dunstan, D. E., *J. Chem. Soc. Faraday Trans.* **89,** 521 (1993).

(7) Kijlstra, J., Leeuwen, H. P. van, Lyklema, J., *Langmuir* **9,** 1625 (1993).

(8) Rosen, L. A., Baygents, J. C., Saville, D. A., *J. Chem. Phys* **98,** 4183 (1993).

(9) Lyklema, J., "Fundamentals of Interface and Colloid Science. Solid-Liquid Interfaces", Vol. II, Academic Press, London, 1995.

(10) Wal, A. van der, Minor, M., Norde, W., Zehnder, A. J. B., Lyklema, J., *Langmuir* **13,** 165 (1997).

(11) Wal, A. van der, Minor, M., Norde, W., Zehnder, A. J. B., Lyklema, J., *J. Colloid Interface Sci.* **186,** 71 (1997).

(12) Minor, M., Linde, A. J. van der, Lyklema, J., submitted to *J. Colloid Interface Sci.* (chapter 2 of this thesis).

(13) Minor, M., Leeuwen, H. P. van, Lyklema, J., submitted to *J. Colloid Interface Sci.* (chapter 3 of this thesis).

(14) Lyklema, J., Minor, M., *Colloids Surfaces A* , in press.

(15) Scheutjens, J. M. H. M., Fleer, G. J., *J. Phys. Chem.* **83,** 1619 (1979).

(16) Scheutjens, J. M. H. M., Fleer, G. J., *J. Phys. Chem.* **84,** 178 (1980).

(17) Fleer, G. J., Scheutjens, J. M. H. M., Cohen Stuart, M. A., Cosgrove, T., Vincent, B., Chapman & Hall, Londen, 1993.

(18) O'Brien, R. W., *J. Colloid Interface Sci.* **92,** 204 (1983).

(19) O'Brien, R. W., *J. Colloid Interface Sci.* **110,** 477 (1986).

(20) Kapur, V., Charkoudian, J. C., Anderson, J. L., submitted.

(21) Kapur, V., Charkoudian, J. C., Kessler, S. B., Anderson, J. L., *Ind. Eng. Chem. Res.* **35,** 3179 (1996).

(22) Tong, J., Anderson, J. L., *Biophysical J.* **70,** 1505 (1996).

(23) Brinkman, H. C., *Appl. Sci. Res.* **A1,** 27 (1947).

(24) Solomentsev, Y. E., Anderson, J. L., *Phys. Fluids* **8,** 1119 (1996).

(25) Gennes, P. -G. de, "Scaling Concepts in Polymer Physics", Cornell University Press: Ithaca, New York, 1979.

(26) Donath, E., Voigt, A., *J. Colloid Interface Sci.* **109,** 122 (1985).

(27) Donath, E., Voigt, A., *Biophys. J.* **49,** 493 (1986).

(28) Fixman, M., *J. Chem. Phys.* **72,** 5177 (1980).

(29) Fixman, M., *J. Chem. Phys.* **78,** 1483 (1983).

(30) Edwards, S. F., *Proc. Phys. Soc.* **85,** 613 (1965).

(31) Barneveld, P. A., Scheutjens, J. M. H. M., Lyklema, J., *Langmuir* **8,** 3122 (1992).

(32) Evers, O. A., Scheutjens, J. M. H. M., Fleer, G. J., *Macromolecules* **23,** 5221 (1990).

(33) Goodwin, J. W., Hearn, J., Ho, C. C., Ottewill, R. H., *Colloid and Polymer Sci.* **252,** 464 (1974).

(34) Kijlstra, J., Wegh, R. A. J., Leeuwen, H. P. van, *J. Electroanal. Chem.* **366,** 37 (1994).

(35) Pelssers, E. G. M., Ph. D. Thesis, Wageningen Agricultural University, 1988.

(36) A detailed description of the apparatus is available on request at the department.

(37) Lyklema, J., "Fundamentals of Interface and Colloid Science. Fundamentals", Vol. I, Academic Press, London, 1991.

Chapter 5

STREAMING POTENTIALS AND CONDUCTIVITIES OF POROUS SILICA PLUGS[1]

ABSTRACT. Streaming potentials and conductivities of close-packed plugs of spherical Stöber-silica particles were measured. Stöber silica is highly porous; more than 98% of the countercharge may be situated inside the particle. Only the countercharge in the double layer region outside the porous particle contributes to the plug conductivity and the streaming potential. The countercharge obtained from plug conductivities is less than the double layer charge obtained from titrations. The countercharge obtained from streaming potentials is less than obtained from plug conductivities, which indicates the occurrence of conduction behind the shear plane. It is essential to take this conduction into proper account in order to arrive at more realistic ζ-potentials.

---

[1] Submitted for publication in *Colloids Surfaces A* in coauthorship with Linde, A. J. van der, Leeuwen, H. P. van, Lyklema, J.

1. INTRODUCTION

Silica sols are one of the most topical systems for studies of stability and electrokinetics. Many authors have contributed to our knowledge of these systems, not in the least H. Sonntag and his co-workers (1,2). In the electrokinetic characterization of the solid-liquid interface, ζ-potentials play an important role. Electrokinetic potentials cannot be measured directly but must be inferred from experiments with the help of a model. However, application of the "standard electrokinetic model" shows that ζ-potentials inferred from different electrokinetic experiments rarely give unique ζ-potentials. The ζ-potentials obtained from conductivity experiments are generally much larger than those obtained from particle mobilities or streaming potentials in plugs (3-14). The cause for this inconsistency is believed to be due to the neglect of conduction behind the shear plane in this model. Dukhin and co-workers (15,16) were the first to incorporate the effect of conduction behind the shear plane into the standard theory. More recently, similar adaptations were made in a number of investigations (9,10,14,17). By doing so, the inconsistencies between the ζ-potentials obtained via different methods could be removed. In a previous study we determined ζ-potentials of constant-charge polystyrene sulphate latices from plug conductivities and streaming potentials (14). By taking conduction behind the shear plane into account, realistic ζ-potentials were obtained. In this paper, plugs composed of monodisperse spherical Stöber silica are the subject of study. In contrast to the latex, the charge of this system is controlled by the pH and the ionic strength which allows for the investigation of electrokinetic properties as a function of the surface charge density. Furthermore, Stöber silica is porous. The interior of the particle contains an enormous amount of charge. We are interested in the question whether or not this charge is electrokinetically mobile and contributes to the plug conductivity.

2. THEORY

2.1. Plug conductivity

O'Brien and Perrins (4) derived that for a plug, composed of close-packed monodisperse non-conducting spheres with relatively thin double layers ($\kappa a \gg 1$), in a symmetrical electrolyte, the conductivity K^* is related to the relative surface conductivity Du_2 according to:

$$\frac{K^*}{K^\infty} = 1 + 3\phi\left[f(0) + \frac{e^2 z_2^2 n_2^\infty / f_2^\infty}{K^\infty}\left(f(Du_2) - f(0)\right)\right] \qquad [1]$$

where ϕ is the particle volume fraction, ez_i is the i-type ion charge, f_i^∞ is the ion friction coefficient beyond the double layer and n_i^∞ the equilibrium ion density beyond the double layer. The subscript i=1 refers to the co-ion, i=2 to the counterion, K^∞ is the electric conductivity of the bulk electrolyte

$$K^{\infty} = \sum_{i=1}^{i=2} K_i^{\infty}, \quad K_i^{\infty} = e^2 z_i^2 n_i^{\infty} / f_i^{\infty} \qquad [2]$$

and $f(Du_2)$ is a tabulated function of Du_2, the particle volume fraction, and the type of packing of the particles. Du_2 is related to the absolute surface conductivity K_2^{σ} via:

$$Du_2 = \frac{K_2^{\sigma}}{aK_2^{\infty}} \qquad [3]$$

where a is the particle radius. Du_2 can be related to the ζ-potential (4,14):

$$Du_2 = \frac{2}{\kappa a}\left(1 + \frac{3m_2}{z_2^2} + \Theta_2\right)\left[\exp(-z_2 e\zeta/2kT) - 1\right] \qquad [4]$$

where m_i is the non-dimensional ionic drag coefficient: $m_i = 2\varepsilon kT f_i^{\infty}/3\eta e^2$, ε the dielectric permittivity of the liquid, k the Boltzmann constant, T the temperature, η the liquid viscosity, and $\Theta_i = \tilde{u}_i^i \sigma_i^i / \tilde{u}_i^{\infty} \sigma_i^d$ reflects the relative amount of conduction behind the shear plane. σ_i^i and σ_i^d are the (surface) charge densities behind and beyond the shear plane, respectively, $\tilde{u}_i^i$ and $\tilde{u}_i^{\infty}$ are the ion mobilities behind and beyond the shear plane, respectively, including their sign: $\tilde{u}_i = z_i e / f_i$ and $u_i = |\tilde{u}_i|$.

Equation [1] can be reduced to a more simple expression (14) if Du_2 is small ($Du_2 < 1/2$):

$$K^{*} = (1 + 3\phi f(0))K^{\infty} - \frac{6\phi f(0)}{a} K_2^{\sigma} \qquad [5]$$

In a plot of K^{*} versus K^{∞}, Eq. [5] describes a straight line if the surface conductivity K_2^{σ} does not change with the electrolyte concentration. The slope of the curve is determined by the particle volume fraction and the type of array. The intercept is proportional to the surface conductivity and the amount of surface in the *close-packed* plug which is proportional to a^{-1}.

2.2. Streaming currents in plugs

The current density $\langle \bar{i}_s \rangle$ due to an imposed pressure gradient is known as the streaming current. O'Brien related $\langle \bar{i}_s \rangle$ to Du_2 and the ζ-potential for a close-packed plug of monodisperse non-conducting spherical particles (18):

$$\langle \bar{i}_s \rangle = -\frac{\varepsilon kT}{\eta e}\left(\frac{e\zeta}{kT}[1 + 3\phi f(0)] - \left[\frac{e\zeta}{kT} - \frac{2}{z_1}\ln 2\right] g(Du_2)\right)\langle -\vec{\nabla} p \rangle \qquad [6]$$

where p is the pressure and $g(Du_2)$ is a tabulated function of Du_2 also depending on the volume fraction and type of packing of the particles.

The above theories were developed for non-conducting particles. As long as conduction within the particles does occur, but remains restricted to an outer layer that is thin compared to a, these theories remain applicable. This additional conduction may then be interpreted as surface

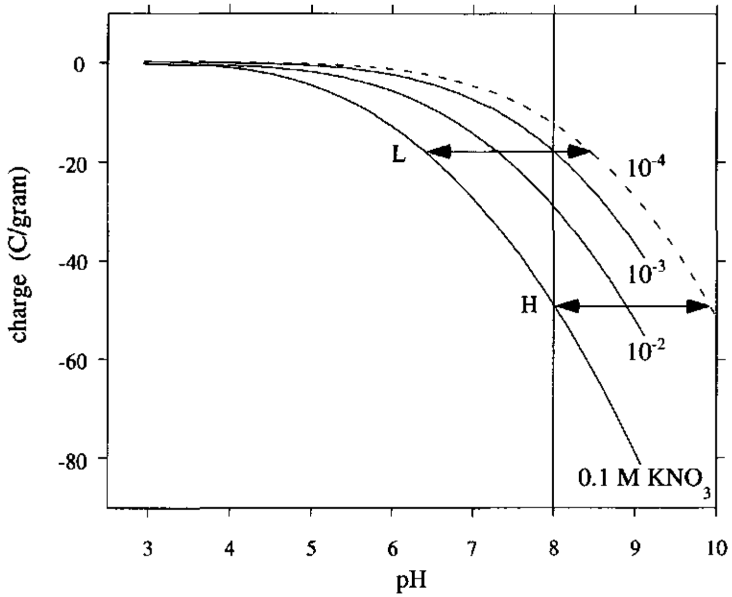

Figure 1. Charge of Stöber silica as a function of pH in 100, 10, and 1 mM KNO_3. The curve for 0.1 mM KNO_3 is determined via extrapolation. H an L refer to high and low-charged samples studied in this paper.

conduction and leads to adaptations in Du_2. However, if the bulk of the particles is conducting, the theories need to be revisited drastically. We will start with the interpretation of the experiments according to the above theories for non-conducting particles. It will turn out that this is justified since the particles appear to be virtually non-conducting.

3. EXPERIMENTAL SECTION

3.1. Characteristics of Stöber silica

De Keizer and co-workers (19) prepared monodisperse spherical silica particles by the method of Stöber (20). A full description of the preparation and characterization of this silica can be found in their paper. We summarize the most pertinent characteristics. The particle radius, found by dynamic light scattering, is 310 nm. Potentiometric acid-base titrations were performed in an automatic titration unit at 20°C. In Fig. 1 the titration charge is depicted as a function of pH in the presence of KNO_3 as the electrolyte in the concentration range 100, 10, and 1 mM. The fact that the titration charge is high can be ascribed to the high porosity of this silica.

Values for the density ρ_{SiO_2} for most SiO_2-minerals were reported to be around $2.2 \cdot 10^3$ kg/m^3 but can be as high as $2.6 \cdot 10^3$ kg/m^3 for quartz (21). We have determined the average density of a particle from a sedimentation experiment. To this end, some drops of the silica dispersion were added to a measuring cylinder filled with water, and stored at 25.0 °C. The scattering of light enables one to follow the moving boundary which appears between the clear supernatant and the dilute dispersion upon particle sedimentation. By equating the velocity of this boundary to the particle velocity, the interpretation according to the Stokes equation for particle friction yields $\bar{\rho}_p = 1.78 \cdot 10^3$ kg/m^3. This value is much lower than any of the reported values for SiO_2. A large part of the particle volume probably consists of pores filled with electrolyte solution. The volume fraction of SiO_2 within a particle, defined as the fraction of volume inside the particle which is taken by the silica, is calculated from $\bar{\rho}_p = \phi_p \rho_{SiO_2} + (1-\phi_p)\rho_w$ to be $\phi_p = 0.65$ ($\rho_{SiO_2} = 2.2 \cdot 10^3$ kg/m^3, ρ_w is the density of water). From sedimentation experiments De Keizer and co-workers found a slightly lower particle density ($\bar{\rho}_p = 1.66 \cdot 10^3$ kg/m^3), which can be caused by the relatively high volume fraction of particles in their experiment.

In the present paper another volume fraction plays an important role, viz. the volume fraction ϕ in the plug which is occupied by the particles. The real volume fraction of solid SiO_2 in the complete plug is simply given by the product $\phi\,\phi_p$.

3.2. Plug preparation

Two porous plugs with different particle charges were made. The low-charge plug (plug L) was made by bringing an intensively washed silica stock suspension, with $\phi = 0.20$, to a bulk ionic strength of 1 mM KCl. In the determination of the amount of KCl solution necessary to obtain this ionic strength we accounted for the porosity of the particles (the water volume fraction was assumed to be $(1-\phi\,\phi_p)$). Then, the pH of the dispersion was brought to 8.0 by adding 0.1 M KOH. Titrations were performed in KNO_3. We will assume that these titration results are also valid for KCl as the electrolyte. This is a reasonable assumption since NO_3^- and Cl^- are indifferent (especially as co-ionic species) and the counterionic species K^+ is identical for the two electrolytes. The charge -18 C/gram is read from the titration curve at pH 8.0 in 1 mM KNO_3. Close-packed plugs were obtained by centrifugation of the suspension ($7 \cdot 10^3 \times g$ m/s^2 for 30 min.). The particles were directly centrifuged into the plug holder (cylinder with length 1.5 cm, diameter 1.0 cm). The plug is placed between two platinum-blacked circular electrodes with small holes to allow for liquid transport. Two membranes (Millipore, 650 nm) were needed between the electrodes and plug to prevent the plug from disintegration upon application of pressure. A high-charge plug (plug H) with -49 C/gram was created by bringing the suspension to an ionic strength of 0.1 M KCl, followed by adjustment of the pH to 8.0. The remaining procedure for making plug H is identical to that described for plug L.

By measuring the mass of the wet plug, ϕ is accessible via $\phi = (\bar{\rho} - \rho_w)/(\rho_p - \rho_w)$ where $\bar{\rho}$ is the macroscopic density of the plug (total mass of the wet plug divided by its volume). This value was determined for plug L after completing all the conductivity and streaming potential experiments: $\phi^w = 0.65 \pm 0.02$ where the error is estimated via the mass of a drop of water

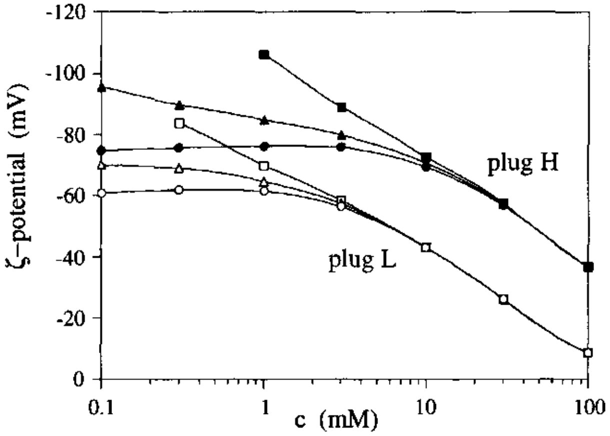

Figure 4. ζ-potentials calculated for plug L according to different theories: (○) ζ^{Smol}, (△) $\zeta^{\Theta_2=0}$, and (□) ζ^{comb} as a function of the bulk electrolyte concentration. Filled symbols for plug H.

move from the pores to the outer double layer resulting in a higher surface conductivity. This can explain the behaviour at low ionic strength.

The slope of the curves is given by $1+3\phi f(0)$. Since the two slopes are identical, the volume fractions of the plugs must also be the same. Using the approximation $f(0)\approx -0.4$ (see Refs. (23,4,14)), the volume fraction is readily obtained. However, $f(0)$ still is a weak function of ϕ. Therefore, ϕ was determined more accurately according to an iteration procedure (14) from the conductivity data for the four highest ionic strength values as $\phi^{\mathrm{con}} = 0.652 \pm 0.001$. The error accounts for the differences between the two plugs. True errors will be larger as can be seen from Fig. 2; obtaining the slope from the three or two points at the highest ionic strengths yields higher slopes and lower volume fractions. The value of ϕ^{con} is very close to ϕ^{w} obtained independently above. For latex plugs (14), we have found $\phi^{\mathrm{con}} = 0.633 \pm 0.008$ which does not differ significantly from the silica values. It is interesting to note that in spite of the high porosity of Stöber silica (35 vol % of the particles consists of aqueous solution) the pores are not filled with *neutral* electrolyte in which ions can move freely. Otherwise, the slopes should have been much closer to unity. The cause must be related to the pore size distribution. Let us consider in more detail a particle with a radius of 310 nm and a total pore volume of 35 %. If the total pore charge is 55 times larger than the outer surface charge (see below), it may be assumed that the total pore surface area is about 55 times larger than the outer surface area. For cylindrical pores with constant radius this would require as much as 10^7 nm of pore length and a pore diameter of about 3 nm. These figures point at serious double-layer overlap inside the pores. Further observations by De Keizer et al. (19) reveal that larger tetraalkylammonium ions are not able to enter part of the pores. This indicates that there is a distribution of pore sizes, with - necessarily - pores wider than 3 nm and pores more narrow than 3 nm. Irrespective of the precise nature of the pore size distribution, it is mandatory that there is extensive double-layer overlap. Hence, mainly counterions are present inside the particle. Since their number is approximately independent of the ionic strength of the medium, these counterions can only influence the intercept of the $K^*(K^\infty)$ curves. In the wider pores the double-layer overlap is less serious, but apparently the ions are not able to move through the particle from one side to the other. It thus seems that these wider pores are not interconnected, or only connected by narrow pores through which the ions move much more slowly. Taken together, the above features illustrate the drastic reduction of ionic mobility inside the particle.

The intercept of the straight lines for the high-charge plug H is much larger than that for the low-charge plug L. Via Eq. [5] we have calculated $K^{\sigma}_{2,L} = 0.10 \cdot 10^{-8}$ S and $K^{\sigma}_{2,H} = 0.42 \cdot 10^{-8}$ S. Note that it is not necessary to know $f(0)$ because the product $\phi f(0)$ to calculate the surface conductivity is readily obtained from the slope. However, for the determination of ϕ^{con}, $f(0)$ must be known. These surface conductivities are of the order of the ones found for latex (14). We can estimate the surface charge density σ^0 under the assumptions that the electroosmotic contribution to the surface conductivity is negligibly small, which usually is the case, and that the ions within the complete double layer have the bulk mobility. Then, $\sigma^0_L = -K^{\sigma}_{2,L} / \tilde{u}^{\infty}_2 = -0.013\ \mathrm{C/m^2}$ and $\sigma^0_H = -0.055\ \mathrm{C/m^2}$. Values of this order of magnitude are commonly found on Aerosil which is a hard, non-porous silica (19). De Keizer and co-workers performed titrations of spherical Stöber silica particles with different radii and were able to divide the particle charge into a part which scales with the (geometrical) outer particle surface area and a part which scales with the particle volume. The first part can be interpreted as a surface charge density (the double layer charge density), the latter as a volume charge density due to the pores, ρ^{po}. For plug H, the particle charge at pH 8.0 in 100 mM KNO_3 is approximately equal to the charge at pH 9 in 10 mM KNO_3 (see Fig. 1) for which De Keizer et al. (19) determined $\rho^{po}_H = -9.6 \cdot 10^7\ \mathrm{C/m^3}$. The surface charge density could not be determined accurately in KNO_3, but this value will differ not much from the value obtained from titrations with $TMeA^+$ as the counterions, as shown by the results on Aerosil. Hence the charge $\sigma^0_{H,tit}$ from titrations will be close to $-0.18\ \mathrm{C/m^2}$. This value is three times larger than the $-0.055\ \mathrm{C/m^2}$ found from the conductivity experiments. The double layer is partly situated beyond the particle, and partly in the porous phase of the particle. The ions in the latter part are obstructed and practically immobile. Only a fraction of the double layer charge is mobile (order of 30%).

Till now the volume charge density ρ^{po} was left out of the interpretation of the conductivity experiments. According to the above values, the ratio between the charge in the porous phase and that on the surface is $a\rho^{po}_H / 3\sigma^0_H \approx 55$. Since σ^0_H, obtained from the plug conductivities, is much smaller than σ^0_H obtained from titrations (albeit of the same order of magnitude) it is likely that the immense amount of countercharge within the particles does not at all contribute to the plug conductivity. The countercharge in the outer part of the double layer is exclusively responsible for the observed conductivity. This seems to be in contradiction with the fact that the interior of the particles is titrated, which implies that small counterions can penetrate into the pores. Hence, the mobility of these in the pores is not nihil. In the appendix we have proposed a simple model to estimate the contribution of interior counterions to the plug conductivity. If $u_2^{po} / u_2^{\infty} < 1.2 \cdot 10^{-3}$, the porous-phase contribution to the macroscopic conductivity is less than 10% of that for counterions in the double layer. This is below the limit of detectability. Titration data are typically measured on a time scale of minutes. The characteristic time to diffuse into the particle (i.e. over a distance of the order a) is $O(a^2 / D_2{}^{po})$ where $D_2{}^{po}$ is the counterion diffusion coefficient in the pores. Over a time interval of 1 minute, we estimate $D_2^{po} / D_2^{\infty} = u_2^{po} / u_2^{\infty} = 8 \cdot 10^{-7}$. Hence, the relative (average) mobility of counterions in the porous phase must lie within the range $O(10^{-6}) \le u_2^{po} / u_2^{\infty} \le O(10^{-3})$.

In Fig. 3 the streaming currents per unit of applied pressure gradient are given as a function of the ionic strength. The streaming currents for the high-charge plug H are, as expected, larger than those in plug L. Maxima due to double layer polarization, as observed for latex (14,24), are also present here. However, they are less distinct. They are situated around 1 mM KCl.

In Fig. 4 we show the ζ-potentials versus the electrolyte concentration, calculated from the streaming currents according to the primitive Smoluchowski theory, (ζ^{Smol}), the O'Brien theory, ($\zeta^{\Theta_2=0}$), and from the combination of the streaming potentials and plug conductivities, (ζ^{comb}). The latter method correctly accounts for polarization of the double layer because conduction behind the shear plane is taken into account. For a detailed description of the calculation procedure we refer to our previous papers (14,24). Especially for lower ionic strengths where double layer polarization is important, Smoluchowski's theory seriously underestimates the ζ-potential. O'Brien accounts for polarization of the double layer due to conduction beyond the shear plane, giving rise to a lower but still significant underestimate of the ζ-potentials at low ionic strengths. By also taking surface conduction behind the shear plane into account, the maximum in ζ which would be unrealistic for a (nearly) constant-charge surface disappears. Furthermore, the trend in the $\zeta(c)$-dependence as observed at higher concentrations continues at lower electrolyte concentrations. This trend of course may not depend on whether or not polarization of the double layer occurs. The values for Θ_2 calculated for these plugs are of the order of 1. Hence, a significant part of the surface conduction is situated behind the shear plane.

5. CONCLUSIONS

The charge of Stöber-silica particles can be controlled by the pH and the ionic strength. However, since the plugs are concentrated systems with high buffering capacities, the particle charge hardly changes throughout series of experiments at different electrolyte concentrations. In spite of the estimate that 35% of the particle volume consists of electrolyte solution, these pores are not filled with *neutral* electrolyte through which ions are able to pass easily.

From the combination of De Keizer's titration data and our electrokinetic data we have constructed the following kinetic model for the distribution of charge in and around a particle in plug H. The double layer charge, i.e., the charge which scales with the particle surface area in a titration experiment, is approximately $-0.18\ \mathrm{C/m^2}$. The double layer is situated partly beyond the particle surface, partly inside the porous particle. The mobility of ions in the porous phase is very low, if not negligible. Therefore, only 30% of the double layer charge is "seen" in a conductivity experiment. Since we had to account for substantial conduction behind the shear plane, the charge seen in a streaming potential experiment is much less than that in a conductivity experiment. The shear plane is situated at some distance from the particle surface.

The surface charge density which was estimated from the measured conductivity is smaller than that observed for non-porous silica (Aerosil), albeit of the same order of magnitude. Hence, the countercharge situated inside the particle, which is about 55 fold of that in the double layer, does not significantly contribute to the plug conductivity. Only the countercharge in the outer double layer regime is sufficiently mobile and therefore seen in the plug conductivity. On the other hand, on the typically much longer time scale of a titration, counterions are able to move in and out of the pores. We estimated that the counterion mobility in the pores relative to that in the bulk is between 10^{-6} and 10^{-3}. This low average mobility is probably caused by the pores having dead ends, a large labyrinth factor, or connected via very narrow pores. In order to increase the insight into the dynamics of the (retarded) ion exchange process, we suggest the use of fast titrations in future studies.

The electrokinetic potential computed according to Smoluchowski shows a maximum when plotted against the electrolyte concentration. For surface with a nearly constant charge this must be an artefact. O'Brien's theory, under the assumption of absence of conduction behind the shear plane, makes the underestimation in ζ at low ionic strengths less severe. But the $\zeta(c)$-trend is still qualitatively not correct since it changes when polarization of the double layer gets important. However, if the surface conductivity behind the slip plane is also taken into account, the trend in the ζ-potential is rather insensitive to whether or not double layer polarization occurs, as it should be. Moreover, the spurious maximum disappears. A significant part of the conduction takes place behind the plane of shear ($\Theta_2 = O(1)$ for the two plugs).

APPENDIX

Consider the porous inner phase of the particle as a Donnan phase with a not too low Donnan potential so that, to a good approximation, only counterions are present inside, i.e., the expulsion of co-ions is complete. The suspending electrolyte is symmetrical and the two ionic species have the same bulk mobilities. Furthermore, relatively thin double layers are considered, i.e., $\kappa a >> 1$. Inside the particle where the potential has attained its Donnan value, as well as beyond the electric double layer, the perturbations in the counterionic and co-ionic electrochemical potentials, $\delta\mu_2$ and $\delta\mu_1$ respectively, obey Laplace's equation:

$$\nabla^2\delta\mu_2 = 0 \qquad r < a^-, \quad r > a^+ \qquad [A.1]$$

$$\nabla^2\delta\mu_1 = 0 \qquad r > a^+ \qquad [A.2]$$

where a^- denotes a position just inside the particle where the equilibrium potential has attained the Donnan value, and a^+ is the position just beyond the double layer where the equilibrium potential is zero. The solution to these linear equations can be expressed in an infinite series where the coefficients of the terms must be determined by the boundary conditions. In dilute dispersions only a minimum number of terms is needed:

$$\delta\mu_2 = \alpha_2 r\cos\theta \qquad r < a^- \qquad [A.3]$$

$$\delta\mu_2 = \left(\beta r + \gamma / r^2\right)\cos\theta \qquad r > a^+ \qquad [A.4]$$

$$\delta\mu_1 = \alpha_1 r\cos\theta \qquad r > a^+ \qquad [A.5]$$

where α_i, β and γ are constants determined by the boundary conditions at the particle surface and in infinity. We consider the situations where the jump in electrochemical potential over the double layer is negligibly small. This local quasi-equilibrium assumption (see also Ref. (16)) implies $\delta\mu_2\big|_{a^-} = \delta\mu_2\big|_{a^+}$.

Co-ions may not enter the double layer from beyond:

$$\frac{\partial}{\partial r}\delta\mu_1\Big|_{a^+} = 0 \qquad [A.6]$$

Counterions entering the double layer regime from beyond may go into the Donnan phase or migrate along the surface via the double layer:

$$\frac{\partial}{\partial r}\delta\mu_2\Big|_{a^+} - \frac{K_2^{po}}{K_2^{\infty}}\frac{\partial}{\partial r}\delta\mu_2\Big|_{a^-} + aDu_2\nabla_t^2\delta\mu_2\big|_{a^+} = 0 \qquad [A.7]$$

where K_2^{po} is the conductivity of the Donnan phase. Since

$$\frac{\partial}{\partial r}\delta\mu_2\Big|_{a^-} = \frac{\delta\mu_2}{a}\Big|_{a^-} = \frac{\delta\mu_2}{a}\Big|_{a^+} = \frac{-a}{2}\nabla_t^2\delta\mu_2\big|_{a^+} \qquad [A.8]$$

boundary condition [A.7] can be transformed into a boundary condition applying to the field beyond the double layer only

$$\frac{\partial}{\partial r}\delta\mu_2\bigg|_{a^+} + aDu_2^*\nabla_t^2\delta\mu_2\big|_{a^+} = 0 \qquad [A.9]$$

where

$$Du_2^* = Du_2 + \frac{K_2^{po}}{2K_2^{\infty}} \qquad [A.10]$$

In this way, the problem is reduced to finding the conductivity of a suspension of non-conducting particles with relative surface conductivity Du_2^*. The solution to this problem is known (17). The conductivity of the dilute suspension, K^*, is directly given by:

$$K^* = K^{\infty} + 3\phi K^{\infty}\left[-\frac{1}{2} + \frac{3}{4}\frac{Du_2^*}{1+Du_2^*}\right] \qquad [A.11]$$

The interior contributes to the macroscopic conductivity as much as the outer surface if $K_2^{\sigma} = \frac{1}{2}aK_2^{po}$, or equivalent, $\sigma^0 u^{\infty} = \frac{1}{2}a\rho^{po}u^{po}$ where we have neglected ionic transport due to electroosmosis and assumed that the ions in the double layer have the bulk mobility. Although these results were derived for dilute dispersions, they can be used as a first estimate for concentrated systems.

REFERENCES

(1) Sonntag, H., Pilgrimm, H., *Progr. Colloid Polym. Sci.* **61,** 87 (1976).

(2) Sonntag, H., Itschvisky, V., Koleznikova, R., *Croat. Chem. Acta.* **60,** 383 (1987).

(3) Put, A. G. van der, Bijsterbosch, B. H., *J. Colloid Interface Sci.* **75,** 512 (1980).

(4) O'Brien, R. W., Perrins, W. T., *J. Colloid Interface Sci.* **99,** 20 (1984).

(5) Myers, D. F., Saville, D. A., *J. Colloid Interface Sci.* **131,** 448 (1989).

(6) Rosen, L. A., Saville, D. A., *Langmuir* **7,** 36 (1991).

(7) Rosen, L. A., Saville, D. A., *J. Colloid and Interface Sci.* **149,** 542 (1992).

(8) Dunstan, D. E., *J. Chem. Soc. Faraday Trans.* **89,** 521 (1993).

(9) Kijlstra, J., Leeuwen, H. P. van, Lyklema, J., *Langmuir* **9,** 1625 (1993).

(10) Rosen, L. A., Baygents, J. C., Saville, D. A., *J. Chem. Phys* **98,** 4183 (1993).

(11) Lyklema, J., "Fundamentals of Interface and Colloid Science. Solid-Liquid Interfaces", Vol. II, Academic Press, London, 1995.

(12) Wal, A. van der, Minor, M., Norde, W., Zehnder, A. J. B., Lyklema, J., *Langmuir* **13,** 165 (1997).

(13) Wal, A. van der, Minor, M., Norde, W., Zehnder, A. J. B., Lyklema, J., *J. Colloid Interface Sci.* **186,** 71 (1997).

(14) Minor, M., Linde, A. J. van der, Lyklema, J., submitted to *J. Colloid Interface Sci.* (chapter 2 of this thesis).

(15) Shilov, V. N., Dukhin, S. S., *Kolloidn. Zh.* **32,** 117 (1970).

(16) Dukhin, S. S., Shilov, V. N., "Dielectric Phenomena and the Double Layer in Disperse Systems and Polyelectrolytes", Wiley, New York, 1974.

(17) Minor, M., Leeuwen, H. P. van, Lyklema, J., submitted to *J. Colloid Interface Sci.* (chapter 3 of this thesis).

(18) O'Brien, R. W., *J. Colloid Interface Sci.* **110,** 477 (1986).
(19) Keizer, A. de, Ent, E. M. van der, Koopal, L. K., submitted to *Colloids Surfaces A.*
(20) Stöber, A., Fink, A., Bohn, E., *J. Colloid Interface Sci.* **26,** 62 (1968).
(21) "CRC Handbook of Chemistry and Physics", 1992.
(22) A detailed description of the apparatus is available on request at the department.
(23) Lyklema, J., Minor, M., *Colloids Surfaces A* , in press.
(24) Minor, M., Leeuwen, H. P. van, Lyklema, J., submitted to *Langmuir* (chapter 4 of this thesis).

JOURNAL OF COLLOID AND INTERFACE SCIENCE **189**, 370–375 (1997)
ARTICLE NO. CS974844

Dynamic Aspects of Electrophoresis and Electroosmosis: A New Fast Method for Measuring Particle Mobilities

M. Minor, A. J. van der Linde,[1] H. P. van Leeuwen, and J. Lyklema

Department of Physical and Colloid Chemistry, Wageningen Agricultural University, Dreijenplein 6, 6703 HB Wageningen, The Netherlands

Received December 16, 1996; accepted February 20, 1997

Measuring the dc electrophoretic mobility in a microelectrophoretic setup is traditionally performed at the stationary levels where the electroosmotic flow due to charge on the capillary wall is absent. Small deviations in the measuring position can give significant errors in the measured mobility, especially if the cell wall is highly charged. An electroosmotic streaming profile does not arise instantaneously upon switching on a field, but develops within a characteristic time, typically of the order of 1 s in a common capillary of 1 mm radius. From a theoretical study of the most pertinent relaxation times in electrophoresis and electroosmosis it is shown that, under the usual microelectrophoretic conditions, a colloidal particle responds much faster to an applied electric field than does the liquid inside the capillary. Therefore, it is possible to apply an alternating electric field with such a frequency that electroosmosis is suppressed, whereas the particles are still able to follow the field according to their dc mobility. Measurements were performed with a commercial laser-Doppler microelectrophoretic device in an alternating electric field as a function of frequency and position in order to demonstrate this principle. This new method for measuring particle mobilities overcomes the problems associated with electroosmosis, e.g., finding the stationary levels. © 1997 Academic Press

Key Words: **electrokinetics; relaxation in electrophoresis and electroosmosis; particle mobility, stationary and dynamic.**

1. INTRODUCTION

Upon switching on an electric field, a charged colloidal particle starts to move to attain a stationary motion after a certain period of time. Finding relations between the stationary velocity per unit field strength and the double-layer characteristics has been subject of study for many years. In the beginning of the 20th century, Smoluchowski (1, 2) improved a relation between the mobility u and the ζ-potential found by Helmholtz (3) in 1879. The resulting relation is known as the Helmholtz–Smoluchowski law which is applicable in the case of relatively thin double layers (local curvature much greater than the double-layer thickness κ^{-1}). Polarization of the double layer was not taken into account.

In 1948, Henry (4) and Booth (5) independently took double-layer polarization into account in the case of spherical particles with thin double layers ($\kappa a \gg 1$, where a is the particle radius). It turned out that the extent to which the electric double layer is polarized depends on the value of the dimensionless ratio Du (after Dukhin (6)). Du represents the surface conductivity relative to the bulk conductivity (times a). When Du is of the order one or higher, the electric double layer is polarized significantly and, as a consequence, the electrophoretic velocity is retarded.

Henry and Booth did not consider the polarization of neutral electrolyte (concentration polarization) around the particle. Deviations from the bulk densities extend from the surface into the solution over distances of the order of the particle radius a, i.e., well beyond the double layer if κa is large.

In 1970, Dukhin and Semenikhin (7) took concentration polarization into account. They solved the conservation equations for both ionic species in a symmetrical electrolyte (whereas Henry and Booth solved one conservation equation for the total electric current). In tackling the problem, Dukhin realized that the double layer practically is in local equilibrium with the surrounding electrolyte. This "local equilibrium assumption" is a cornerstone in many important theories for electrokinetic phenomena. It is also successfully applied in theories for the dielectric response of dilute suspensions (6, 8–10) as is shown by comparison with exact numerical results (10, 11). In fact, Henry and Booth also used a local equilibrium assumption to compute double-layer polarization. Therefore, they considered the double layer as an extremely thin sheet. As a consequence, the perturbation in electric potential in the sheet is nearly independent of the radial position within the sheet and it is identical to the perturbation in the electric potential just beyond the sheet in the neighboring electrolyte. However, the potential in an undisturbed diffuse double layer, no matter how thin, shows a fast radial decay. Also the perturbation in the electric potential inside the electric double layer due to double-layer polarization has a strong decay (10, 12). Dukhin noticed that

---

[1] To whom correspondence should be addressed. E-mail: ab@fenk.wau.nl. Fax: (NL) 317 483777.

0021-9797/97 $25.00

Copyright © 1997 by Academic Press
All rights of reproduction in any form reserved.

not the electric potential but the electrochemical potential is nearly constant.

Outline of the paper. In this article we are interested in the time needed for a particle to attain a stationary velocity relative to the solution in which it is moving after switching on an electric field. For this purpose, the most pertinent relaxation processes are studied in Section 2.2. The corresponding relaxation times, as we will see, divide the time-axis in regions where the different theories discussed above are applicable. So it is outlined that a particle with a relatively thin double layer moves according to Helmholtz–Smoluchowski shortly after switching on the field when the double layer is not yet polarized, and according to Dukhin–Semenikhin after longer times when the double layer is completely relaxed.

Mobilities are usually measured in a microelectrophoresis setup in closed capillaries. The response of the liquid to an applied electric field is given by the well-known parabolic velocity profile. This flow field is described by solution of the Stokes equations. However, electroosmosis will be absent immediately after switching on a field. It takes a certain characteristic time τ_{eo} for the electroosmotic profile to develop. In Section 2.1 we will find an expression relating the characteristic time τ_{eo} to the capillary radius R, the liquid density ρ, and the liquid viscosity η by considering the Navier–Stokes equations.

It will be shown that in a conventional microelectrophoresis setup, a particle reaches the stationary velocity much faster than the liquid inside the measuring capillary.

Section 3 demonstrates the principles on the basis of measurements, performed with a commercial laser-Doppler microelectrophoretic device in an alternating applied electric field as a function of frequency and position.

2. THEORY

2.1. *Dynamic Aspects of Electroosmosis*

In order to guarantee well-defined hydrodynamic conditions in microelectrophoretic experiments, closed cells are usually used. However, closing the cell does not imply immobilization of the fluid. The cell wall usually carries charge which induces an electroosmotic displacement.

The velocity profile in the stationary situation is well known. For the most common cylindrical cell, *beyond* the electric double layer, this profile is given by (6)

$$\mathbf{v} = v_{eo}[2(r/R)^2 - 1]\mathbf{e}_z, \qquad [1]$$

which is the sum of the linear electroosmotic profile and a Poisseuille-type back flow. Here, R is the capillary radius, $\mathbf{e}_z$ is a unit vector along the capillary axis, r is the distance from the capillary axis, and $v_{eo}\mathbf{e}_z$ is the electroosmotic slip velocity, i.e., the velocity just beyond the diffuse double layer. The stationary plane is located at position $r = (1/2)\sqrt{2}R$. The velocity inside the double layer has a much stronger radial position dependency due to the extra electric force term. The velocity changes from 0 at the shear plane to $v_{eo}\mathbf{e}_z$ just beyond the double layer.

Under nonstationary conditions (just after switching on the electric field) the velocity beyond the double layer is found by solving the Navier–Stokes equations

$$\rho \frac{\partial \mathbf{v}}{\partial t} = \eta\nabla^2\mathbf{v} - \nabla p \qquad [2]$$

$$\nabla \cdot \mathbf{v} = 0, \qquad [3]$$

where ρ is the liquid density, p is the pressure, and η is the liquid viscosity. The nonlinear term is omitted since we are interested in solutions for low electric fields, i.e., low $\mathbf{v}$.

We will study the response to a harmonic oscillating electric field with magnitude E_0 and angular frequency ω:

$$\mathbf{E} = E_0\exp(i\omega t)\mathbf{e}_z \qquad [4]$$

subject to the boundary condition

$$\mathbf{v} = v_{eo}\exp(i\omega t)\mathbf{e}_z \qquad [5]$$

at the capillary surface.[2] The double layer is thin compared to the capillary radius ($\kappa R \gg 1$) and the liquid inside the double layer will respond nearly instantaneously to the applied field in the frequency regime of interest where inertia of the liquid beyond the double layer is studied. Hence, v_{eo} is a real number. The condition of no net flow in the closed system mathematically completes the problem.

Equations [2] and [3] are linear. This means that in finding τ_{eo}, it is sufficient to study transport in an open capillary, for which $\nabla p = \mathbf{0}$, and the pressure-induced backflow separately. For an open system at higher frequencies, oscillations of the liquid are restricted to a small region close to the capillary surface. Then we may solve the equations for a flat geometry

$$\rho \frac{\partial v_z}{\partial t} = \eta \frac{\partial^2 v_z}{\partial y^2} \qquad [6]$$

subject to the boundary conditions

$$\mathbf{v} = v_{eo}\exp(i\omega t)\mathbf{e}_z \quad \text{at } y = 0 \qquad [7]$$

$$\mathbf{v} = \mathbf{0} \quad \text{as} \quad y \to \infty. \qquad [8]$$

---

[2] In principle this boundary condition must be applied just beyond the double layer. However, since the velocity beyond the double layer does not change significantly over distances κ^{-1}, this position may be identified with position R.

The y-axis is perpendicular to the capillary surface (pointing inward) and has the origin at this surface. The solution is well-known (13):

$$\mathbf{v} = v_{\mathrm{eo}}\exp(-l^{-1}y + i\omega t)\mathbf{e}_z, \quad l^{-1} = (1+i)\sqrt{\frac{\omega\rho}{2\eta}}. \qquad [9]$$

Equation [9] represents damped harmonic oscillations. The velocity profile is oscillating with a characteristic penetration depth δ

$$\delta = \sqrt{\frac{2\eta}{\omega\rho}} \qquad [10]$$

into the solution. This result is valid for such high frequencies that $\delta/R \ll 1$. Still, we may use it to estimate the order of magnitude of the characteristic time τ_{eo}, which corresponds to the time for δ to become of the order of the capillary radius R:

$$\tau_{\mathrm{eo}} = \mathrm{O}\left(\frac{R^2\rho}{\eta}\right). \qquad [11]$$

Inspection of the pressure-induced backflow shows that it develops in the same characteristic time. Hence τ_{eo} is also the characteristic time for the full development of flow in a closed system.

In microelectrophoresis, the capillary radius is typically 1 mm and measurements are usually performed in aqueous solutions. For this situation it follows from Eq. [11] that $\tau_{\mathrm{eo}} = \mathrm{O}(1)$s.

2.2. *Dynamic Aspects of Particle Electrophoresis*

In this section we will consider the response of a charged particle with a thin double layer ($\kappa a \gg 1$) subjected to an electric field switched on at time $t = 0$.

Hydrodynamic relaxation. Since the dielectric permittivity of the particle is usually much smaller than that of the aqueous solvent, the electric field will initially be nearly tangential to the particle surface. As a result, liquid in the double layer starts to move along the surface. This thin layer attains its quasi-stationary velocity nearly instantaneously, in contradistinction to the liquid beyond the double layer, where in the stationary state the velocity profile extends over distances of the order a. By comparing the viscous term and the time-derivative term in the Navier–Stokes equations, the typical time τ_{h} to attain a stationary hydrodynamic profile beyond the double layer is found to be of the order (11)

$$\tau_{\mathrm{h}} = \mathrm{O}\left(\frac{a^2\rho}{\eta}\right). \qquad [12]$$

This expression is identical to [11] except for the characteristic length scale which is now the particle radius. For a 100-nm particle in an aqueous solution, $\tau_{\mathrm{h}} = \mathrm{O}(10^{-8})$s.

In order to just estimate the effect of inertia due to the particle mass on the response, we assume that the velocity of the fluid around the particle is relaxed ($t \gg \tau_{\mathrm{h}}$). Then the force on the particle is given by a Stokes-type relation (6, 14) resulting in an exponential increase to the quasi-stationary velocity. The characteristic time for this process is

$$\tau_{\mathrm{p}} = \mathrm{O}\left(\frac{a^2\rho_{\mathrm{p}}}{\eta}\right) \qquad [13]$$

where ρ_{p} is the density of the particle. Usually ρ_{p} is close to ρ so that $\tau_{\mathrm{p}} = \mathrm{O}(\tau_{\mathrm{h}})$ which means that the two relaxation processes occur essentially simultaneously.

If we suppose that the electric double layer is still unpolarized, all conditions for the Helmholtz–Smoluchowski expression are obeyed for t beyond a few times the highest value of τ_{h} or τ_{p}. Hence, the particle movement can be interpreted according to this expression.

Double-layer polarization. The double layer however does not remain unaffected by the field. For simplicity we consider a symmetrical electrolyte where the cations and anions have identical diffusion coefficients. The current flowing in the double-layer regime due to the (initially nearly tangential) electric field is locally not balanced and this leads to local changes in the double layer charge and hence to its polarization. This polarization process continues until the currents induced by the extra dipole field balance the initial currents; i.e., the sum of the charges entering and leaving any portion of the double layer per unit time equals zero. The dipole strength attains a quasi-stationary value in the typical time τ_{dl} (15):

$$\tau_{\mathrm{dl}} = \mathrm{O}\left(\frac{1}{\kappa^2 D}\right), \qquad [14]$$

where D is the diffusion coefficient of the ions. For example, for 1 mM KI in water, $\tau_{\mathrm{dl}} = \mathrm{O}(10^{-7})$s.

The Henry–Booth theory is applicable and the particle will move according to this theory at times beyond a few times τ_{dl}, provided concentration polarization is still absent.

Concentration polarization. After the relatively rapid adjustment of the electric double layer, a much slower process will take place as we will see now. The electric currents are balanced; however, this is not yet the case for the fluxes of the individual ionic species. In the electric double layer, the current is mainly carried by counterions, whereas beyond the double layer this current is equally carried by co-ions and counterions. This unbalance makes the particle behave as a source for neutral electrolyte at one side and as a sink at the other. As a result, neutral ion density changes spread out into the electrolyte. In the stationary situation, deviations from the bulk densities extend over distances of the order of the particle radius a. The time for diffusion over a distance a is typically

$$\tau_{\mathrm{cp}} = \mathrm{O}\left(\frac{a^2}{D}\right), \quad [15]$$

which is $\mathrm{O}(10^{-5})$s for a 100-nm particle in an aqueous KI solution. For t beyond a few times τ_{cp}, not only the electric current but also the fluxes for the two individual ionic species are stationary and the particle will move according to the Dukhin–Semenikhin theory for the dc mobility. Usually this is the relaxation process with the largest characteristic time in electrophoresis. Hence, for not too extreme situations $\tau_{\mathrm{eo}} \gg \tau_{\mathrm{cp}}$. In this respect we mention that for a very large particle of 30 μm in an aqueous KI solution, $\tau_{\mathrm{cp}} = \mathrm{O}(1)$s which is comparable to τ_{eo} in a microelectrophoretic experiment so that the condition $\tau_{\mathrm{eo}} \gg \tau_{\mathrm{cp}}$ is violated. However, polarization of the double layer for such a huge particle and its effect on the mobility are negligible. The particle will move according to Helmholtz–Smoluchowski. This can be seen from the derivation below.

Particle mobility. In an alternating electric field the particle will follow the field according to its dc mobility for frequencies well below τ_{cp}^{-1}. Around the frequencies where relaxation processes occur, the mobility will show dispersion in the velocity, i.e., an out-of-phase motion. This will now be demonstrated for frequencies around τ_{cp}^{-1}. From the flux balances for the individual ions and the local equilibrium assumption, the electric potential and ionic concentrations are calculated for frequencies around τ_{cp}^{-1}. From these, the electrochemical potentials for the individual ionic species are derived. The mobility is related to the tangential gradients of the electrochemical potentials in the double layer regime (10, 12, 16, 17). Using these relationships, one obtains the following expression for the mobility:

$$\frac{\eta e u}{\varepsilon k T} = \frac{e\zeta}{kT} + \frac{Du}{1 + Du(1 - \frac{1}{2}\gamma(\omega\tau))} \times \left\{\frac{2\ln 2}{z} - \frac{e\zeta}{kT} - \gamma(\omega\tau)\left(\frac{2\ln 2}{z} - \frac{e\zeta}{2kT}\right)\right\}, \quad [16]$$

which is an explicit form of the equation given by Hinch *et al.* (12). Here, ε is the dielectric permittivity of the liquid, k is the Boltzmann constant, T is the temperature, z is the co-ion valence, $\gamma(\omega\tau)$ is a complex function of the nondimensional angular frequency $\omega\tau$,

$$\gamma(\omega\tau) \equiv \frac{\omega\tau\sqrt{\omega\tau} + i\omega\tau}{(1 + \sqrt{\omega\tau})(1 + \omega\tau)}, \quad \tau = \frac{a^2}{2D}, \quad [17]$$

and Du is the relative surface conductivity parameter (6):

$$Du = \frac{2}{\kappa a}\left(1 + \frac{3m}{z^2} + \Theta\right)[\exp(ze\zeta/2kT) - 1],$$

$$m = \frac{2\varepsilon k^2 T^2}{3\eta e^2 D}, \quad [18]$$

where Θ reflects the conduction behind the shear plane (6, 18). The first term on the right-hand side of Eq. [16] is the Helmholtz–Smoluchowski result. The second term shows the retardation due to polarization of the double layer and becomes unimportant for $Du \ll 1$.

TABLE 1

Theories, Applicable for the Different Time Domains after Switching on an Electric Field at $t = 0$

Time domain	Theory applicable
$\tau_h, \tau_p \ll t \ll \tau_{dl}$	Helmholtz–Smoluchowski
$\tau_h, \tau_p, \tau_{dl} \ll t \ll \tau_{cp}$	Henry–Booth, Eq. [20]
$\tau_{cp} \ll t$	Dukhin–Semenikhin, Eq. [19]

Two limiting cases immediately follow from Eq. [16]:

$$\frac{\eta e u}{\varepsilon k T} = \frac{e\zeta}{kT} + \frac{Du}{1 + Du}\left\{\frac{2\ln 2}{z} - \frac{e\zeta}{kT}\right\} \quad \text{as} \quad \omega\tau \ll 1, \quad [19]$$

which is equivalent to the Dukhin–Semenikhin expression for the dc mobility (7, 19) and

$$\frac{\eta e u}{\varepsilon k T} = \frac{e\zeta}{kT} + \frac{Du}{2 + Du}\left\{-\frac{e\zeta}{kT}\right\} \quad \text{as} \quad \omega\tau \gg 1, \quad [20]$$

which reduces to the Henry–Booth expression for the mobility if $\Theta = 0$ (4, 5, 19). Around $\omega = \tau^{-1}$ the mobility shows dispersion and the motion is out of phase. For particles with low relative surface conductivity (large a and/or low surface charge density), $Du \ll 1$. Then polarization of the double layer and its influence on the mobility are negligible so that the particles move according to Helmholtz–Smoluchowski.

Measuring the mobility for frequencies around $\omega = \tau^{-1}$ would yield extra information and the correct ζ-potential if $Du \geqslant \mathrm{O}(1)$. The particle radius a can be obtained from the relaxation frequency. From the two limiting mobilities, ζ and Θ are obtained.

The relaxation times discussed in this section depend on the particle radius, double-layer thickness, medium viscosity, and diffusion coefficient of the ions. This means that the magnitudes will be changed for other numerical examples.

In Table 1 we have summarized the results of this section.

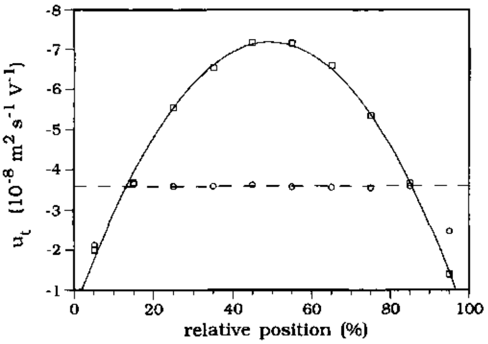

FIG. 1. Total mobility u_t as a function of the relative radial position inside the measuring capillary for (□) $\omega/2\pi$ = 0.5 Hz and (○) $\omega/2\pi$ = 50 Hz.

3. EXPERIMENTS

Mobilities were measured with a commercial laser-Doppler device (Malvern, Zetasizer 3). The reader is referred to (20, 21) for details concerning the apparatus. In the common measuring mode, a rectangular alternating electric field of relatively low frequency is applied to suppress electrode polarization and the measurements are performed in the stationary plane. The measurements can also be performed in fields with higher frequencies without making alterations of any kind to the hardware. This is done via the standard software by adjusting the mirror modulation frequency and correlation interval. The radius of the capillary is 2 mm.

Mobility measurements were performed with silver iodide particles ($\bar{a}$ = 120 nm obtained from dynamic light scattering) in an aqueous 1 m*M* KI solution. This classical colloid is easy to make and the surface potential is controlled by KI. The relative surface conductivity under these conditions is O(1) so that the mobility may be significantly retarded due to polarization of the double layer. The velocity per unit field strength was measured in an alternating field as a function of the radial position in the closed capillary. The measured total mobility u_t (sum of electrophoresis and electroosmosis) is presented in Fig. 1 for two frequencies. At 0.5 Hz, the velocity of the particle has the well-known parabolic dependence on position. This is the result of the static electrophoretic velocity and the parabolic velocity profile caused by electroosmosis. The measured velocity at 50 Hz, indicated by circles, was constant throughout the major part of the capillary and identical to the measured velocity in the stationary planes (14.65 and 85.35%) at 0.5 Hz. The deviations from this constant value near the capillary wall can be caused by light scattered from the wall or residual electroosmosis occurring near the wall. From these measurements we conclude that electroosmosis is absent in the major part of the capillary at 50 Hz.

Furthermore, measurements were performed in the middle of the capillary as a function of frequency in the range 0.25–50 Hz and shown in Fig. 2. The curve is the empirical fit with a Debye-type of relaxation given by the expression $u_t = -(3.65 + 4.42/(1 + (\omega\tau_{eo})^2)) \times 10^{-8}\ \mathrm{m^2\,s^{-1}\,V^{-1}}$. The measured velocity changed from the electrophoretic velocity at high frequencies to the sum of the electrophoretic and electroosmotic velocity at low frequencies. The observed characteristic time τ_{eo} for the development of the electroosmotic profile is 0.13 s. This is one order too small compared to the theoretical value of 4 s resulting from Eq. [11]. In a more precise study, it would be necessary to compute the exact velocity profiles as a function of frequency from the Navier–Stokes equations. This should be the object of future studies.

As a remark we want to mention here that measurements on other systems such as monodisperse latex and oxides have shown similar results.

4. CONCLUSIONS

Studying relaxation processes in electrokinetics is not only of great scientific interest. It can also contribute to solving practical problems. Via a theoretical analysis and experiments it was shown in this article that colloidal particles respond to the electric field much faster than the liquid inside the measuring capillary. This enables one to suppress electroosmosis in mobility measurements by measuring the mobility at a sufficiently high frequency. The principles were illustrated by experiments.

The new method for measuring mobilities overcomes the problems associated with electroosmosis. In this respect we can mention that no stationary planes have to be searched and, hence, errors due to small misplacements are absent. Furthermore, the ζ-potential of the capillary surface can be a function of position due to inhomogeneous contamination

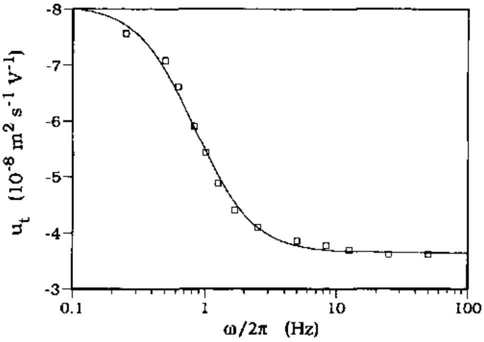

FIG. 2. Total mobility u_t measured in the center of the capillary versus the frequency $\omega/2\pi$: (□) measurements. The empirical fit is given by the curve.

or sedimentation of particles. In the latter case the bottom of the capillary has the particle ζ-potential, whereas the top has the capillary ζ-potential and the stationary planes would deviate from the theoretical positions. This problem occurs when relatively heavy particles are subject of investigation, e.g., in soil science studies. We conclude that inclusion of the frequency as a variable in capillary electrophoresis avoids these problems and directly yields the correct particle mobility.

REFERENCES

1. von Smoluchowski, M., *Bull. Int. Acad. Sci. Cracovie* 184 (1903).
2. von Smoluchowski, M., *Z. Phys. Chem.* **92,** 129 (1918).
3. von Helmholtz, H., *Ann. Phys.* **7,** 337 (1879).
4. Henry, D. C., *Trans. Faraday Soc.* **44,** 1021 (1948).
5. Booth, F., *Trans. Faraday Soc.* **44,** 955 (1948).
6. Lyklema, J., "Fundamentals of Interface and Colloid Science: Solid–Liquid Interfaces," Vol. II. Academic Press, London, 1995.
7. Dukhin, S. S., and Semenikhin, N. M., *Kolloid. Zh.* **32,** 366 (1970).
8. Dukhin, S. S., and Shilov, V. N., "Dielectric Phenomena and the Double Layer in Disperse Systems and Polyelectrolytes." Wiley, New York, 1974.
9. Fixman, M., *J. Chem. Phys.* **72,** 5177 (1980).
10. Fixman, M., *J. Chem. Phys.* **78,** 1483 (1983).
11. DeLacey, E. H. B., and White, L. R., *J. Chem. Soc. Faraday Trans.* **77,** 2007 (1981).
12. Hinch, E. J., Sherwood, J. D., Chew, W. C., and Sen, P. N., *J. Chem. Soc. Faraday Trans. 2* **80,** 535 (1984).
13. Batchelor, G. K., "An Introduction to Fluid Dynamics." Cambridge Univ. Press, Cambridge, 1977.
14. Anderson, J. L., and Prieve, D. C., *Langmuir* **7,** 403 (1991).
15. O'Brien, R. W., *J. Colloid Interface Sci.* **113,** 81 (1986).
16. O'Brien, R. W., *J. Colloid Interface Sci.* **92,** 204 (1983).
17. Hunter, R. J., "Foundations of Colloid Science," Vol II. Oxford Univ. Press, New York, 1989.
18. Minor, M., van der Wal, A., and Lyklema, J., *in* "Fine Particles Science and Technology" (E. Pelizzetti, Ed.), p. 225. Kluwer, Dordrecht, 1996.
19. Dukhin, S. S., and Derjaguin, B. V., *in* "Surface and Colloid Science" (E. Matijevic, Ed.), Vol. 7. Wiley, New York, 1974.
20. Hunter, R. J., "Zeta Potential in Colloid Science: Principles and Applications." Academic Press, London, 1981.
21. Hunter, R. J., "Introduction to Modern Colloid Science." Oxford Univ. Press, New York, 1993.

Chapter 7

POLARIZATION OF THE STERN LAYER AND ITS ROLE IN THE LOW-FREQUENCY DIELECTRIC RESPONSE AND ELECTROPHORETIC MOBILITY[1]

ABSTRACT. This paper discusses the influence of finite mobilities of the ions in the non-diffuse part of the double layer on the low-frequency dielectric dispersion (LFDD) and the electrophoretic mobility. The classical thin double layer theory of Fixman (1) concerning polarization of the diffuse part of the double layer is generalized by rigorously including polarization of charge in the dense part of the double layer. Using different models for the exchange of charge between the Stern layer and the diffuse layer, the cases of free exchange, absence of exchange and the intermediate situation of retarded exchange are all included. Retarded exchange is characterised by the absence of local equilibrium between the Stern layer and the diffuse layer. The charge in a perturbed Stern layer relaxes to a new stationary distribution via the simultaneous processes of *ion exchange* and *lateral transport in the Stern layer*. This results into one extra dispersion in LFDD spectra (next to the classical dispersion induced by the diffuse layer). The faster process determines the position of this extra dispersion on the frequency axis.

If ions in the Stern layer are able to exchange with the neighbouring diffuse layer, the dc-particle mobility is retarded. The more freely the ions are able to exchange, the more the particle mobility is retarded.

---

[1] Submitted for publication in *J. Chem. Soc. Faraday Trans.* in coauthorship with Leeuwen, H. P. van, Lyklema, J.

1. INTRODUCTION

Over the past few decades several models for the polarization of the electric double layer have been developed in order to interpret the low-frequency dielectric dispersion (LFDD) observed for colloidal suspensions. Originally, Schwarz (2) proposed lateral transport of counterions in the Stern layer as the main mechanism for double-layer polarization. Ions were supposed to be unable to exchange between the Stern layer and the diffuse layer. Dukhin and Shilov (3) suggested an alternative mechanism. In their theory the quasi-equilibrium polarization of the complete double layer is responsible for the LFDD. Free exchange between the double layer and the adjacent electrolyte is the main assumption in this theory. More recently, Kijlstra et al. (4), and Rosen et al. (5) developed similar models for a Stern layer in equilibrium with the neighbouring diffuse layer in order to interpret experimental LFDD and mobility results. Dukhin and Shilov did not reject the Schwarz mechanism for polarization of the Stern layer as a possible option. They modified the Schwarz theory by incorporating the necessary screening by the diffuse layer in the absence of an equilibrium diffuse layer (in the iso-electric point) (3). This effect was not taken into account by Schwarz. Lyklema et al. (6) further modified this theory for situations of non-zero Stern potentials, still under the restriction of small values of the relative surface conductivity parameter Du ($Du \ll 1$, see e.g. Ref. (7,8) for the precise definition of Du) where concentration polarization is negligible. More recently, Razilov and Dukhin (9) and Razilov et al. (10) extended this theory for moderate values of Du ($Du = O(1)$) by studying the mutual influence of polarization of the Stern layer and the diffuse layer.

Hence, theory describing polarization of the Stern layer is available for the extreme situations of free exchange with the neighbouring electrolyte and complete absence of exchange. An intermediate situation has been the object of a study by Hinch et al. (11) They took into account retarded surface site reactions and showed their effect on the LFDD. However, surface ions were not allowed to move along the surface.

Outline of the paper. As a next step, we want to develop a thin double-layer theory where ions in the compact part of the double layer are mobile and able to exchange at some rate with the adjacent diffuse layer. In the following section we introduce the phenomenon of Stern-layer polarization by considering a Stern layer subjected to an alternating electric field in some pertinent limiting situations. In section 3 the electrokinetic equations and proper boundary conditions are set out. In section 4 we give the solutions to these equations, valid beyond the electric double layer. In these solutions there remain a few of undetermined quantities which must be determined by boundary conditions imposed on the fields in the vicinity of the particle surface. In section 5, these so called "inner boundary conditions" are related to perturbations in the Stern-layer charge. These perturbations depend on the physical mechanisms which may be operative in the double layer. Some simple models for the description of ionic exchange between the diffuse and the

Stern layer are derived in section 6 after which in section 7 their effects on the LF dielectric dispersion are derived. To provide more insight in the consequences of Stern-layer polarization, approximate expressions for the permittivity, the conductivity and the dc particle mobility are given in section 8. In the section "results and discussion" some typical cases are calculated and discussed.

2. DYNAMIC ASPECTS OF STERN-LAYER POLARIZATION

Phenomenologically, four limiting situations of Stern-layer relaxation can be distinguished. To this end we introduce the characteristic times $\tau_{//}$ needed for tangential redistribution of ions in the Stern layer and $\tau_{\perp}$ needed for establishing equilibrium between the Stern layer and the diffuse layer (in the absence of tangential redistribution). Consider:

1) the period of the applied electric field is small compared to $\tau_{\perp}$ and small compared to $\tau_{//}$, i.e.:

$$1/\tau_{\perp} << \omega, \quad 1/\tau_{//} << \omega \qquad [1]$$

where ω is the angular frequency of the field. In this situation ions are not able to exchange between the diffuse and the Stern layer. Furthermore, ions in the Stern layer cannot redistribute tangentially. Consequently the Stern layer stays unpolarized.

2) the period of the applied field is large compared to $\tau_{\perp}$ and large compared to $\tau_{//}$:

$$1/\tau_{\perp} >> \omega, \quad 1/\tau_{//} >> \omega \qquad [2]$$

Now, ions are able to exchange between the layers, as well as to redistribute by moving tangentially to the surface. The two mechanisms occur simultaneously and are responsible for polarization of the Stern layer.

3) the period of the applied field is large compared to $\tau_{\perp}$ and small compared to $\tau_{//}$:

$$1/\tau_{//} << \omega << 1/\tau_{\perp} \qquad [3]$$

Redistribution of ions in the Stern layer by movement along the surface is not possible. However, ions are able to exchange between the Stern and diffuse layer. This is the only mechanism operational for the polarization of the Stern layer. O'Brien (12) studied the effect of fast surface-dissociation reactions on the dipole strength. Ions in the Stern layer were not able to move along the surface. This situation obeys conditions [3].

4) the period of the applied field is small compared to $\tau_{\perp}$ and large compared to $\tau_{//}$:

$$1/\tau_{\perp} << \omega << 1/\tau_{//} \qquad [4]$$

Ions are unable to exchange between the Stern and diffuse layer, but polarization of the bound layer is possible by the tangential redistribution of ions. This is the mechanism proposed by Schwarz (2) to explain the LFDD.

3. ELECTROKINETIC EQUATIONS

We consider a spherical particle with radius a in a suspending electrolyte where the ion charge, ion friction coefficient and number density of the i-th type of ionic species ($i = 1,2,\ldots,N$) are $z_i e$, f_i and n_i, respectively. The origin of our spherical co-ordinate system is located at the centre of the particle. The distance to this centre is r. We will identify the position just inside the particle with a^-, the position in the inner part of the diffuse layer, adjacent to the surface, with a, the position of the shear plane with a^ζ and the position just beyond the thin diffuse double layer with a^+.

An oscillating electric field with magnitude E_0 and (angular) frequency ω is imposed:

$$\vec{E} = \vec{E}_0 \exp(i\omega t), \quad E_0 = \left|\vec{E}_0\right| \tag{5}$$

The electric potential ψ, the space charge density ρ and the dielectric permittivity $\varepsilon = \varepsilon_0 \varepsilon_r$ are related via Poisson's equation:

$$\vec{\nabla} \cdot \varepsilon \vec{\nabla} \psi = -\rho = -\sum_{i=1}^{N} z_i e n_i \tag{6}$$

where $\varepsilon = \varepsilon_0 \varepsilon_r$ is the permittivity of the medium.

The ions are convectively transported by the fluid with velocity $\vec{v}$ and are able to move relative to the solvent under the influence of electric and thermodynamical forces. The ionic flux density $\vec{J}_i$ is given by the Nernst-Planck equation:

$$\vec{J}_i = n_i \vec{v} - \frac{kT}{f_i}\left(n_i \frac{z_i e}{kT} \vec{\nabla} \psi + \vec{\nabla} n_i \right) \tag{7}$$

The motion of the fluid is described by the Navier-Stokes equations restricted to incompressible fluid flow and low Reynolds numbers, extended with an electrostatic force term. In the LF domain to be considered here, the time-derivative term may be neglected (13):

$$\eta \vec{\nabla}^2 \vec{v} - \vec{\nabla} p - \rho \vec{\nabla} \psi = \vec{0} \tag{8}$$

$$\vec{\nabla} \cdot \vec{v} = 0 \tag{9}$$

where η is the liquid viscosity and p is the pressure.

Conservation of ions implies:

$$\frac{\partial n_i}{\partial t} + \vec{\nabla} \cdot \vec{J}_i = 0 \tag{10}$$

If the applied electric field strength is low, the equations can be linearized around the equilibrium values in the absence of the imposed field (subscript *eq*). To that end we write:

$$\begin{aligned} \psi &= \psi_{eq} + \delta\psi + \mathrm{O}(E_0^2) \\ n_i &= n_{i,eq} + \delta n_i + \mathrm{O}(E_0^2) \qquad [11] \\ &\text{etc.} \end{aligned}$$

The liquid velocity $\vec{v}$ is first-order in E_0. Substituting these expressions in the above equations and omitting the small non-linear $\mathrm{O}(E_0^2)$ terms we obtain a set of equations linear in the perturbation quantities:

$$\vec{\nabla} \cdot \varepsilon \vec{\nabla} \delta\psi = -\delta\rho = -\sum_i z_i e \delta n_i \qquad [12]$$

$$\begin{aligned} \vec{J}_i &= n_{i,eq}\vec{v} - \frac{kT}{f_i}\left(\frac{z_i e}{kT}\left(n_{i,eq}\vec{\nabla}\delta\psi + \delta n_i \vec{\nabla}\psi_{eq}\right) + \vec{\nabla}\delta n_i\right) \\ &= n_{i,eq}\vec{v} - n_{i,eq}\frac{kT}{f_i}\vec{\nabla}\left[\frac{z_i e}{kT}\delta\psi + \frac{\delta n_i}{n_{i,eq}}\right] \end{aligned} \qquad [13]$$

$$\eta\vec{\nabla}^2\vec{v} - \vec{\nabla}\delta p - \rho_{eq}\vec{\nabla}\delta\psi - \delta\rho\vec{\nabla}\psi_{eq} = \vec{0}, \quad \vec{\nabla}\cdot\vec{v} = 0 \qquad [14]$$

$$\frac{\partial \delta n_i}{\partial t} + \vec{\nabla}\cdot\vec{J}_i = 0 \qquad [15]$$

The term between square brackets in Eq. [13] is just the first-order perturbation in the non-dimensional electrochemical potential, $\delta\mu_i$.

It remains to determine the boundary conditions of the functions $\delta\psi$, δn_i and $\vec{v}$. Far away from the particle the electric field approaches the applied electric field and the ion density approaches its bulk value (superscript "∞"):

$$\vec{\nabla}\delta\psi = -\vec{E} \quad \text{as} \quad r \to \infty \qquad [16]$$

$$\delta n_i \to 0 \quad \text{as} \quad r \to \infty \qquad [17]$$

In order to keep the mathematics tractable but nevertheless to capture the essential physical features we restrict the situation to the case of very high inner layer capacitances. In fact this means that the surface ions, giving rise to the surface charge σ^0, and the Stern ions giving rise to the Stern charge σ_i^s are virtually located in the same plane and experience the same electric field. Lyklema et al. used the same approximation in their Stern-relaxation study (6). As a further elaboration the case of lower Stern-layer capacitances may be considered. We shall refer to this combined layer with the symbol "S". The perturbation in potential at the surface is related to perturbation in the surface charge density by Gauss's law:

$$\left(\varepsilon\frac{\partial\delta\psi}{\partial r}\right)\Bigg|_{a^-}^{a} = -\delta\sigma^s \qquad [18]$$

Here, $\delta\sigma^s$ is the sum of the perturbations in surface charge density and Stern layer charge density.

Ions are supposed to be unable to be transferred through the particle surface (which excludes certain types of colloids like AgI):

$$\vec{J}_i \cdot \vec{e}_r = 0 \quad \text{at} \quad r = a^- \qquad [19]$$

where $\vec{e}_r$ is the unit vector, normal to the surface.

Furthermore,

$$\begin{aligned} \vec{v} &= \vec{0} \quad \text{at} \quad r \le a^\zeta \\ \vec{v} &= -\vec{v}_{ef} \quad \text{as} \quad r \to \infty \end{aligned} \qquad [20]$$

where $\vec{v}_{ef}$ denotes the electrophoretic velocity. The liquid between $r = a^-$ and $r = a^\zeta$ is supposed to be stagnant.

4. EQUATIONS AND FIELDS BEYOND THE THIN DOUBLE LAYER

Beyond the relatively thin diffuse double layer with thickness:

$$\kappa^{-1} = \sqrt{\varepsilon^\infty kT \Big/ \sum_i z_i^2 e^2 n_i^\infty} \qquad [21]$$

the electrolyte is unperturbed by the equilibrium double layer

$$\psi_{eq} = 0, \quad n_{i,eq} = n_i^\infty \qquad [22]$$

and the set of governing equations simplifies. The solutions to these simplified equations define the so called "far fields" and are labelled with the superscript "*f*".

Beyond the double layer the Poisson equation reads:

$$\nabla^2 \delta\psi^f = -\frac{1}{\varepsilon^\infty} \sum_i z_i e \delta n_i^f \qquad [23]$$

Using the Nernst-Planck expression, the conservation equation for each species turns into:

$$\frac{f_i^\infty}{kT} \frac{\partial \delta n_i^f}{\partial t} = \nabla^2 \left(n_i^\infty \frac{z_i e}{kT} \delta\psi^f + \delta n_i^f \right) \qquad [24]$$

The convective term cancelled because of incompressibility. From hereon we will consider the far less complex but common situation of a symmetrical (in valence) suspending electrolyte. Adding the conservation equations [24] for the two ionic species results in:

$$\nabla^2 \delta n^f = \mathrm{i}\omega \frac{\overline{f^\infty}}{kT} \delta n^f, \quad \overline{f^\infty} \equiv (f_1^\infty + f_2^\infty)/2 \qquad [25]$$

Subtraction of the conservation equations yields:

$$\nabla^2 \delta\psi^f = \mathrm{i}\omega \frac{kT}{e} \frac{\overline{f^\infty/z}}{kT} \frac{1}{n^\infty} \delta n^f, \quad \overline{f^\infty/z} \equiv (f_1^\infty / z_1 + f_2^\infty / z_2)/2 \qquad [26]$$

In obtaining Eqs. [25] and [26] we used the electroneutrality condition $\delta n_1^f = \delta n_2^f = \delta n^f$. These equations are exact if the ions have equal diffusion coefficients, and are good approximations if $f_1^\infty \neq f_2^\infty$, as long as the frequency is much smaller than the Maxwell-Wagner frequency ($= \mathrm{O}(K^\infty / \varepsilon)$). This was explained by Dukhin and Shilov (3) and Hinch et al. (11) by including Poisson's equation. The electroneutrality condition only cancels insignificant terms. To a very good approximation, Eq. [26] still accounts for the space charge that arises beyond the electric double layer if $f_1^\infty \neq f_2^\infty$. The right-hand-side is directly proportional to the space charge density via Poisson's equation. If $f_1^\infty = f_2^\infty$, Laplace's equation for the potential is operative everywhere beyond the double layer. Hence charge generation beyond the double layer is absent and there are no associated diffusion potentials.

The unique solution of Eq. [25] for δn^f, which tends to zero far away from the particle, and which is able to satisfy the boundary conditions just beyond the double layer, is:

$$\delta n^f = \frac{d_n a^3 E_0}{r^2} (1 + \lambda r) \exp(-\lambda r) \cos(\theta) \exp(\mathrm{i}\omega t) \qquad [27]$$

where

$$\lambda a \equiv (1 + \mathrm{i})\sqrt{\omega\tau}, \quad \tau \equiv \frac{\overline{f^\infty} a^2}{2kT} \qquad [28]$$

Here, τ is the characteristic time necessary for the diffusion layer (with typical dimension a) to develop. The potential beyond the double layer is given by:

$$\delta\psi^f = \left(-E_0 r + \frac{d_\psi a^3 E_0}{r^2} \right) \cos(\theta) \exp(\mathrm{i}\omega t) + \frac{kT}{e} \frac{\overline{f^\infty / z}}{\overline{f^\infty}} \frac{\delta n^f}{n^\infty} \qquad [29]$$

where d_ψ and d_n are polarization parameters, to be determined by boundary conditions imposed just beyond the double layer, the so-called "inner boundary conditions".

5. THE INNER BOUNDARY CONDITIONS

By subtracting the conservation equation for the far fields from the general conservation equation [13] and integration over the diffuse part of the double layer (d), we obtain the integrated flux balance for the perturbations in the diffuse layer:

$$\begin{aligned} &\frac{\partial}{\partial t} \int_d \left(\delta n_i - \delta n_i^f \right) dr - \nabla_t^2 \left(\frac{z_i e}{kT} \delta\psi^f + \frac{\delta n_i^f}{n_i^\infty} \right) \int_d \frac{kT}{f_i^\infty} \left(n_{i,eq} - n_i^\infty \right) dr + J_i^{d \to S} \\ &- \frac{kT}{f_i^\infty} n_i^\infty \frac{\partial}{\partial r} \left(\frac{z_i e}{kT} \delta\psi^f + \frac{\delta n_i^f}{n_i^\infty} \right) \Bigg|_{a^+} + \int_d \vec{\nabla} \cdot \left(n_{i,eq} - n_i^\infty \right) \vec{v} dr = 0 \end{aligned} \qquad [30]$$

$J_i^{d\rightarrow S}$ expresses the flux of i-type ions exchanging from the diffuse to the Stern layer. Fixman considered particles with fixed surface charge density and could neglect accumulation in the diffuse layer and normal transport from the diffuse to the Stern layer (14,1) but in the present study these two extra contributions must be taken into account. In the derivation of conditions [30] we have assumed that local equilibrium between the diffuse layer and the adjacent electrolyte is maintained. Following this assumption, $\delta\mu_i$ was considered to be equal to $\delta\mu_i^f$ in the double-layer region. The two extra contributions will be expressed in the far fields evaluated at the particle surface and eventually appear in the inner boundary conditions for the far fields.

Since the surface charge and the Stern-layer charge are located in one single plane, the surface potential ψ^0 and the Stern potential ψ^s are identical. The shear plane may be located somewhere beyond the particle surface, $|\zeta| \leq |\psi^0|$. Henceforth, the surface charge will be identified as just one of the i-type Stern ions. First we obtain the accumulation in the diffuse double layer. In leading order, there is no normal flux in the perturbed diffuse layer. Hence, the local ion density in the diffuse double layer will obey a Boltzmann distribution:

$$n_i \propto \exp(-z_i e\psi / kT) \qquad [31]$$

Just outside the diffuse double layer the potential is equal to $\delta\psi^f\big|_{r=a}$ [2] and as the ion density equals $n_i^f\big|_{r=a}$ the proportionality constant can be determined:

$$n_i = n_i^f\Big|_a \exp\left(-\frac{z_i e}{kT}\left[\psi - \delta\psi^f\Big|_a\right]\right) \qquad [32]$$

Subtracting the equilibrium distribution and omitting small second-order terms yields the perturbation in the ion density:

$$\delta n_i = \exp(-z_i e\psi_{eq} / kT)\left(\delta n_i^f\Big|_a - n_i^\infty \frac{z_i e}{kT}\left[\delta\psi - \delta\psi^f\Big|_a\right]\right) \qquad [33]$$

By substituting this expression into Poisson's equation, Hinch et al. (11) found, in the case of a symmetrical binary electrolyte, the potential profile in the perturbed flat diffuse double layer:

$$\delta\psi = \delta\psi^f\Big|_a + \frac{d\psi_{eq}}{dr}\left(B + \frac{1}{2}\frac{\delta n^f\big|_a}{n^\infty}(r-a)\right) \qquad [34]$$

where B is a constant determined by the boundary condition on the potential at $r = a$.

Using Eqs. [33] and [34], and the potential profile for a flat diffuse double layer we obtain the perturbations in the excess amount of accumulated ions in the diffuse part of the double layer $\delta\Gamma_i^d$:

---

[2] Far fields can only change significantly over distances of the order of the particle radius, so $\delta\psi^f\big|_{r=a^+}$ is in good approximation equal to $\delta\psi^f\big|_{r=a}$.

$$\begin{aligned}\delta\Gamma_i^d &\equiv \int_a^\infty (\delta n_i - \delta n_i^f)\,dr \\ &= \frac{n^\infty}{\kappa}\left(-\kappa B\left[\exp(-z_i e\psi_{eq}/kT)-1\right]+\frac{\delta n^f}{n^\infty}\left[\exp(-z_i e\psi_{eq}/2kT)-1\right]\right)\Bigg|_{r=a}\end{aligned} \qquad [35]$$

B follows from[3]:

$$\varepsilon^\infty \frac{\partial \delta\psi}{\partial r}\bigg|_a = -\delta\sigma^s \qquad [36]$$

All adsorbed species contribute to the total bound charge:

$$\delta\sigma^s = \sum_i \delta\sigma_i^s \equiv \sum_i z_i e\,\delta\Gamma_i^s \equiv \sum_i z_i e \int_S \delta n_i^s\,dr \qquad [37]$$

Needed are the perturbations in the adsorbed amounts. By integration of the conservation equation over the Stern layer (S) we obtain the integrated flux balance for the Stern layer:

$$\frac{\partial}{\partial t}\int_S \delta n_i\,dr - \int_S \vec{\nabla}_t \cdot \frac{kT}{f_i^s}\left(\frac{z_i e}{kT} n_{i,eq}\vec{\nabla}_t\delta\psi + \vec{\nabla}_t\delta n_i\right)dr - J_i^{d\to S} = 0 \qquad [38]$$

Because perturbations in the Stern-layer charge may also be generated by exchange of charge between the Stern layer and the diffuse layer, the development of a dynamic model for the description of this exchange is the next step of our analysis.

6. DYNAMIC MODELS FOR ION EXCHANGE BETWEEN THE STERN LAYER AND THE DIFFUSE LAYER

In this section we present two simple models for ion exchange between the Stern layer and the diffuse layer. The first model is specific and considers a site-binding mechanism. The second model is not specific and assumes the presence of an average, short-range ($<< \kappa^{-1}$) interaction potential responsible for accumulation of ions in the Stern layer. This interaction potential has a peaked narrow maximum at the boundary of the Stern and the diffuse layer. This maximum limits the rate of ion exchange between the two layers. Comparison between the two models yields a more general expression for ion exchange.

6.1. Site binding model

Consider the simple first-order site binding reaction of an ion of kind i, B_i, with a surface site S to form a surface complex B_iS. The reaction rate constants for adsorption and desorption are $k_{i,a}$ and $k_{i,d}$, respectively. Then:

---

[3] We assumed the permittivity of the particle to be small.

$$B_i + S \underset{k_{i,d}}{\overset{k_{i,a}}{\rightleftarrows}} B_iS \tag{39}$$

For this reaction, the net rate at which surface sites are occupied by species *i* is given by:

$$\frac{\partial \Gamma_i^s}{\partial t} = k_{i,a}\Gamma^{es} n_i\big|_a - k_{i,d}\Gamma_i^s \tag{40}$$

where Γ^{es} and Γ_i^s are the number of empty sites and that of occupied sites per unit surface area, respectively. In the equilibrium situation the net rate is equal to zero which relates the rate constants:

$$\frac{\Gamma_{eq}^{es} n_{i,eq}\big|_a}{\Gamma_{i,eq}^s} = \frac{k_{i,d}}{k_{i,a}} \equiv K_{i,eq} \tag{41}$$

If the applied electric field is small, we can linearize the rate equations. First we introduce small perturbation terms linear in the applied electric field:

$$\begin{gathered}\Gamma_i^s = \Gamma_{i,eq}^s + \delta\Gamma_i^s + \mathrm{O}(E_0^2) \\ \Gamma^{es} = \Gamma_{eq}^{es} + \delta\Gamma^{es} + \mathrm{O}(E_0^2) \\ \text{etc.}\end{gathered} \tag{42}$$

Substituting these expressions in the rate equation and omitting the small $\mathrm{O}(E_0^2)$ non-linear terms gives us the linearized rate equation:

$$\frac{\partial \delta\Gamma_i^s}{\partial t} = k_{i,a}\left(\Gamma_{eq}^{es}\,\delta n_i\big|_a + \delta\Gamma^{es} n_{i,eq}\big|_a\right) - k_{i,d}\Gamma_i^s \tag{43}$$

Using Eq. [41] to eliminate $k_{i,a}$ yields:

$$\frac{\partial \delta\Gamma_i^s}{\partial t} = k_{i,d}\Gamma_{i,eq}^s\left(\left.\frac{\delta n_i}{n_{i,eq}}\right|_a - \frac{\delta\Gamma^{es}}{\Gamma_{eq}^{es}} + \frac{\delta\Gamma_i^s}{\Gamma_{i,eq}^s}\right) \tag{44}$$

With the use of conservation of sites

$$\delta\Gamma^{es} + \sum_i \delta\Gamma_i^s = 0 \tag{45}$$

we obtain:

$$J_i^{d\to S} = \frac{\partial \delta\Gamma_i^s}{\partial t} = k_{i,d}\Gamma_{i,eq}^s\left(\left.\frac{\delta n_i}{n_{i,eq}}\right|_a - \frac{\delta\Gamma_i^s}{\Gamma_{i,eq}^s}\left[1 + \frac{\sum_i \delta\Gamma_i^s}{\delta\Gamma_i^s}\frac{\Gamma_{i,eq}^s}{\Gamma_{eq}^{es}}\right]\right) \tag{46}$$

6.2. Average interaction-potential adsorption model

In this model an ion of species *i* near the surface is supposed to experience an average specific interaction energy u_i^{int}. The Nernst-Planck equation for this situation is given by:

$$\vec{j}_i \cdot \vec{e}_r = -\frac{kT}{f_i}\left(n_i\left[\frac{z_i e}{kT}\frac{d\psi}{dr} + \frac{1}{kT}\frac{du_i^{int}}{dr} \right] + \frac{dn_i}{dr} \right) \qquad [47]$$

For small applied electric fields this equation can be linearized. First we introduce terms linear in the applied field:

$$\begin{aligned} \psi &= \psi_{eq} + \delta\psi + O(E_0^2) \\ u_i^{int} &= u_{i,eq}^{int} \\ n_i &= n_{i,eq} + \delta n_i + O(E_0^2) \end{aligned} \qquad [48]$$

The interaction potential is considered to be not perturbed by the applied electric field. Substituting these expressions and omitting small non-linear terms yields:

$$\vec{j}_i \cdot \vec{e}_r = -\frac{kT}{f_i} n_{i,eq} \frac{d}{dr}\left(\frac{ez_i}{kT}\delta\psi + \frac{\delta n_i}{n_{i,eq}} \right) = -\frac{kT}{f_i} n_{i,eq} \frac{d}{dr}\delta\mu_i \qquad [49]$$

Gradients in the electrochemical potential are the driving force for transport. Solving for $-kTd\delta\mu_i$ and integrating from a position $(a-\Delta)$ somewhere in the interior of the thin Stern layer to position a just beyond the bound layer (but in the inner part of the diffuse layer adjacent to the surface) yields:

$$\vec{j}_i \cdot \vec{e}_r \int\limits_{a-\Delta}^{a} \frac{f_i}{n_{i,eq}} dr = -kT \int\limits_{r=a-\Delta}^{r=a} d\delta\mu_i = -kT\left(\delta\mu_i\big|_a - \delta\mu_i\big|_{a-\Delta} \right) \qquad [50]$$

We assumed the energy barrier to be narrow and high. Then the normal flux through the barrier does not depend on the position (only a negligible fraction of the flux entering the barrier will be transported tangentially in the barrier or will be "used" to alter the chemical part of the electrochemical potential in the barrier in an alternating field at moderate frequencies) and can be taken out of the integration. The major contribution to the integral on the left-hand side in Eq. [50] stems from the small interval containing the barrier. There the equilibrium number density is small which yields a huge integrand. This is why the positions $(a-\Delta)$ and a do not have to be specified more precisely.

In this picture the major jump in electrochemical potential is in the barrier. The electrochemical potentials throughout the Stern and diffuse layers both are approximately constant in radial direction but in general not equal. Transport through the barrier is driven by the difference in electrochemical potential. By defining the effective transfer coefficient $\alpha_i^{\neq}$, Eq. [50] can be written in the form:

$$\vec{J}_i \cdot \vec{e}_r = -n_i^\infty \frac{kT}{\alpha_i^{\neq}} \left(\delta\mu_i\big|_a - \delta\mu_i\big|_{a-\Delta} \right), \quad \alpha_i^{\neq} \equiv f_i^\infty \int_{a-\Delta}^{a} \frac{f_i}{f_i^\infty} \frac{n_i^\infty}{n_{i,eq}} dr \qquad [51]$$

The Stern layer is considered to be thin. This means that the electric potential in the bound layer is equal to the potential in the inner part of the diffuse layer adjacent to the surface[4], i.e., the potential terms in Eq. [51] cancel:

$$\vec{J}_i \cdot \vec{e}_r = -n_i^\infty \frac{kT}{\alpha_i^{\neq}} \left(\frac{\delta n_i}{n_{i,eq}}\bigg|_a - \frac{\delta n_i}{n_{i,eq}}\bigg|_{a-\Delta} \right) \qquad [52]$$

Because the electrochemical potential and the electric potential in the Stern layer are constant, the chemical part of the electrochemical potential is also constant which implies:

$$\frac{\delta n_i}{n_{i,eq}}\bigg|_{a-\Delta} = \text{constant} \Rightarrow \frac{\delta n_i}{n_{i,eq}}\bigg|_{a-\Delta} = \frac{\int_S \delta n_i dr}{\int_S n_{i,eq} dr} = \frac{\delta \Gamma_i^s}{\Gamma_{i,eq}^s} \qquad [53]$$

Substituting this expression in Eq. [52] and noting that $J_i^{d\to S} = -J_i$ yields:

$$J_i^{d\to S} = \frac{n_i^\infty}{\Gamma_{i,eq}^s} \frac{kT}{\alpha_i^{\neq}} \Gamma_{i,eq}^s \left(\frac{\delta n_i}{n_{i,eq}}\bigg|_a - \frac{\delta \Gamma_i^s}{\Gamma_{i,eq}^s} \right) \qquad [54]$$

6.3. Comparison of the two adsorption models

An interesting case occurs in the situation where a small fraction of the surface sites is occupied. Then the term between square brackets in Eq. [46] is close to 1 and the normal flux in both models can be written in the form:

$$J_i^{d\to S} = \frac{1}{\tau_{i,\perp}} \Gamma_{i,eq}^s \left(\frac{\delta n_i}{n_{i,eq}}\bigg|_a - \frac{\delta \Gamma_i^s}{\Gamma_{i,eq}^s} \right) \qquad [55]$$

with, in case of the surface site model (Eq.[46]): $\frac{1}{\tau_{i,\perp}} = k_{i,d}$ (in reciprocal units of time)

and in case of the average potential model (Eq.[54]) $\frac{1}{\tau_{i,\perp}} = \frac{n_i^\infty}{\Gamma_{i,eq}^s} \frac{kT}{\alpha_i^{\neq}}$ (in reciprocal units of time)

More complex models can be developed but are not the object of study in this analysis. Eq. [55] is simple but bears the physics of retarded exchange in it and will be used in the integrated flux balance previously deduced.

---

[4] Stern layer capacities are not taken into account. This can easily be done but would add a lot of parameters.

7. THE POLARIZATION PARAMETER d_ψ AND THE LOW-FREQUENCY DIELECTRIC RESPONSE

By substituting the explicit form for $J_i^{d\to S}$ (Eq. [55]) in the integrated flux balance [38] and carrying out the integration we obtain:

$$\mathrm{i}\omega\delta\Gamma_i^s + \frac{2kT}{a^2 f_i^s}\left(\frac{z_i e}{kT}\delta\psi^s\Gamma_{i,eq}^s + \delta\Gamma_i^s\right) - \frac{1}{\tau_{i,\perp}}\Gamma_{i,eq}^s\left(\delta\mu_i^f\Big|_a - \frac{z_i e}{kT}\delta\psi^s - \frac{\delta\Gamma_i^s}{\Gamma_{i,eq}^s}\right) = 0 \qquad [56]$$

Solving for $\delta\Gamma_i^s$ yields:

$$\delta\Gamma_i^s = \left\{\frac{\dfrac{-z_i e}{kT}\Gamma_{i,eq}^s}{1+\mathrm{i}\omega\tau_i}\right\}\delta\psi^s + \frac{\tau_i}{\tau_{i,\perp}}\frac{\Gamma_{i,eq}^s}{1+\mathrm{i}\omega\tau_i}\delta\mu_i^f\Big|_a \qquad [57]$$

In this expression we recognised the relaxation times $\tau_{i,//}$ introduced previously:

$$\frac{1}{\tau_i} = \frac{1}{\tau_{i,//}} + \frac{1}{\tau_{i,\perp}}, \qquad \frac{1}{\tau_{i,//}} = \frac{2kT}{a^2 f_i^s} \qquad [58]$$

In the absence of normal exchange ($\tau_{i,\perp} = \infty$) the second term on the right-hand side of Eq. [57] disappears and the interaction between the two layers is completely of an electric nature, i.e., perturbations in Stern layer charge are generated by perturbations in the local potential (Eq. [57]). Vice versa, the Stern potential ψ^s depends on B (Eq. [34]) which, in turn, depends on the perturbations in the Stern layer via condition [36]. At low frequencies, perturbations in the Stern-layer charge are in phase with the driving perturbations in the potential. At frequencies around $1/\tau_{i,//}$ dispersion occurs. Now ion redistribution lags behind the local electric field. At much higher frequencies perturbations in charge are 90 degrees in phase behind as compared to the perturbations in the local potential and almost zero in amplitude, i.e., the ion distribution cannot follow the field.

If normal exchange is possible, the electrochemical potential of the diffuse layer appears in Eq. [57]. The total relaxation time τ_i can now be seen as the effective time of the two processes occurring in parallel. The smallest time is the most important for the resulting τ_i and for the frequency where the extra dispersion is to be expected.

From the combination of Eqs. [34], [36], [37] and [57] we obtain B^{cr}, i.e. B in this situation of "charge regulation":

$$B^{cr} = \left.\frac{-\dfrac{1}{2}\varepsilon^\infty\dfrac{d\psi_{eq}}{dr}\dfrac{\delta n^f}{n^\infty} + \left(\displaystyle\sum_i\frac{\sigma_{i,eq}^s}{1+\mathrm{i}\omega\tau_i}\frac{z_i e}{kT}\right)\delta\psi^f - \left(\displaystyle\sum_i\frac{\sigma_{i,eq}^s}{1+\mathrm{i}\omega\tau_i}\delta\mu_i^f\frac{\tau_i}{\tau_{i,\perp}}\right)}{\varepsilon^\infty\dfrac{d^2\psi_{eq}}{dr^2} - \left(\displaystyle\sum_i\frac{\sigma_{i,eq}^s}{1+\mathrm{i}\omega\tau_i}\frac{z_i e}{kT}\right)\dfrac{d\psi_{eq}}{dr}}\right|_a \qquad [59]$$

Substituting B^{cr} in Eq. [35] gives us the accumulation of ions in the diffuse layer expressed in far-fields evaluated at $r = a$.

The fluxes of ions exchanging from the Stern layer to the neighbouring diffuse layer can be found in a similar way. Using the integrated flux balance for the Stern layer [38] and Eq. [57] we obtain:

$$J_i^{d\to S} = \frac{\tau_i}{\tau_{i,//}\tau_{i,\perp}} \frac{\Gamma^s_{i,eq}}{1+\mathrm{i}\omega\tau_i}\left(-\mathrm{i}\omega\tau_{i,//}\frac{ez_i}{kT}\delta\psi^s + \left(1+\mathrm{i}\omega\tau_{i,//}\right)\delta\mu_i^f\Big|_a\right) \qquad [60]$$

Equation [34] relates the Stern potential to the far fields evaluated at $r = a$:

$$\delta\psi^s = \delta\psi^f\Big|_a + \frac{d\psi_{eq}}{dr}\bigg|_a B^{cr} \qquad [61]$$

Substitution of this expression in Eq. [60] and using [59] yields the required relation between the exchanging fluxes and the far fields evaluated at the surface. It is interesting to formulate the conditions under which the Stern layer is in thermodynamic equilibrium with the adjacent diffuse layer, i.e., $\delta\mu_i^s = \delta\mu_i^f\Big|_a$. It follows immediately from Eq. [57] and $\delta\mu_i^s = \delta\Gamma_i^s / \Gamma^s_{i,eq} + z_i e\delta\psi^s / kT$ that equilibrium is maintained under the conditions:

$$1/\tau_i >> \omega \quad \text{and} \quad \tau_i/\tau_{i,\perp} \approx 1 \qquad [62]$$

which are equivalent to

$$1/\tau_{i,\perp} >> \omega \quad \text{and} \quad \tau_{i,\perp}/\tau_{i,//} << 1 \qquad [63]$$

In this respect, Razilov's single condition $1/\tau_\perp >> \omega$ (15,16) is not sufficient to ensure local equilibrium between the layers.

An interesting situation is the entering flux in the zero frequency limit. Then, Eq. [60] reduces to:

$$J_i^{d\to S}\Big|_{\omega\tau_i\downarrow 0} = \frac{\tau_i}{\tau_{i,\perp}}\frac{2kT}{a^2 f_i^s}\Gamma^s_{i,eq}\delta\mu_i^f\Big|_a \qquad [64]$$

which indicates that, compared to the diffuse layer, the electrochemical potential in the Stern layer is lower by a factor $\tau_i/\tau_{i,\perp}$. This result will be used in section 8.

The charges and the potentials in the equation for B^{cr} are related. We choose to express B^{cr} in the potentials. With the definition of the Stern charge fractions Ω_i

$$\sigma^s_{i,eq} \equiv \Omega_i \sum_i \sigma^s_{i,eq} = -\Omega_i\varepsilon^\infty \frac{d\psi_{eq}}{dr}\bigg|_a \qquad [65]$$

and the diffuse double-layer expressions for flat plates

$$\frac{d\psi_{eq}}{dr} = -2\frac{kT}{ze}\kappa\sinh\left(\frac{ze\psi_{eq}}{2kT}\right), \quad z = |z_i| \qquad [66]$$

$$\frac{d^2\psi_{eq}}{dr^2} = \frac{kT}{ze}\kappa^2 \sinh\left(\frac{ze\psi_{eq}}{kT}\right) = -\kappa\frac{d\psi_{eq}}{dr}\cosh\left(\frac{ze\psi_{eq}}{2kT}\right) \tag{67}$$

substituted in Eq. [59] we obtain:

$$\begin{aligned} B^{cr} &= \left.\frac{1}{\kappa}\frac{\frac{1}{2}\frac{\delta n^f}{n^\infty} + \left(\sum_i \frac{\Omega_i}{1+\mathrm{i}\omega\tau_i}\frac{z_i e}{kT}\right)\delta\psi^f - \left(\sum_i \frac{\Omega_i}{1+\mathrm{i}\omega\tau_i}\delta\mu_i^f\frac{\tau_i}{\tau_{i,\perp}}\right)}{\cosh\left(\frac{ze\psi_{eq}}{2kT}\right) + 2\frac{kT}{ze}\left(\sum_i \frac{\Omega_i}{1+\mathrm{i}\omega\tau_i}\frac{z_i e}{kT}\right)\sinh\left(\frac{ze\psi_{eq}}{2kT}\right)}\right|_a \\ &\equiv \left.\frac{1}{\kappa}\left(\delta h^f B^h + \delta\varphi^f B^\varphi + \sum_i B_i^\mu \delta\mu_i^f\right)\right|_a \end{aligned} \tag{68}$$

where h_i is the non-dimensional ion density, $h_i = n_i / n_i^\infty$, and φ is the non-dimensional potential, $\varphi = e\psi / kT$. The functions B^h, B^φ, and B_i^μ are explicitly given in the appendix. Note that $\psi_{eq}\big|_a = \psi^0$ is the equilibrium surface potential. The extra contributions expressed in the far fields evaluated at the surface read:

$$\mathrm{i}\omega\delta\Gamma_i^d = \mathrm{i}\omega\frac{n^\infty}{\kappa}\left(-\kappa B^{cr}\left[\exp(-z_i e\psi^0/kT) - 1\right] + \delta h^f\left[\exp(-z_i e\psi^0/2kT) - 1\right]\right)\Big|_a \tag{69}$$

$$J_i^{d\to S} = \frac{\tau_i}{\tau_{i,\perp}}\frac{4\Omega_i \sinh(z_i e\psi^0/2kT)}{1+\mathrm{i}\omega\tau_i}\frac{n^\infty}{\kappa}\left\{\left(2\kappa B^{cr}\sinh(z_i e\psi^0/2kT) + \delta h^f\right)\mathrm{i}\omega + \frac{\delta\mu_i^f}{\tau_{i,//}}\right\}\Bigg|_a \tag{70}$$

These adaptations will be implemented in Fixman's boundary condition (1). For the sake of clarity we shall follow Fixman's notation in non-dimensional operators and fields

$$R \equiv \kappa r, \quad \vec{\nabla}_R \equiv \kappa^{-1}\vec{\nabla}, \quad \tilde{E}_0 \equiv \frac{e}{kT\kappa}E_0 \tag{71}$$

The modified non-dimensional boundary conditions are given by:

$$\left.\frac{\partial\delta\mu_i^f}{\partial R}\right|_{R=\kappa a} - \frac{2}{(\kappa a)^2}\sum_j A_{ij}\delta\mu_j^f\Big|_{R=\kappa a} - \frac{f_i^\infty}{kT\kappa n^\infty}\left(\mathrm{i}\omega\delta\Gamma_i^d + J_i^{d\to S}\right) = 0 \tag{72}$$

The functions A_{ij} were calculated by Fixman (1) and are given in the appendix. The extra contributions in equations [69] and [70] that are explicit in $\delta\mu_j^f$ are now implemented in A_{ij} to form A'_{ij}. Furthermore, the extra contributions explicit in δh^f and $\delta\varphi^f$ are collected in the functions D_i^h and D_i^φ, respectively. We obtain:

$$\left.\frac{\partial\delta\mu_i^f}{\partial R}\right|_{R=\kappa a} - \frac{1}{(\kappa a)^2}\left(D_i^h\delta h^f + D_i^\varphi\delta\varphi^f + 2\sum_j A'_{ij}\delta\mu_j^f\right)\Bigg|_{R=\kappa a} = 0 \tag{73}$$

The far-field equations in non-dimensional form read:

$$\nabla_R^2 \delta h^f = \tilde{\lambda}^2 \delta h^f \tag{74}$$

$$\nabla_R^2 \delta \varphi^f = \overline{f^\infty / z}\, \tilde{\lambda}^2 \delta h^f \tag{75}$$

$$\tilde{\lambda} \equiv (1 + \mathrm{i}) \sqrt{\frac{\omega \overline{f^\infty}}{2kT\kappa^2}} \tag{76}$$

with the non-dimensional solutions:

$$\delta h^f = -d_h \tilde{E}_0 \frac{1}{R^2} \left(1 + \tilde{\lambda} R\right) \exp\left(-\tilde{\lambda} R\right) \cos\theta \tag{77}$$

$$\delta \varphi^f = \left(-\tilde{E}_0 R + \frac{d_\psi (\kappa a)^3 \tilde{E}_0}{R^2} \right) \cos\theta + \frac{\overline{f^\infty / z}}{\overline{f^\infty}} \delta h^f \tag{78}$$

Applying the inner boundary conditions to these expressions yields the polarization parameter:

$$d_\psi = \frac{L_1 H_2 - L_2 H_1}{N_1 H_2 - N_2 H_1} \tag{79}$$

where

$$H_i = \frac{1}{\kappa a} \left(2 + 2x + x^2\right) \left(1 + z_i \frac{\overline{f^\infty / z}}{\overline{f^\infty}}\right) + \frac{(1 + x)}{(\kappa a)^2} \left\{ D_i^h + \frac{\overline{f^\infty / z}}{\overline{f^\infty}} D_i^\varphi + 2 \sum_j A'_{ij} \left(1 + z_j \frac{\overline{f^\infty / z}}{\overline{f^\infty}}\right) \right\} \tag{80}$$

$$N_i = -2 z_i - \frac{1}{\kappa a} \left\{ D_i^\varphi + 2 \sum_j A'_{ij} z_j \right\} \tag{81}$$

$$L_i = z_i - \frac{1}{\kappa a} \left\{ D_i^\varphi + 2 \sum_j A'_{ij} z_j \right\} \tag{82}$$

The complex conductivity $\hat{K}$ of a system is defined by

$$\bar{i} = \hat{K} \bar{E} \tag{83}$$

where $\bar{i}$ is the (macroscopic) electric current density. $\hat{K}$ can be decomposed into its real and imaginary components:

$$\hat{K}(\phi, \omega) \equiv K(\phi, \omega) + \mathrm{i}\, \omega \varepsilon_0 \varepsilon_r(\phi, \omega) \tag{84}$$

Here, ϕ denotes the particle volume fraction. In the absence of particles, $\hat{K}$ simply reduces to:

$$\hat{K}(0, \omega) = K^\infty + \mathrm{i}\, \omega \varepsilon_0 \varepsilon_r^\infty \equiv \hat{K}^\infty(\omega) \tag{85}$$

where K^∞ is the dc conductivity of the electrolyte solution and ε_r^∞ the relative dielectric permittivity of the electrolyte solution (≈80 for aqueous solutions) which both are independent of the frequency in the regime of interest ($\omega << K^\infty / \varepsilon_0 \varepsilon_r^\infty$). For dilute dispersions, $\hat{K}$ is related to the electric polarization parameter d_ψ according to (3,13):

$$\hat{K}(\phi,\omega) = \hat{K}^\infty + 3\phi \, d_\psi \hat{K}^\infty \qquad [86]$$

Hence, by combining Eq. [84] and [86], the experimentally accessible $K(\phi,\omega)$ and $\varepsilon_r(\phi,\omega)$ are expressed in terms of d_ψ which, in turn, is related to the polarization processes in the double layer.

Increments are defined as the deviations from the bulk values:

$$\Delta K(\phi,\omega) = K(\phi,\omega) - K^\infty \qquad [87]$$

$$\Delta \varepsilon_r(\phi,\omega) = \varepsilon_r(\phi,\omega) - \varepsilon_r^{\infty} \qquad [88]$$

In dielectric studies often increments due to changes in frequency are considered. The conductivity relative to the same at a reference frequency $\omega_{ref,K}$ much smaller than τ^{-1} is defined as:

$$\Delta_\omega K(\phi,\omega) = K(\phi,\omega) - K(\phi,\omega_{ref,K}) \qquad [89]$$

and the permittivity relative to the value at a reference frequency $\omega_{ref,\varepsilon}$ much larger than τ^{-1}:

$$\Delta_\omega \varepsilon_r(\phi,\omega) = \varepsilon_r(\phi,\omega) - \varepsilon_r(\phi,\omega_{ref,\varepsilon}) \qquad [90]$$

8. LIMITING EXPRESSIONS FOR THE PERMITTIVITY, CONDUCTIVITY AND DC PARTICLE MOBILITY

The polarization of the Stern layer is described by rather untransparant complex functions. In this section we present simple approximate expressions for some important situations. We consider a surface with fixed surface charge density. The countercharge is distributed over the Stern layer and the diffuse layer. Lateral mobilities of Stern ions need not be identical to those in the bulk. For the diffuse part the mobilities of cations and anions are assumed identical, and equal to their values in bulk. Furthermore, we assume that the boundary of the Stern layer coincides with the slip plane. Hence, $\psi^0 = \zeta$.

In section 7 it was concluded that the contribution of the Stern layer to the surface conductivity in the low-frequency limit is the fraction $\tau_i / \tau_{i,\perp}$ of the value of a Stern layer in local equilibrium with the neighbouring diffuse layer. Hence the approximate expressions for the static conductivity derived in our previous study (8) can be adapted in a very simple manner:

$$K(\phi,0) = K^\infty + 3\phi K^\infty \left[-\frac{1}{2} + \frac{3}{4} \frac{Du_2}{1 + Du_2} \right] \qquad [91]$$

where the relative surface conductivity Du_2 is given by (8):

$$Du_2 = \frac{2}{\kappa a}\left(1+3m_2/z_2^2+(\tau_2/\tau_{2,\perp})\Theta_2\right)\left[\exp(-z_2e\zeta/2kT)-1\right] \qquad [92]$$

Here, $\Theta_2=(\sigma_2^s/f_2^s)/(\sigma_2^d/f_2^\infty)$ where σ_2^d is the contribution of the counterions to the countercharge in the diffuse layer. This limiting expression can also be found after some algebra from the results obtained in this study under the appropriate assumptions (8). The subscript "2" refers to the counterions.

The limiting high-frequency conductivity is derived from the results obtained in this study under equivalent assumptions:

$$K(\phi,\omega\tau>>1)=K^\infty+3\varphi K^\infty\left[-\frac{1}{2}+\frac{3}{4}\frac{Du_2'}{2+Du_2'}\right] \qquad [93]$$

where Du_2' is now given by:

$$Du_2'=\frac{2}{\kappa a}(1+3m_2/z_2^2+\Theta_2)\left[\exp(-z_2e\zeta/2kT)-1\right] \qquad [94]$$

Hence, $K(\phi,\omega\tau>>1)$ is completely independent of the extent of exchange. Even if exchange is impossible ($\tau_{2,\perp}=\infty$) the Stern layer completely contributes to the surface conductivity Du_2'. This is because a complete ion redistribution in the Stern layer, and consequently stagnation in ion movement, cannot occur at these high frequencies. Note that the limiting conductivity increment $\Delta_\omega K(\phi,\omega\tau>>1)=K(\phi,\omega\tau>>1)-K(\phi,\omega\tau\downarrow 0)$ is of course depending on $\tau_2/\tau_{2,\perp}$. The particle mobility can be described by the approximate equation given by e.g. O'Brien and Hunter (17,18):

$$\frac{\eta eu}{\varepsilon^\infty kT}=\frac{e\zeta}{kT}+\frac{Du_2}{1+Du_2}\left\{\frac{2\ln 2}{-z_2}-\frac{e\zeta}{kT}\right\} \qquad [95]$$

The Du_2 appearing in this expression is given by Eq. [92]. The particle mobility is more retarded for higher surface conduction, e.g., due to a more easy exchange ($\tau_2/\tau_{2,\perp}$ closer to unity).
Finding equations for the static permittivity increment is not difficult but rather elaborate. For the situation of no exchange ($\tau_2/\tau_{2,\perp}=0$) we collected the terms in d_ψ which are proportional to $i\omega$ at low frequencies and, after neglect of the unimportant terms as discussed above, obtained

$$\begin{aligned}\Delta_\omega\varepsilon_r(\phi,\omega\tau\downarrow 0) &= \frac{9}{16}\varepsilon_r^\infty(\kappa a)^2\phi\left(\frac{Du_2}{1+Du_2}\right)^2+\\ &+\frac{9}{8}\varepsilon_r^\infty(\kappa a)\phi\frac{2\Omega_2\frac{z^s}{z}\sinh(z\varphi^0)}{\cosh(z\varphi^0/2)+2\Omega_s\frac{z^s}{z}\sinh(z\varphi^0/2)}\left(\frac{1}{1+Du_2}\right)^2\end{aligned} \qquad [96]$$

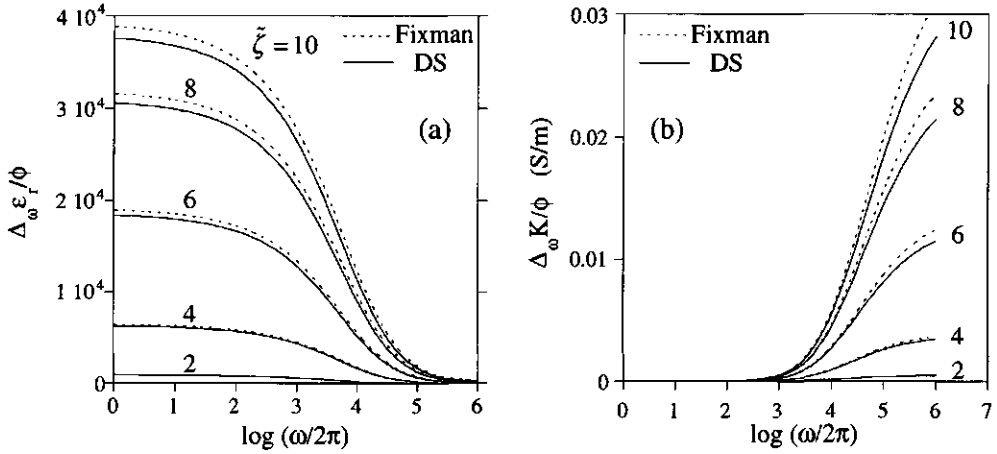

Figure 1. (a) Permittivity and (b) conductivity increment of a dilute dispersion. The particle surface charge density is fixed and no Stern layer is present. Calculations according to Fixman (1) and to our Dynamic Stern-layer model (DS) for various $\tilde{\zeta}$-potentials (indicated).

The first term on the right-hand side is the classical diffuse double-layer contribution (8). The second term is the contribution due to polarization of the Stern layer. It becomes negligibly small at higher surface potentials where $Du_2 >> O(1)$. In the situation of no exchange, ions in the Stern layer may be of a different type than the ions of the suspending electrolyte giving rise to the coefficients z^s/z. For the case of adsorption of suspending electrolyte where $|z^s/z|=1$, Eq. [96] reduces to the one derived by Razilov et al. (9,10).

9. RESULTS AND DISCUSSION

In order to illustrate the dynamic Stern-layer model as developed above, we here present results for some interesting situations. All calculations are performed for particles with radius $a = 250$ nm and relatively thin double layers ($\kappa a = 30$) suspended in an aqueous KCl-solution (ionic strength approximately 1 mM) for which the ions have identical mobilities. Furthermore, we assumed that the shear plane coincides with the particle surface. Hence, $\psi^0 = \zeta$. Ions which have a sign equal to the one of ζ are referred to as the co-ions. The counterions have opposite sign.

The dielectric increment and the conductivity increment are depicted for various surface potentials in Fig. 1. Ions on the surface and in the Stern layer are considered immobile (no tangential motion, no exchange). For this situation the results given by Fixman's theory do not diverge significantly from our dynamic Stern-layer model (DS). Under the restriction of a constant surface charge density, the accumulations of (both type) ions in the diffuse part of the double

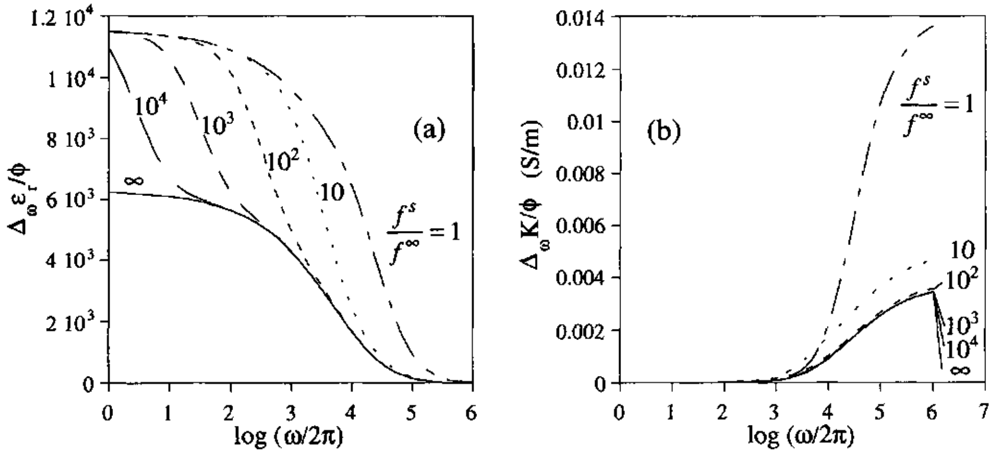

Figure 2. (a) Permittivity and (b) conductivity increment according to our DS-model for $\tilde{\zeta} = 4$. Half of the immobile surface charge is screened by mobile charge in the Stern layer ($\Omega_2 = -1,\ \Omega_1 = 0$). The mobility in the Stern layer is varied between the bulk value ($f^s = f^\infty$) and zero ($f^s = \infty$).

layer are small but not exactly zero and this results in the small differences obtained (see Eq. [69]).

Fig. 2 shows the dielectric increment and the conductivity increment for $\tilde{\zeta} = e\zeta / kT = 4$. Half of the immobile surface charge is screened by the mobile Stern-layer charge ($\Omega_2 = -1,\ \Omega_1 = 0$). Ions in the Stern layer are unable to exchange with the neighbouring diffuse layer. An extra dispersion occurs at the frequency where ion movement in the Stern layer is just able to significantly polarize the Stern layer. With decreasing mobility in the Stern layer this dispersion is shifted to lower frequencies. The mobility was decreased in steps of a factor of 10 starting with the bulk mobility. Accordingly, the dispersion frequency shifts downwards by the same factor. At low frequencies ($\omega\tau_{i,//} << 1$) the polarization of the Stern layer is relaxed and independent of the Stern-ion mobility. The currents responsible for the accumulations (proportional to the time derivative of the accumulation) are out of phase and contribute to the observable macroscopic current density as an iω-term. Hence the response near zero frequency is independent of the mobility in the Stern layer. This is shown by Fig. 2 as well as by expression [96]. The asymptotic conductivity increment $\Delta_\omega K / K^\infty(\omega >> \tau, \tau_i)$ reduces to the increment of solely the diffuse layer for low Stern-layer mobilities (see also Eqs. [91] and [92]). We note that identical results are obtained for the situation where the surface charge is absent ($\Omega_2 = 0,\ \Omega_1 = 1,\ \tilde{\zeta} = -4$).

In order to investigate the influence of the surface potential on the dispersion we depict in Fig. 3 the permittivity increments for the previously chosen charge distribution ($\Omega_2 = -1,\ \Omega_1 = 0$) but

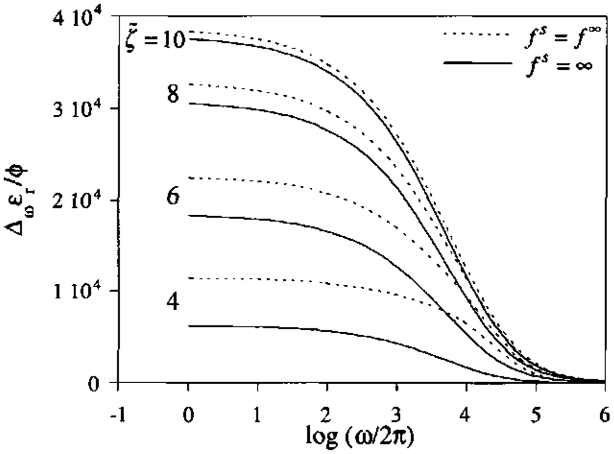

Figure 3. Permittivity increment according to our DS-model for various $\tilde{\zeta}$-potentials. Half of the immobile surface charge is screened by mobile charge in the Stern layer ($\Omega_2 = -1,\ \Omega_1 = 0$). The response for every $\tilde{\zeta}$-potential is calculated for situations where the ions in the Stern layer are immobile or have the bulk mobility.

now as a function of the surface potential. Ions in the Stern layer are considered as mobile as in the bulk. At low ζ-potentials the Stern-layer response prevails over the diffuse-layer response. With increasing ζ-potentials the Stern-layer contribution decreases and eventually only the diffuse-layer dispersion remains. This behaviour is in line with Eq. [96].

In Fig. 4 we plot the zero-frequency limit of the dielectric increment as a function of the ζ-potential according to different theories. Half of the immobile surface charge is screened by the mobile Stern-layer charge ($\Omega_2 = -1,\ \Omega_1 = 0$). For low ζ-potentials the results according to Lyklema et al. (6) are identical to those of Razilov et al. (9,10) and our DS-model. When concentration polarization of the diffuse layer sets in ($Du_2 = O(1)$), deviations appear. The occurrence of concentration polarization reduces the extra response. Some of the aspects of the situations shown in the figures 2, 3 and 4 were already investigated by Razilov et al. (9,10). We basically find the same characteristics in these situations.

Figure 5 depicts the dielectric response in the situation of a Stern layer in local equilibrium (free exchange) with the diffuse layer in comparison with the situation of absence of exchange. The ions in the Stern layer have no lateral mobility. Half of the immobile surface charge is screened by the immobile Stern-layer charge ($\Omega_2 = -1,\ \Omega_1 = 0,\ \tilde{\zeta} = 6$). There is no substantial difference between the responses in the two situations. The reason for this is that if a counterion adsorbs from the diffuse layer into the Stern layer to increase the Stern-layer charge locally by $z_2 e$, the non-linear diffuse layer (we suppose $|\tilde{\zeta}| >> 1$) tends to respond by locally loosing a counterion.

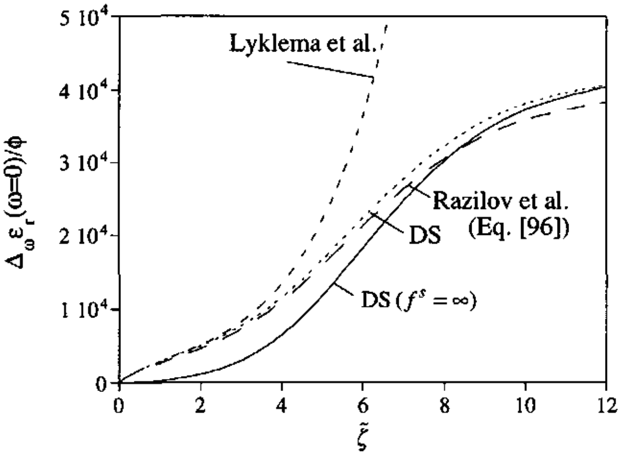

Figure 4. Zero-frequency dielectric increment as a function of the $\tilde{\zeta}$-potential for the situation as in Fig. 3 ($\Omega_2 = -1$, $\Omega_1 = 0$), calculated according to different theories: Lyklema et al., Razilov et al. (Eq. [96]), and DS. For comparison, the data in absence of Stern layer transport (DS ($f^s = \infty$)) are also included.

However, this just occurred by the counterion skipping position. Hence the far fields (concentration and potential) as well as the dielectric dispersion are unaffected.

We have included in Fig. 5 the results of a comparable situation, but now in the absence of surface charge. Then the Stern layer is occupied by co-ions by definition ($\Omega_2 = 0$, $\Omega_1 = 1$, $\tilde{\zeta} = -6$). In this situation the response is indeed affected by free exchange and it is significantly higher. The reason for this is that when a co-ion adsorbs from the diffuse layer into the Stern layer to increase the Stern-layer charge locally by $z_1 e$, the non-linear diffuse layer prefers to respond by locally gaining a counterion instead of loosing a co-ion. Hence, via tangential transport in the diffuse double layer co-operative with normal transport induced by the far fields both a co-ion and a counterion are delivered locally to the diffuse layer. Hence the far fields are affected, and so is the dielectric response. In Fig. 5 we have also plotted a situation of retarded co-ion exchange ($\tau_{1,\perp} / \tau = 10^3$). An extra dispersion is obtained around 300 Hz. For frequencies much higher than 300 Hz, the Stern layer is unable to respond via normal exchange. Then, the response is due to the diffuse layer only. For frequencies much lower than 300 Hz, the Stern layer is able to relax completely via exchange and the permittivity increment is equal to that of free co-ion exchange. The relaxation frequency depends on $\tau_{1,\perp}$ but the zero-frequency limit of the permittivity increment does not.

In Fig. 6 we plot the zero-frequency limit of the dielectric increment in the situation of free counterion exchange ($\Omega_2 = -1$, $\Omega_1 = 0$, $\tilde{\zeta} = 6$), and free co-ion exchange ($\Omega_2 = 0$, $\Omega_1 = 1$, $\tilde{\zeta} = -6$) as a function of the ratio f_i^∞ / f_i^s, i.e., the ratio between the mobility in the Stern layer

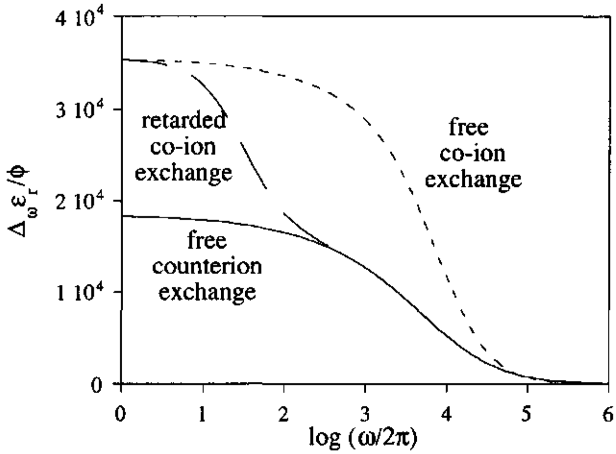

Figure 5. Dielectric increment according to our DS-model for three different Stern layers. The ions in the Stern layer have no lateral mobility in any of the three situations. 1) Free counterion exchange: the Stern layer is in local equilibrium (free exchange) with the diffuse layer. Half of the immobile surface charge is screened by the immobile charge in the Stern layer ($\Omega_2 = -1$, $\Omega_1 = 0$, $\tilde{\zeta} = 6$). 2) Free co-ion exchange: a situation comparable to the previous one, but now in the absence of surface charge ($\Omega_2 = 0$, $\Omega_1 = 1$, $\tilde{\zeta} = -6$). 3) Retarded co-ion exchange ($\Omega_2 = 0$, $\Omega_1 = 1$, $\tilde{\zeta} = -6$, $\tau_{1,\perp}/\tau = 10^3$). Here, an extra dispersion is obtained.

and the mobility in the bulk. In the case of counterion exchange, Kijlstra et al's model for a Stern layer in equilibrium with the diffuse layer (4) is in good agreement with our dynamic Stern-layer model. Then at $f_2^\infty / f_2^s = 0$ only the diffuse layer contributes to the dielectric increment. With increasing f_2^∞ / f_2^s the counterions in the Stern layer increasingly contribute. The Stern layer is polarized by concentration polarization which can be described by the classical concentration-polarization theory for polarization of the complete double layer. In the case of co-ion exchange, results are different. At $f_1^\infty / f_1^s = 1$, co-ions and counterions in the double layer are individually responsible for (nearly) half the conductivity in the (complete) double layer as well as in the bulk. Hence, concentration polarization is (nearly) absent and the permittivity increment is small. The classical theory for polarization of the complete double layer due to concentration polarization is not suitable for co-ion exchange as shown by the discrepancy in Kijlstra's results.

The main interest of this study is the situation of ions in the Stern layer which are mobile and able to exchange retardedly with the adjacent diffuse layer. The permittivity increment for retarded counterion exchange for the situation $\Omega_2 = -1$, $\Omega_1 = 0$, $\tilde{\zeta} = 4$ is presented in Fig. 7. Ions in the Stern layer are chosen to be 1000 times less mobile than in the bulk. In Fig. 2a we showed this situation for complete absence of exchange. Here, we varied $\tau_{2,\perp}/\tau_{2,//}$ between ∞ and 0 as indicated. Typically around $\tau_{2,\perp}/\tau_{2,//} = 1$ the dielectric increment changes from the increment in

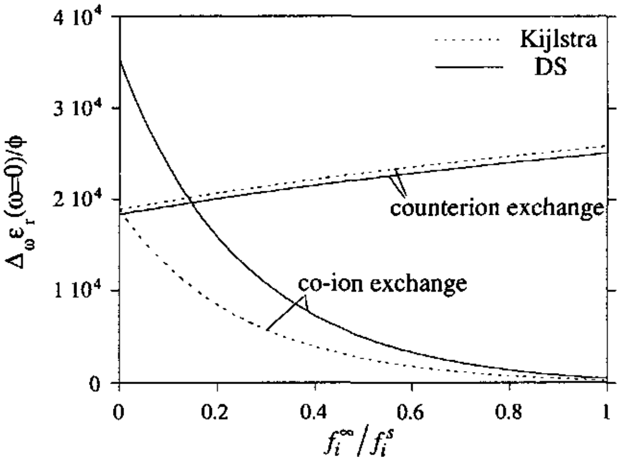

Figure 6. Zero-frequency limit of the dielectric increment as a function of the ratio f_i^∞ / f_i^s for free counterion exchange ($\Omega_2 = -1,\ \Omega_1 = 0,\ \bar{\zeta} = 6$) and for free co-ion exchange ($\Omega_2 = 0,\ \Omega_1 = 1,\ \bar{\zeta} = -6$). Calculations according to Kijlstra are included for comparison.

the situation of no exchange to the classical situation of the complete double layer in local equilibrium. Since ions in the Stern layer have a very low mobility compared to ions in the diffuse layer, the dielectric increment of the complete double layer in equilibrium (free exchange) is (almost) fully determined by the diffuse layer. Furthermore, the conductivity increment is insensitive to processes in the Stern layer due to the low Stern-layer ion mobility. This immediately follows from Eqs. [93] and [94].

10. CONCLUSIONS

We were able to incorporate the influence of a dynamic Stern layer in Fixman's boundary conditions and have investigated its effect on the complex conductivity of a dilute dispersion in the low-frequency regime, and on the particle dc mobility. In the limiting situations of no exchange or free exchange of counterions, the results generated by our dynamic Stern-layer model are in agreement with those of existing theories.

The intermediate situation of retarded exchange was investigated. Transitions between the situations of complete absence of exchange and completely free exchange typically occurred around $\tau_\perp / \tau_{//} = O(1)$.

The dc particle mobility can only be retarded by lateral mobile charge inside the Stern layer if this charge is able to leave the Stern layer. The extent to which the Stern charge contributes to the surface conduction and retardation of the particle mobility depends on the ratio $\tau_\perp / \tau_{//}$.

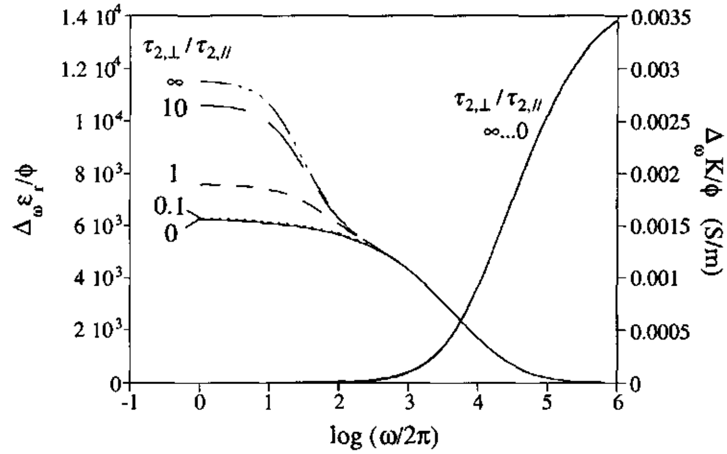

Figure 7. Permittivity and conductivity increments for retarded counterion exchange in the situation $\Omega_2 = -1$, $\Omega_1 = 0$, $\tilde{\zeta} = 4$. Ions in the Stern layer are chosen to be 1000 times less mobile than those in the bulk ($f^s / f^\infty = 10^{-3}$). The ratio $\tau_{2,\perp} / \tau_{2,//}$ was varied between ∞ and 0.

This dynamic Stern layer model may be helpful in explaining the extremely high dielectric response (19,20), extra dispersions, or dispersion frequencies which differ from the theoretical values (21,22). Information on the dynamics of charge redistribution in the Stern layer, important in modern stability theories, is in principle accessible by LFDD experiments.

APPENDIX

$$D_i^h = x^2 \frac{f_i^\infty}{f^\infty} \left\{ B^h \left(-\left[\exp(-z_i\varphi^0) - 1 \right] + 2M_i \sinh(z_i\varphi^0/2) \right) + \left[\exp(-z_i\varphi^0/2) - 1 \right] + M_i \right\} \quad \text{[A.1]}$$

$$D_i^\varphi = x^2 \frac{f_i^\infty}{f^\infty} B^\varphi \left\{ -\left[\exp(-z_i\varphi^0) - 1 \right] + 2M_i \sinh(z_i\varphi^0/2) \right\} \quad \text{[A.2]}$$

$$M_i = 4\Omega_i \frac{\tau_i}{\tau_{i,\perp}} \frac{\sinh(z_i\varphi^0/2)}{1 + \frac{1}{2}x_i^2} \quad \text{[A.3]}$$

$$B^h = \frac{1}{2\mathrm{Den}}, \quad B^\varphi = \frac{1}{\mathrm{Den}} \sum_i \frac{\Omega_i\, z_i}{1 + \frac{1}{2}x_i^2}, \quad B_j^\mu = -\frac{1}{\mathrm{Den}} \frac{\Omega_j}{1 + \frac{1}{2}x_j^2} \frac{\tau_j}{\tau_{j,\perp}} \quad \text{[A.4]}$$

$$\mathrm{Den} = \cosh(z\varphi^0/2) + \frac{2}{z} \left(\sum_i \frac{\Omega_i\, z_i}{1 + \frac{1}{2}x_i^2} \right) \sinh(z\varphi^0/2) \quad \text{[A.5]}$$

$$A'_{ij} = A_{ij} + G_{ij} \qquad [A.6]$$

$$G_{ij} = \frac{1}{2} x^2 \frac{f_i^\infty}{\overline{f^\infty}} B_j^\mu \left\{ -\left[\exp(-z_i \varphi^0) - 1 \right] + 2M_i \sinh(z_i \varphi^0 / 2) \right\} + \delta_{ij} \frac{f_i^\infty}{f_i^s} M_i \qquad [A.7]$$

$$\delta_{ij} = 0 \text{ if } i \neq j, \quad \delta_{ii} = 1 \qquad [A.8]$$

$$x = (1 + \mathrm{i})\sqrt{\omega\tau}, \quad \tau \equiv \frac{\overline{f^\infty} a^2}{2kT}, \quad x_i = (1 + \mathrm{i})\sqrt{\omega\tau_i} \qquad [A.9]$$

The expressions for A_{ij} read:

$$A_{ij} = I_i^d \delta_{ij} - \frac{3m_i}{4z^2} I_{ij} \qquad [A.10]$$

where

$$I_i^d = -4K_i / (1 + K_i) \qquad [A.11]$$

$$m_i = \frac{2\varepsilon^\infty kT f_i^\infty}{3\eta e^2} \qquad [A.12]$$

$$I_{ij} = -8\ln(1 - K_i^2) \text{ if } i \neq j, \quad I_{ii} = 16\left[K_i / (1 + K_i) - \ln(1 + K_i) \right] \qquad [A.13]$$

$$K_i = \tanh(z_i \tilde{\zeta} / 4) \qquad [A.14]$$

REFERENCES

(1) Fixman, M., *J. Chem. Phys.* **78,** 1483 (1983).

(2) Schwarz, G., *J. Phys. Chem.* **66,** 2636 (1962).

(3) Dukhin, S. S., Shilov, V. N., "Dielectric Phenomena and the Double Layer in Disperse Systems and Polyelectrolytes", Wiley, New York, 1974.

(4) Kijlstra, J., Leeuwen, H. P. van, Lyklema, J., *J. Chem. Soc., Faraday Trans. 2* **88,** 3441 (1992).

(5) Rosen, L. A., Baygents, J. C., Saville, D. A., *J. Chem. Phys* **98,** 4183 (1993).

(6) Lyklema, J., Dukhin, S. S., Shilov, V. N., *J. Electroanal. Chem.* **143,** 1 (1983).

(7) Minor, M., Linde, A. J. van der, Lyklema, J., submitted to *J. Colloid Interface Sci.* (chapter 2 of this thesis).

(8) Minor, M., Leeuwen, H. P. van, Lyklema, J., submitted to *J. Colloid Interface Sci.* (chapter 3 of this thesis).

(9) Razilov, I. A., Dukhin, S. S., *Colloid J.* **57,** 364 (1995).

(10) Razilov, I. A., Gonzales-Caballero, F., Delgado, A. V., Dukhin, S. S., *Colloid J.* **58,** 222 (1996).

(11) Hinch, E. J., Sherwood, J. D., Chew, W. C., Sen, P. N., *J. Chem. Soc., Faraday Trans. 2* **80,** 535 (1984).

(12) O'Brien, R. W., *Adv. Colloid Interface Sci.* **16,** 281 (1982).

(13) DeLacey, E. H. B., White, L. R., *J. Chem. Soc., Faraday Trans. 2* **77,** 2007 (1981).

(14) Fixman, M., *J. Chem. Phys.* **72,** 5177 (1980).

(15) Razilov, I. A., Pendze, G., Dukhin, S. S., *Colloid J.* **56,** 612 (1994).

(16) Razilov, I. A., Pendze, G., Lyklema, J., Dukhin, S. S., *Colloid J.* **56,** 736 (1994).
(17) O'Brien, R. W., Hunter, R. J., *Canad. J. Chem.* **59,** 1878 (1981).
(18) Hunter, R. J., "Foundations of Colloid Science", Vol II, Oxford University Press, New York, 1989.
(19) Springer, M. M., Ph. D. Thesis, Wageningen Agricultural University, 1979.
(20) Springer, M. M., Korteweg, A., Lyklema, J., *J. Electroanal. Chem.* **153,** 55 (1989).
(21) Rosen, L. A., Saville, D. A., *J. Colloid Interface Sci.* **140,** 82 (1990).
(22) Rosen, L. A., Baygents, J. C., Saville, D. A., *J. Chem. Phys.* **98,** 4183 (1993).

Chapter 8

SURFACE CHARGE RELAXATION IN PARTICLE COAGULATION

Abstract. The stability of colloids was connected to the rate at which the surface charge on the particles relaxes towards equilibrium. Since more than one surface charge relaxation mechanism (desorption and surface migration) occurs simultaneously, the faster of the two dominates the extent of disequilibration during particle interaction. Only small disequilibrations are dealt with. Furthermore, a first attempt is made to generalize by taking into account all possible trajectories leading to particle-particle contact. This is necessary for the study of coagulation under conditions far from equilibrium (in between constant potential and constant charge) where the extent of disequilibration is large. This situation can be approached via extension of the diffusion equation in that not only the *positions* of the particles but also their *surface charge densities* are followed during particle interaction. Near equilibrium, the equations could be solved analytically. The results slightly diverge from existing theories. Far from equilibrium these equations have to be solved numerically.

In this paper, a link is made between stability against coagulation and dielectric spectroscopic properties.

1. INTRODUCTION

Conservation of the probability $P(r)$ of locating a second particle at separation r relative to a test particle implies (1)

$$\frac{\partial P}{\partial t}+\vec{\nabla}\cdot P\,\vec{v}_p=0 \qquad [1]$$

where $\vec{v}_p$ is the velocity of the second particle relative to the test particle and t is the time. After a short period, coagulation is steady which implies $\partial P/\partial t=0$. The flux $\vec{J}$ of a particle is given by:

$$\vec{J}=P\,\vec{v}_p \qquad [2]$$

Both the Brownian motion and the interparticle force $\vec{F}$ contribute to the motion:

$$\vec{v}_p=\frac{1}{f_{hyd}}(-kT\,\vec{\nabla}\ln P+\vec{F}) \qquad [3]$$

where $f_{hyd}=6\pi\eta a$ is the Stokes friction coefficient, kT is the thermal energy and η is the viscosity of the solvent. The particles are assumed to be spherical (radius a). Hydrodynamic interactions are ignored. Under non-equilibrium conditions, the force consists of a conservative interparticle part $\vec{F}_{con}$, and a non-conservative dynamic part, $\vec{F}_{dyn}$:

$$\vec{F}=\vec{F}_{con}+\vec{F}_{dyn} \qquad [4]$$

The conservative force can be written as the gradient of a potential function $\vec{F}_{con}=-\vec{\nabla}V_{con}$. If we suppose that transient deviations from equilibrium in the surface charge density are small ($\vec{F}_{dyn}=\delta\vec{F}$), the dynamic force is small and proportional to the particle velocity:

$$\delta\vec{F}=-\delta f\,\vec{v}_p \qquad [5]$$

where δf is the dynamic friction coefficient. Solving Eqs. [3]-[5] for $\vec{v}_p$ yields

$$\vec{v}_p=\frac{1}{f_{hyd}+\delta f}(-kT\,\vec{\nabla}\ln P+\vec{F}_{con}) \qquad [6]$$

This expression is equivalent to [3] with $1/(f_{hyd}+\delta f)$ replacing $1/f_{hyd}$ and $\vec{F}=\vec{F}_{con}$. The colloidal stability ratio W is now given by (2)

$$W=2a\int_2^{\infty}(1+\delta f(r)/f_{hyd})\exp(V_{con}(r)/kT)dr/r^2 \qquad [7]$$

where r is the distance between the centres of the particles. Usually $V_{con}(r)$ has a pronounced maximum and the integration is dominated by the exponent in a small region for which $\delta f(r)$ is nearly constant. We may write:

$$W = 2a(1 + \delta f / f_{hyd}) \int_{2}^{\infty} \exp(V_{con}(r)/kT) dr / r^2 \qquad [8]$$

where δf must be evaluated at the position for which $V_{con}(r)$ attains its maximum. This is typically at separations $r = 2a + O(\kappa^{-1})$.

There is another way of looking at this problem close to equilibrium. We may expand $\delta\vec{F}$ in terms of δf:

$$\delta\vec{F} = -\delta f\, \vec{v}_{p,eq} + O(\delta f^2) \qquad [9]$$

where $\vec{v}_{p,eq} = \vec{J}_{eq} / P_{eq}$ is the velocity under "equilibrium conditions" ($\delta f = 0$). Note that $\vec{v}_p = \vec{v}_{p,eq} + O(\delta f)$. Substitution of Eq. [9] in [3] yields:

$$\vec{v}_p = \frac{1}{f_{hyd}}(-kT\, \vec{\nabla} \ln P + \vec{F}_{con} - \delta f\, \vec{v}_{p,eq}) + O(\delta f^2) \qquad [10]$$

Since $\delta f\, \vec{v}_{p,eq}$ is a function of the interparticle distance only, it can also be written as the gradient of a potential. Hence, diffusion under near-equilibrium conditions may be interpreted as diffusion in a modified conservative force field $\vec{F}_{con} - \delta f\, \vec{v}_{p,eq}$. The two views are equivalent in the limit of small δf.

Dukhin and Lyklema (3,4) have investigated the effect of small transient deviations from the equilibrium double layer structure due to retarded desorption of charge-determining ions or transport of these ions along the surface away from the interaction area. They showed that the diffuse part of the double layer usually relaxes fast and therefore maintains a Boltzmann distribution.

Kijlstra et al. (5) proposed an electrodynamic approach applicable to large disequilibrations of charge-determining ion distributions. As can be shown easily, Kijlstra's procedure reduces to diffusion in a modified force field in the limit of small disequilibration. Hence, the method of Kijlstra et al. (5) and Dukhin and Lyklema (3,4) are similar in this limit. Additionally, Kijlstra et al.'s model generates interaction at constant charge in the limit of very slow relaxation of surface charge. This is in contradiction to Dukhin and Lyklema's theory which does not work in this limit (an infinite repulsion is generated in this limit). In two more recent papers, Shulepov et al. (6,7) applied Kijlstra's procedure to interacting particles which exhibit more complicated mechanisms of surface charge relaxation.

Kijlstra's electrodynamic theory generates interaction at constant potential and constant charge in the limits of fast and slow charge relaxation, respectively. However, for the interesting intermediate situations Kijlstra's procedure has its limitations. In this regime, the surface charge is extremely sensitive to the trajectory followed by the particles from just beyond the interaction zone (at separations of a few times κ^{-1}) to their actual position of interaction (8). Therefore, particles situated at a certain specified separation may have various surface charge densities.

Kijlstra ascribed an *average* surface charge density to all particles at separation r. However, in order to find the total rate of coagulation, one has to consider the complete distribution of surface charge densities and associated distribution of interaction forces at every separation.

The goals of this chapter are twofold. (i) In a previous study (9), we have related the low-frequency dielectric dispersion (LFDD) to the rates at which surface charge is able to desorb from a surface, or to migrate along it. Since these mechanisms also determine the extent of disequilibration of the surface during particle-particle interaction, we will express stability in terms of the parameters introduced previously (9). Hence, our first goal is to link LFDD and sol stability against coagulation. In this part of the work, we will restrict ourselves to interaction close to equilibrium.

(ii) Our second goal is to make an attempt in dealing with non-equilibrium interaction by following the complete distributions of particles with all possible surface-charge densities during interaction.

2. THEORY

2.1. Coagulation near equilibrium

In this paragraph we will relate the stability ratio W to the rates at which surface charge is able to leave the interaction area by means of desorption from the surface, or migration along it. These mechanisms were introduced previously (9). It is presumed that the diffuse part of the double layer is able to adjust rapidly and that therefore it is always in equilibrium during interaction. We study the situation where the double layer is relatively thin ($\kappa a >> 1$). Low surface potentials are considered which allows us to work in the Debye-Hückel approximation. Furthermore, disequilibration is considered small which reduces the problem to finding the corrected friction coefficient.

Let us start by introducing the concepts involved with the more simple case of two interacting flatspots instead of two spheres. In general we may write for the Gibbs energy per unit surface area, $G_A(r,\sigma)$, of the two-plate system area around equilibrium:

$$G_A(r,\sigma) = G_{A,eq}(r) + \overline{g}_A(r)\left(\sigma - \sigma_{eq}(r)\right)^2 \qquad [11]$$

where σ_{eq} is the equilibrium charge density at separation r, $\overline{g}_A(r)$ is a function of the plate separation r, reflecting the width of the energy minimum around the equilibrium charge. Parameters given per unit surface area are referred to with subscript "A". Surface charge relaxation can be described by the phenomenological relation

$$\frac{\partial\sigma}{\partial t} = -\frac{1}{f_\sigma}\frac{\partial G_A(r,\sigma)}{\partial\sigma} = -\frac{2}{f_\sigma}\overline{g}_A(\sigma - \sigma_{eq}) \qquad [12]$$

where the generalized friction coefficient f_σ describes the rate at which surface charge relaxes. If the two surfaces approach each other at net velocity v, Eq. [12] can be written as:

$$\frac{\partial\sigma}{\partial r}v = -\frac{2}{f_\sigma}\bar{g}_A(\sigma-\sigma_{eq}) \qquad [13]$$

For low velocities, perturbations in the surface charge are small and the charge on the plates nearly follows the equilibrium value:

$$\frac{\partial\sigma}{\partial r} = \frac{d\sigma_{eq}}{dr} + \mathrm{O}(v) \qquad [14]$$

Hence,

$$\frac{d\sigma_{eq}}{dr}v = -\frac{2}{f_\sigma}\bar{g}_A(\sigma-\sigma_{eq}) + \mathrm{O}(v^2) \qquad [15]$$

or

$$\sigma = \sigma_{eq} - \frac{d\sigma_{eq}}{dr}\frac{f_\sigma}{2\bar{g}_A}v + \mathrm{O}(v^2) \qquad [16]$$

We note that the perturbation in the surface charge density is proportional to the change of charge density, $d\sigma_{eq}$, in an approaching step dr. Fast relaxation (low f_σ) results in small perturbations in charge density. Furthermore, the broader the energy minimum (the smaller $\bar{g}_A$), the larger the perturbation in σ is. The perturbation is only determined by the distance r. In this limit of low f_σ v surfaces a distance r apart have already "forgotten" what the charge on the plates was at separation $r+\Delta r$. In this situation the memory is negligibly short.

The perturbation in the force per unit surface area is given by:

$$\delta F_A = -\frac{\partial G_A}{dr}\bigg|_{\sigma_{eq}}^{\sigma} = -\left(\frac{dG_{A,eq}}{dr} + \frac{d\bar{g}_A}{dr}(\sigma-\sigma_{eq})^2 - 2\bar{g}_A(\sigma-\sigma_{eq})\frac{d\sigma_{eq}}{dr}\right)\bigg|_{\sigma_{eq}}^{\sigma} \qquad [17]$$

For the force between the two plates per unit surface area we find

$$\delta F_A = -f_\sigma(d\sigma_{eq}/dr)^2 v + \mathrm{O}(v^2) \qquad [18]$$

The dynamic force acts like a friction force inhibiting the displacement. The dynamic friction coefficient per unit surface area is given by:

$$\delta f_A = f_\sigma(d\sigma_{eq}/dr)^2 + \mathrm{O}(v) \qquad [19]$$

We note that $\delta F_A = \mathrm{O}(v)$ while $\delta G_A = \mathrm{O}(v^2)$. All the extra work performed by bringing the plates together with velocity v does not contribute to the Gibbs energy of the two-plate system. It is dissipated immediately as heat which emphasises the purely frictional, and hence, non-conservative nature of the dynamic force in this near-equilibrium limit.

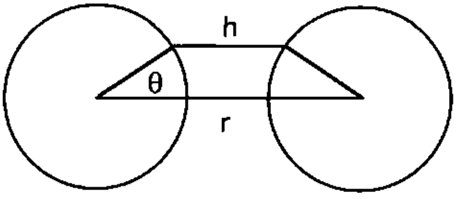

Figure 1. Geometrical parameters.

Now let us continue with spherical particles. In Fig. 1 the geometrical parameters are defined. The distance between the centres of the spheres is referred to by r and h is the distance between the surfaces at a certain angle θ. As shown previously (9), conservation of ions within the surface layer (or Stern layer) is described by:

$$\frac{\partial \Gamma^s}{\partial t} = \frac{kT}{f^s} \Gamma^s_{eq} \nabla_t^2 \delta\mu^s - \frac{1}{\tau_\perp} \Gamma^s_{eq} \delta\mu^s \qquad [20]$$

where Γ^s is the amount of ions in the surface layer per unit surface area, f^s is the friction coefficient of these ions for lateral movement, $\delta\mu^s$ is the perturbation in the non-dimensional electrochemical potential in the surface layer and $\tau_\perp$ is the characteristic time for desorption. Since $\delta\mu^s$ as well as $\nabla_t \delta\mu^s$ characteristically decay over a distance along the surface for which the separation h has increased by an amount κ^{-1}, we approximate $\nabla_t^2 \delta\mu^s$ by $-(\kappa / a)^{-1} \delta\mu^s$. Furthermore, $\partial \Gamma / \partial t = d\Gamma^s_{eq} / dr \; v$. Hence,

$$\frac{v}{\Gamma^s_{eq}} \frac{d\Gamma^s_{eq}}{dr} \approx -\frac{1}{\tau_{int}} \delta\mu^s + \mathrm{O}(v^2) \qquad [21]$$

where

$$\frac{1}{\tau_{int}} = \frac{1}{\tau_{int,//}} + \frac{1}{\tau_\perp}, \quad \frac{1}{\tau_{int,//}} = \frac{kT}{a\kappa^{-1} f^s} \qquad [22]$$

$\tau_{int,//}$ is the characteristic time for ions to diffuse along the surface out of the interaction area, i.e., over a distance of the order $\sqrt{a/\kappa}$. In the theory for the LFDD, the characteristic time $\tau_{//}$ for diffusion along the surface over distances of the order a is important. We note that $\tau_{int,//} = \tau_{//} / \kappa a$.

In the surface layer the perturbation in electrochemical potential is related to the perturbation in the electric potential and the perturbation in adsorption

$$\delta\mu^s = \frac{ze}{kT} \delta\psi^s + \frac{\delta\Gamma^s}{\Gamma^s_{eq}} \qquad [23]$$

and in the low surface-potential limit ($| ze\psi^s_{eq} / kT | \leq 1$):

$$\delta\psi^s = \frac{ze\delta\Gamma^s}{\varepsilon\kappa\tanh(\kappa h/2)} \qquad [24]$$

Furthermore, under equilibrium conditions the surface potential and the adsorption are related according to (9):

$$\ln\Gamma^s_{eq} + \frac{ze}{kT}\psi^s_{eq} = \text{constant} \qquad [25]$$

Combining Eqs. [21], [23]-[25]yields:

$$ze\delta\Gamma^s = \delta\sigma = -\sigma_{eq}\tau_{int}v\frac{ze}{kT}\frac{d\psi^s_{eq}}{dr}\bigg/\left(\frac{ze\sigma_{eq}}{\varepsilon\kappa kT\tanh(\kappa h/2)}+1\right) \qquad [26]$$

The friction coefficient has to be evaluated at a separation for which G attains its maximum, i.e., typically at separation $r = \mathrm{O}(\kappa^{-1})$ (10). Since at this separation $\psi^s_{eq} = \mathrm{O}(\psi^{s,\infty}_{eq})$, $\sigma_{eq} = \mathrm{O}(\sigma^{\infty}_{eq})$ and $d\psi^s_{eq}/dr = \mathrm{O}(-\psi^{s,\infty}_{eq}\kappa)$, where the additional superscript "∞" refers to the value at infinite separation, we estimate:

$$\delta\sigma = \mathrm{O}(\sigma^{\infty}_{eq}\tau_{int}v\frac{ze}{kT}\psi^{s,\infty}_{eq}\kappa) \qquad [27]$$

The perturbation in force per unit surface area is proportional to the perturbation in surface charge density (see appendix A):

$$\delta F(r) = -\frac{\partial\psi^s(r,\sigma_{eq})}{\partial r}\delta\sigma = \mathrm{O}(-\psi^{s,\infty}_{eq}\kappa\delta\sigma) \qquad [28]$$

Since the interaction area is $\mathrm{O}(a/\kappa)$ the perturbation in force between the spheres, δF, is related to the force per unit surface area according to

$$\delta F(r) = \mathrm{O}\big(\delta F_A(r)a/\kappa\big) \qquad [29]$$

Combination of Eqs. [27]-[29] yields:

$$\delta f = -\delta F/v = \mathrm{O}\left(\tau_{int}\sigma^{\infty}_{eq}(\psi^{s,\infty}_{eq})^2\frac{ze}{kT}\kappa a\right) \qquad [30]$$

The stability ratio under non-equilibrium conditions, W, is related to the stability ratio in the situation of instantaneous surface relaxation, W_{eq}:

$$W/W_{eq} = 1 + \mathrm{O}\left(\tau_{int}\sigma^{\infty}_{eq}(\psi^{s,\infty}_{eq})^2\frac{ze}{kT}\kappa a\bigg/6\pi\eta a\right) \qquad [31]$$

Since surface charge relaxation via desorption and surface migration occur simultaneously, the faster of the two mechanisms determines the extent of disequilibration and the corresponding deviation in stability compared to the stability in the case of infinitely fast adjustment. From [31] we can formulate the dynamic condition for which constant-potential interaction will occur:

$\tau_{int} << 6\pi kT\eta / ze\sigma_{eq}^{\infty}(\psi_{eq}^{s,\infty})^2\kappa$, which allows a direct comparison between the characteristic time constants of the relaxation process and the equilibrium double-layer parameters $\psi_{eq}^{s,\infty}$ and κ. The rate parameters of the pertinent relaxation processes can be inferred from dielectric spectroscopy (9).

2.2. Arbitrary departures from equilibrium; all possible trajectories considered

In the limiting situations of interaction at equilibrium (constant electrochemical potential) and interaction without charge relaxation (constant charge), the surface charge density is independent of the trajectories made by the particles. In the former case of complete relaxation, the actual separation determines the surface charge and the electric force originating from double-layer overlap. In the two limits the interparticle force is conservative and the stability ratio is straightforwardly related to this force, as shown by Smoluchowski (11,12) and Fuchs (13). In the intermediate situation, which generally involves large deviations from equilibrium (8), the surface charge and the interparticle electric force are functions of the trajectories. The interparticle force is non-conservative and hence the classical approach of Smoluchowski and Fuchs cannot be applied. Particles separated by a certain distance may exhibit a charge density somewhere between the value of a completely relaxed surface and the equilibrium density at infinite separation. The charge distribution is the result of the possible trajectories of the particle. Hence, the interparticle force is not only determined by the separation, but also by the *charge density*. A theory is needed which keeps track of both parameters during interaction. We model the interaction between the spherical particles as the interaction between two interacting *flatspots*, located on spheres, with characteristic area A. We introduce a new probability density $P(r,\sigma|t)$ of locating at time t the second flatspot with surface charge density σ at separation r-$2a$ (r is the centre to centre distance). The interparticle force is related to the Gibbs energy:

$$F = -\frac{\partial G(r,\sigma)}{\partial r} \qquad [32]$$

where $G = AG_A$. The flux of a plate in (r,σ)-space, $\vec{J}(r,\sigma|t)$, is given by:

$$\vec{J}(r,\sigma|t) = -\frac{1}{f_{hyd}}\frac{\partial}{\partial r}\left[kT\frac{\partial P}{\partial r} + P\frac{\partial G}{\partial r}\right]\vec{e}_r - \frac{1}{f_\sigma A}\left[kT\frac{\partial P}{\partial \sigma} + P\frac{\partial G}{\partial \sigma}\right]\vec{e}_\sigma \qquad [33]$$

where $\vec{e}_r$ and $\vec{e}_\sigma$ are the unit vectors in r- and σ-space, respectively. Surface charge relaxation is involved in the way, described by Eq. [12]. Furthermore, since thermal motion generates fluctuations in the charge density, the diffusive (Brownian) term $\propto \partial P / \partial \sigma$ is added in such a way that $P \propto \exp(-G/kT)$ in equilibrium (see appendix B).

After a short transient, coagulation is steady:

$$-\vec{\nabla}_{r,\sigma}\cdot\vec{J} = \frac{1}{r^2}\frac{\partial}{\partial r}\left(r^2\frac{1}{f_{hyd}}\left[kT\frac{\partial P}{\partial r} + P\frac{\partial G}{\partial r}\right]\right) + \frac{\partial}{\partial \sigma}\left(\frac{1}{f_\sigma A}\left[kT\frac{\partial P}{\partial \sigma} + P\frac{\partial G}{\partial \sigma}\right]\right) = 0 \qquad [34]$$

Thus, the problem has been reduced to a stationary diffusion problem in (r,σ)-space. What remains is the formulation of the boundary conditions. The test particle is taken as a perfect sink:

$$P(r,\sigma)=0 \quad \text{as} \quad r=2a \tag{35}$$

At large separations the surface is undisturbed and the surface charge attains a Boltzmann distribution:

$$P(r,\sigma)=\frac{\exp(-G^{\infty}/kT)}{\int_{\sigma}\exp(-G^{\infty}/kT)d\sigma'}=\frac{\exp\left(-\bar{g}^{\infty}(\sigma-\sigma_{eq})/kT\right)}{\sqrt{kT\pi/\bar{g}^{\infty}}} \quad \text{as} \quad r\rightarrow\infty \tag{36}$$

We may ask ourselves how these equations evolve in the limit of immediate surface-charge relaxation.

Instantaneous relaxation. In this limit where $f_{\sigma}=0$, P obeys a Boltzmann distribution in the σ-direction and can generally be written as:

$$P(r,\sigma)=l_{eq}(r)\exp(-G(r,\sigma)/kT) \tag{37}$$

where $l_{eq}(r)$ is a function of r only. The *total* flux reaching the test particle is given by:

$$J_{eq}=\int_{\sigma}-\frac{4\pi r^{2}}{f_{hyd}}(kT\frac{\partial P}{\partial r}+P\frac{\partial G}{\partial r})\exp(-G/kT)d\sigma'=-4\pi r^{2}\frac{kT}{f_{hyd}}\frac{dl_{eq}}{dr}\int_{\sigma}\exp(-G/kT)d\sigma' \tag{38}$$

Solving for dl_{eq} yields

$$dl_{eq}=-\frac{J_{eq}f_{hyd}}{4\pi r^{2}kT}\frac{dr}{\int_{\sigma}\exp(-G/kT)d\sigma'} \tag{39}$$

and, integrating from $r=2a$ to infinity

$$l_{eq}^{\infty}=\int_{r=2a}^{r=\infty}dl_{eq}=\frac{-J_{eq}f_{hyd}}{4\pi kT}\int_{2a}^{\infty}\frac{dr/r^{2}}{\int_{\sigma}\exp(-G/kT)d\sigma'} \tag{40}$$

Solving for J_{eq} yields

$$J_{eq}=-\frac{4\pi kT}{f_{hyd}}\frac{1}{\int_{2a}^{\infty}\exp(G_{eq}/kT)\sqrt{\bar{g}/\bar{g}^{\infty}}dr/r^{2}} \tag{41}$$

The stability ratio is given by

$$W=2a\int_{2}^{\infty}\exp(G_{eq}/kT)\sqrt{\bar{g}/\bar{g}^{\infty}}dr/r^{2} \tag{42}$$

As long as the width of the energy minimum is independent of the separation ($\bar{g} = \bar{g}^{\infty}$), the classical expression for the stability ratio is obtained. However, in general $\bar{g}$ becomes larger for decreasing separation which yields deviations from the classical expression. We want to stress here that the way in which fluctuations are incorporated in Eq. [33] is primitive. There is, e.g., no correlation between fluctuations within one flatspot. Furthermore, the fluctuations on both the flatspots are assumed to be identical which is, of course, not real. Therefore, the factor $\sqrt{\bar{g}/\bar{g}^{\infty}}$ will not be quantitatively correct. Still, qualitatively interesting phenomena appear due to the fluctuations in charge. For instance, particles may lose their charge due to thermal fluctuations and coagulate without further obstructions since an energy barrier is absent then. This route is no option in the classical theory.

Particle interaction near equilibrium (f_σ small).

Near equilibrium we may write

$$l(r,\sigma) = l_{eq}(r) + \delta l(r,\sigma) + \mathrm{O}(f_\sigma^2) \qquad [43]$$

and

$$P = l(r,\sigma)\exp(-GA/kT) = \left(l_{eq}(r) + \delta l(r,\sigma)\right)\exp(-G/kT) + \mathrm{O}(f_\sigma^2) \qquad [44]$$

Here the distribution is written as the equilibrium distribution plus an extra perturbation. Under steady coagulation conditions, δl obeys

$$\frac{1}{r^2}\frac{\partial}{\partial r}\left[r^2\frac{1}{f_{hyd}}\frac{\partial}{\partial r}(l_{eq}+\delta l)\exp(-G/kT)\right] + \frac{1}{f_\sigma A}\frac{\partial}{\partial\sigma}\left[\frac{\partial\delta l}{\partial\sigma}\exp(-G/kT)\right] + \mathrm{O}(f_\sigma) = 0 \qquad [45]$$

Small $\mathrm{O}(f_\sigma)$ terms can be neglected:

$$\frac{1}{r^2}\frac{\partial}{\partial r}\left[r^2\frac{1}{f_{hyd}}\frac{dl_{eq}}{dr}\exp(-G/kT)\right] + \frac{1}{f_\sigma A}\frac{\partial}{\partial\sigma}\left[\frac{\partial\delta l}{\partial\sigma}\exp(-G/kT)\right] = 0 \qquad [46]$$

After substitution of Eq. [11], this expression is equivalent to:

$$\begin{gathered}\frac{1}{r^2}\left[\frac{d}{dr}\left(r^2\frac{1}{f_{hyd}}\frac{dl_{eq}}{dr}\right) - \left(r^2\frac{1}{f_{hyd}}\frac{dl_{eq}}{dr}\right)\left(\frac{dG_{eq}}{dr} + \frac{d\bar{g}}{dr}(\sigma-\sigma_{eq})^2 - 2\bar{g}(\sigma-\sigma_{eq})\frac{d\sigma_{eq}}{dr}\right)\frac{1}{kT}\right] + \\ \frac{1}{f_\sigma A}\left[\frac{\partial^2\delta l}{\partial\sigma^2} - \frac{\partial\delta l}{\partial\sigma}2\bar{g}(\sigma-\sigma_{eq})\frac{1}{kT}\right] = 0\end{gathered} \qquad [47]$$

The above equation has to be solved under the appropriate boundary conditions:

$$\delta l(r,\sigma) = 0 \quad \text{as} \quad r = 2a \qquad [48]$$

Particles far apart are unperturbed:

$$\delta l(r,\sigma) = 0 \quad \text{as} \quad r \to \infty \qquad [49]$$

No particles enter at, or leave to $\sigma = \pm\infty$:

$$\frac{\partial \delta l(r,\sigma)}{\partial \sigma}\exp(-G/kT) \to 0 \quad \text{as} \quad |\sigma| \to \infty \tag{50}$$

This boundary condition is in principle not very important as we will see later. With the help of Eq. [38] we find

$$\frac{d}{dr}\left(r^2 \frac{1}{f_{hyd}} \frac{dl_{eq}}{dr}\right) = -\frac{J_{eq}}{4\pi kT} \frac{\int\limits_{\sigma} \exp(-G/kT)\left(\frac{dG_{eq}}{dr} + \frac{d\overline{g}}{dr}\left(\sigma - \sigma_{eq}\right)^2\right)\frac{1}{kT}d\sigma'}{\left(\int\limits_{\sigma} \exp(-G/kT)d\sigma'\right)^2} \tag{51}$$

Now, combining the Eqs. [38] and [51] results in:

$$\frac{d}{dr}\left(r^2 \frac{1}{f_{hyd}} \frac{dl_{eq}}{dr}\right) = \left(r^2 \frac{1}{f_{hyd}} \frac{dl_{eq}}{dr}\right)\left(\frac{dG_{eq}}{dr} + \frac{d\overline{g}}{dr} \frac{\int\limits_{\sigma} (\sigma - \sigma_{eq})^2 \exp\left(-\overline{g}(\sigma - \sigma_{eq})^2/kT\right)d\sigma'}{\int\limits_{\sigma} \exp\left(-\overline{g}(\sigma - \sigma_{eq})^2/kT\right)d\sigma'}\right)\frac{1}{kT} \tag{52}$$

which, after integrating the expression in the numerator by parts, converts into:

$$\frac{d}{dr}\left(r^2 \frac{1}{f_{hyd}} \frac{dl_{eq}}{dr}\right) = \left(r^2 \frac{1}{f_{hyd}} \frac{dl_{eq}}{dr}\right)\left(\frac{dG_{eq}}{dr}\frac{1}{kT} + \frac{d\overline{g}}{dr}\frac{1}{2\overline{g}}\right) \tag{53}$$

Substitution of Eq. [53] in [47] yields a linear inhomogeneous second order differential equation:

$$\begin{gathered}\frac{1}{f_{hyd}} \frac{\partial l_{eq}}{\partial r}\left(\frac{d\overline{g}}{dr}\frac{1}{2\overline{g}} - \frac{d\overline{g}}{dr}(\sigma - \sigma_{eq})^2 \frac{1}{kT} + 2\overline{g}(\sigma - \sigma_{eq})\frac{d\sigma_{eq}}{dr}\frac{1}{kT}\right) + \\ \frac{1}{f_\sigma A}\left[\frac{\partial^2 \delta l}{\partial \sigma^2} - \frac{\partial \delta l}{\partial \sigma} 2\overline{g}(\sigma - \sigma_{eq})\frac{1}{kT}\right] = 0\end{gathered} \tag{54}$$

Integrating once yields:

$$\frac{\partial \delta l}{\partial \sigma} = \frac{f_\sigma A}{f_{hyd}} \frac{dl_{eq}}{dr}\left[-\frac{d\overline{g}}{dr}\frac{(\sigma - \sigma_{eq})}{2\overline{g}} + \frac{d\sigma_{eq}}{dr}\right] + \delta m(r)\exp\left(\overline{g}(\sigma - \sigma_{eq})^2 \frac{1}{kT}\right) \tag{55}$$

where $\delta m(r)$ is an arbitrary function of r. The three contributions can be interpreted in the following way. The last term on the right-hand side generates a flux in the σ-direction which is independent of the magnitude of σ. Applying boundary condition [50] yields $\delta m(r) = 0$. However, every other value for $\delta m(r)$ leaves the rate of coagulation unchanged since the rate in the r-direction is unaltered. The second term yields fluxes that are parallel to the σ_{eq} curve in (r,σ)-space. If the width of the free-energy minimum de- or increases, additional particles fluxes will flow from or towards the equilibrium charge-density value, respectively. This process is represented by the first term.

Integrating once again yields:

$$\delta l(r,\sigma) = \delta n(r) + \frac{f_\sigma A}{f_{hyd}}\frac{dl_{eq}}{dr}\left[-\frac{d\bar{g}}{dr}\frac{(\sigma-\sigma_{eq})^2}{4\bar{g}} + (\sigma-\sigma_{eq})\frac{d\sigma_{eq}}{dr}\right] \qquad [56]$$

where $\delta n(r)$ is an arbitrary function of r. All terms except $\delta n(r)$ satisfy the boundary conditions [48] and [49] since

$$\frac{dl_{eq}}{dr} = 0 \quad \text{as} \quad r = 2a \quad \text{(see Eq. [38])} \qquad [57]$$

$$\frac{dl_{eq}}{dr} \to 0, \quad \frac{d\bar{g}}{dr} \to 0 \quad \text{and} \quad \frac{d\sigma_{eq}}{dr} \to 0 \quad \text{as} \quad r \to \infty \qquad [58]$$

This means that $\delta n(r)$ also has to satisfy the boundary conditions [48] and [49]. From hereon we will assume $\bar{g}$ to be constant. We may write for the retarded flux:

$$\begin{aligned} J &= -4\pi r^2 \frac{kT}{f_{hyd}}\int_\sigma \left[\frac{dl_{eq}}{dr} + \frac{\partial \delta l}{\partial r}\right]\exp(-G/kT)d\sigma' \\ &= -4\pi r^2 \frac{kT}{f_{hyd}}\left[\frac{dl_{eq}}{dr} + \frac{d\delta f}{dr} - \frac{f_\sigma}{f_{hyd}}\frac{dl_{eq}}{dr}(d\sigma_{eq}/dr)^2 A\right]\int_\sigma \exp(-G/kT)d\sigma' \\ &= -4\pi r^2 \frac{kT}{f_{hyd}}\left[\left(\frac{dl_{eq}}{dr} + \frac{d\delta f}{dr}\right)\left(1 - \frac{f_\sigma}{f_{hyd}}(d\sigma_{eq}/dr)^2 A\right)\right]\int_\sigma \exp(-G/kT)d\sigma' + \mathrm{O}(f_\sigma) \end{aligned} \qquad [59]$$

Applying the same procedure as before we find

$$l_{eq}^{\infty} = \int_{r=2a}^{r=\infty} d\left(l_{eq} + \delta f\right) = -\frac{Jf_{hyd}}{4\pi kT}\int_{r=2a}^{r=\infty}\frac{dr/r^2}{\left(1 - \frac{f_\sigma}{f_{hyd}}(d\sigma_{eq}/dr)^2 A\right)\int_\sigma \exp(-G/kT)d\sigma'} \qquad [60]$$

Hence,

$$J = -\frac{4\pi kT}{f_{hyd}} l_{eq}^{\infty} \frac{1}{\displaystyle\int_{2a}^{\infty}\frac{dr/r^2}{\left(1 - \frac{f_\sigma}{f_{hyd}}(d\sigma_{eq}/dr)^2 A\right)\int_\sigma \exp(-G/kT)d\sigma'}} \qquad [61]$$

which becomes

$$J = -\frac{4\pi kT}{f_{hyd}} \frac{1}{\displaystyle\int_{2a}^{\infty}\left(1 + \frac{f_\sigma}{f_{hyd}}(d\sigma_{eq}/dr)^2 A\right)\exp(G_{eq}/kT)dr/r^2} \qquad [62]$$

if small $O(f_\sigma)$-terms are neglected. Hence, the dynamic friction coefficient δf is equal to $f_\sigma (d\sigma_{eq} / dr)^2 A$ as it was already found previously (Eq. [19]).

The two limiting situations we have discussed above are close to equilibrium (small f_σ). For situations far from equilibrium the conservation equation [34] must be solved numerically. We note that in the interesting far-from-equilibrium regime, the Brownian term $kT\partial P / \partial\sigma$ may be neglected compared to the dissipative term $P\partial G / \partial\sigma$ in Eq. [34]. Of course, boundary condition [36] then turns into a delta function, $P(r,\sigma) = \delta(\sigma - \sigma_{eq}^{\infty})$ as $r \to \infty$. This removes the problems connected with fluctuations in the charge density as observed near equilibrium.

3. CONCLUSIONS AND PERSPECTIVES

Deviations from constant potential behaviour in the stability of colloids were linked to the rate characteristics of surface charge relaxation. Since surface charge relaxation via desorption and surface migration occur simultaneously, the faster of the two mechanisms determines the extent of disequilibration and the corresponding deviation in stability compared to the stability in the case of infinitely fast adjustment. The rate parameters of the pertinent relaxation processes can be inferred from dielectric spectroscopy (9). The direct link between dielectric relaxation data and surface charge adjustment rates in particle-particle interaction forms an important step in the development of comprehensive knowledge of the electrodynamics of colloids.

A first attempt to take into account all possible trajectories towards particle contact was made by generalization of the diffusion equation from r to (r,σ)-space. Our theory does not exactly reduce to existing theories valid in and nearby equilibrium and nearby equilibrium due to fluctuations in the charge density. To further investigate this aspect and the interesting far-from-equilibrium regime, it will be necessary to numerically solve the conservation equation in order to obtain the width of the charge distribution. This should open the way to rigorous estimation of colloidal stability in the intermediate dynamic regime between constant-potential and constant-charge interaction.

APPENDIX A

The Gibbs energy per unit surface area of a two-plate system may be written as:

$$G_A(r,\sigma) = b(\sigma) + \int_0^{\sigma} \psi^s(\sigma',r)d\sigma' \qquad [A.1]$$

where $b(\sigma)$ is a function of σ. The interparticle force is given by:

$$F_A = -\frac{\partial G_A}{\partial r} = -\int_0^{\sigma} \frac{\partial \psi^s(r,\sigma')}{\partial r} d\sigma' = -\int_0^{\sigma_{eq}} \frac{\partial \psi^s(r,\sigma')}{\partial r} d\sigma' - \int_{\sigma_{eq}}^{\sigma} \frac{\partial \psi^s(r,\sigma')}{\partial r} d\sigma' \qquad [A.2]$$

In the case that $(\sigma - \sigma_{eq}) = \delta\sigma$ is small,

$$F_A = -\frac{dG_{A,eq}}{dr} - \frac{\partial \psi^s_{eq}(r,\sigma_{eq})}{\partial r}\delta\sigma \qquad [A.3]$$

Hence,

$$\delta F_A = -\frac{\partial}{\partial r}\psi^s_{eq}\,\delta\sigma \qquad [A.4]$$

APPENDIX B

For ideally polarizable interfaces, fluctuations in charge density are given by (14):

$$\overline{\delta\sigma^2} = \overline{(\sigma - \sigma_{eq})^2} = \frac{kT}{A}\left(\frac{\partial \psi^s_{eq}(r,\sigma_{eq})}{\partial \sigma_{eq}}\right)^{-1} \qquad [B.1]$$

To a good approximation, the distribution in σ is Gaussian:

$$P(\sigma) = \frac{1}{\sqrt{2\pi\overline{\delta\sigma^2}}}\exp\left(\frac{(\sigma - \sigma_{eq})^2}{2\overline{\delta\sigma^2}}\right) \qquad [B.2]$$

The Gibbs energy of ideally polarizable interacting surfaces per unit area is:

$$G_A(r,\sigma) = -\sigma\psi^s_{eq} + \int_0^\sigma \psi^s(\sigma',r)d\sigma' \qquad [B.3]$$

Expanding the Gibbs energy around σ_{eq} yields:

$$G_A(r,\sigma) = G_{A,eq} + \frac{(\sigma - \sigma_{eq})^2}{2}\frac{\partial \psi^s_{eq}(r,\sigma_{eq})}{\partial \sigma_{eq}} + \mathrm{O}(\sigma - \sigma_{eq})^3 \qquad [B.4]$$

Hence,

$$P(\sigma) \propto \exp(-G/kT) \qquad [B.5]$$

We have assumed that this result is also true for surfaces interacting at constant electrochemical potential dealt with in this chapter.

REFERENCES

(1) Krozel, J. W., *J. Colloid Interface Sci.* **163**, 437 (1994).

(2) Verwey, E. J. W., Overbeek, J. T. G., "Theory of the Stability of Lyophobic Colloids", Elsevier, Amsterdam, 1948.

(3) Dukhin, S. S., Lyklema, J., *Langmuir* **3**, 94 (1987).

(4) Dukhin, S. S., Lyklema, J., *Faraday Discuss. Chem. Soc.* **90**, 261 (1990).

(5) Kijlstra, J., Leeuwen, H. P. van, *J. Colloid Interface Sci.* **160**, 424 (1993).

(6) Shulepov, S. Yu., Dukhin, S. S., Lyklema, J., *J. Colloid Interface Sci.* **171,** 340 (1995).

(7) Shulepov, S. Yu., *J. Colloid Interface Sci.* **189,** 199 (1997).

(8) Kijlstra, J., Ph. D. Thesis, Wageningen Agricultural University, 1992.

(9) Minor, M., Leeuwen, H. P. van, Lyklema, J., submitted to *J. Chem. Soc. Faraday Trans.* (chapter 7 of this thesis).

(10) Lyklema, J., *in* "The Structure, Dynamics and Equilibrium Properties of Colloidal Systems", (D. M. Bloor, Wyn-Jones, E., Ed.), 789, Kluwer Academic Publishers, 1990.

(11) Smoluchowski, M. von, *Phys. Z.* **17,** 557 (1916).

(12) Smoluchowski, M. von, *Z. Phys. Chem.* **17,** 129 (1917).

(13) Fuchs, N., *Z. Phys.* **89,** 736 (1934).

(14) Stafiej, J., *J. Electroanal. Chem* **351,** 1 (1993).

SUMMARY

The goal of the present study is to deepen the insight into the non-equilibrium properties of the electric double layer of colloidal systems. Of basic interest are the ionic mobilities in the different regions of the electric double layer as well as the potential at the plane of shear, i.e., the electrokinetic potential (ζ-potential). These parameters determine the colloidal behaviour under non-equilibrium conditions when the double layer is perturbed, for instance if external fields are applied and in particle-particle interaction during coagulation.

One of the experimental methods utilized in this study is the measurement of the conductivity and the streaming potential of close-packed plugs of particles. From the resulting data we retrieved the ζ-potential, the surface conductivity, and the mobility of the counterions behind the plane of shear. The results are well comparable to those from the experimental low-frequency (LF) dielectric response of dilute dispersions of latex particles.

The electrodynamic parameters can be influenced by adsorbing neutral polymer onto the surface. It is shown that the ζ-potential as well as the mobilities of the ions behind the plane of shear are decreased by the polymer film.

The data in the above studies were successfully interpreted under the assumption of local equilibrium between the (complete) electric double layer and the adjacent electrolyte. However, there are double-layer conditions where this assumption is violated. In order to study these, we theoretically investigated the influence of relaxation of the compact part of the double layer (occupied inner-Helmholtz Stern layer) on the LF dielectric response and electrophoretic mobility. Possible relaxation mechanisms are retarded adsorption/desorption and ion migration along the surface. Along the same lines, the stability of the sol against coagulation was expressed in terms of the relaxation characteristics of the Stern layer.

Chapter 2 dealt with the determination of plug conductivities and streaming potentials of a close-packed porous plug of latex particles for a number of indifferent electrolytes and ionic strengths. From these, the ζ-potentials and surface conductivities were computed. Monodisperse

sulphate latex is an ideal model system since the surface charge consists of strong acidic groups so that a constant surface charge density is maintained throughout all the experiments. It was shown that the surface conductivity is insensitive to the ionic strength and that a large part of the countercharge is situated behind the shear plane. Furthermore, it was demonstrated that the ions in the double layer have a mobility close to the bulk mobility.

In **chapter 3** practical expressions were developed for the low-frequency (LF) dielectric response of dilute dispersions of spherical particles suspended in a binary electrolyte. The LF dielectric response of dilute sulphate latex dispersions was experimentally determined in the frequency range of 500 Hz to 500 kHz as a function of the ionic strength of suspending KCl. The resulting surface conductivities are insensitive to the ionic strength and practically identical to the values obtained by steady state methods (chapter 2). It was proposed that counterion motion can be retarded by specific interaction with the surface and by neutral polymer hairs present on the surface. In order to test the latter effect, the influence of the adsorption of uncharged polymer poly(ethylene) oxide onto the latex surface was investigated by means of LF spectroscopy, plug conductivities and streaming potentials of plugs in **chapter 4**. It was found that the polymer film on the surface reduces the surface conductivity. The drag on the ions in the polymer film can be described by considering the polymer layer as an inhomogeneous Brinkman fluid, characterised by a Darcy permeability which depends on the local polymer volume fraction. The polymer and counterion distributions were calculated from statistical self-consistent field lattice models.

In order to investigate the influence of the surface charge density on the streaming potential and static conductivity, plugs of monodisperse spherical Stöber-silica particles were studied in **chapter 5**. Contrary to the latex, the surface charge density of silica can be controlled by pH. The high-charge silica plug showed more surface conduction than the low-charge plug since more mobile counterions are present in the double layer of the former. Stöber-silica particles are highly porous. For the relatively large particles under consideration, the major part of the countercharge is situated in the micropores of the particles. It was shown that these counterions do not contribute to the plug conductivity because of their low mobility.

Chapter 6 analysed the dynamic aspects of particle electrophoresis. It was shown theoretically as well as experimentally that colloidal particles respond to an applied electric field much faster than does the liquid inside a measuring capillary. Therefore, it is possible to apply an alternating electric field with such a frequency that unwanted electroosmosis, induced by charge on the capillary wall, is suppressed, whereas the particles are still able to follow the field according to their dc mobility. This study illustrates that knowledge of the dynamics and the corresponding relaxation times is not only of purely scientific interest, but that it also offers solutions to very practical problems.

In **chapter 7** the influence of polarization of surface charge (or charge in an inner-Helmholtz layer) on the particle mobility, static conductivity, and low-frequency dielectric response was studied within the framework of the thin double-layer theory. It was shown that the characteristic times of relaxation processes in the Stern layer are accessible from dielectric spectroscopy. The relaxation phenomena under consideration are Stern-layer polarization via retarded adsorption/desorption and polarization via lateral transport in the Stern layer. The two processes may occur simultaneously. Since these relaxation processes are also relevant for particle-particle interaction, **chapter 8** considered the implications for colloidal stability. In the situation of small transient disequilibrations of the surface charge, the stability could be expressed in terms of the characteristic times of surface charge relaxation. This allows the use of electrodynamic data obtained by dielectric spectroscopy in the interpretation of colloidal stability. On an even more rigorous level, the free energy of particle-particle interaction was also considered in the space of the two variables surface charge and separation. This formalism opens the way to investigate coagulation far from equilibrium.

SAMENVATTING

Onder een kolloïd wordt verstaan een mengsel van twee fasen, waarbij de één als minuscule 'deeltjes' is verdeeld (gedispergeerd) in de ander, de continue fase. De deeltjes zijn veel groter dan een atoom, maar nog wel zo klein dat ze niet met het blote oog waarneembaar zijn. Dat wil zeggen, typisch van de orde van 10^{-9} tot 10^{-5} meter. Men zou nu kunnen denken dat kolloïden dan ook wel erg zeldzaam zullen zijn en vast alleen gemaakt kunnen worden door wetenschappers in speciaal daartoe uitgeruste laboratoria. Echter, niets is minder waar. Iedere koe is in staat kolloïden te maken. Melk bestaat immers uit microscopisch kleine vetbolletjes in een waterfase. Zo'n kolloïd is beter bekend als emulsie. Zonder het te beseffen worden we dagelijks vele malen geconfronteerd met kolloïden. Neem b.v. eens een willekeurige werkdag in het bestaan van de schrijver. Het begint al bij het ontbijt. Melk, boter en pindakaas op ons brood zijn kolloïden (emulsies). Evenals de benodigdheden bij het wassen (een zeepoplossing zit vol met groepjes zeepmoleculen, z.g. associatiekolloïden), het scheren met schuim (kolloïdale gasbelletjes in een vloeistof) en het tanden poetsen (vaste kolloïdale deeltjes in een vloeistof zijn het hoofdbestanddeel van tandpasta). Nog even snel de krant doornemen. Zonder inkt (kolloïdale pigmentdeeltjes in een vloeistof) is er geen gedrukt nieuws. Dan op de groene fiets (verf is een kolloïd net als inkt) naar de vakgroep. De route via de dijk (rivierklei bestaat uit kolloïdale kleiplaatjes in water) met kijk over de rivier en de in nevel gehulde uiterwaarden (kolloïdale waterdruppeltjes in de lucht) is fraai. En dan is er koffie (een kolloïd). De koffiekamer is opgedeeld in een deel waar aerosolen gemaakt mogen worden, en een deel waar roken niet is toegestaan. Aerosolen zijn kolloïden waarvan de continue fase een gas is (spray, mist, rook, stof). Dit zijn nog maar enkele voorbeelden van kolloïden die we veel tegenkomen.

Een bijzondere groep van kolloïden wordt gevormd door die waarin vaste deeltjes zijn verdeeld in een vloeistof. Zo'n systeem wordt 'sol' genoemd. Solen zijn het onderwerp in dit proefschrift en we zullen voortaan solen bedoelen wanneer we van kolloïden spreken.

Vrijwel alle kolloïden zijn positief danwel negatief *geladen*, en maar zelden elektrisch neutraal. De elektrische lading is vaak gelokaliseerd aan de buitenkant van de deeltjes en ontstaat b.v.

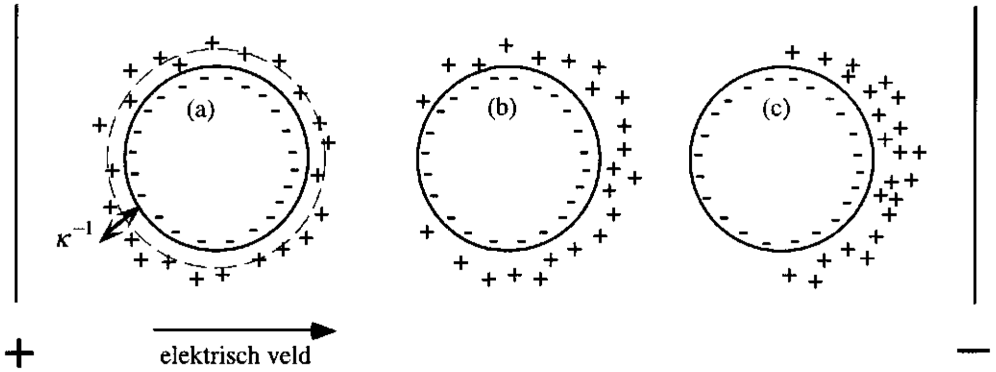

Figuur 1. Respons van een negatief geladen kolloïdaal deeltje op een plotseling aangelegd veld. (a) Voor, en direct na het inschakelen is de elektrische dubbellaag nog onverstoord. (b) De positieve ionen in de elektrische dubbellaag verplaatsen zich in de richting van de negatieve pool. (c) Uiteindelijk stelt zich een nieuwe situatie in waarin de dubbellaag volledig is gepolariseerd. Aangenomen is hier dat de negatieve oppervlaktelading zo sterk gefixeerd is dat zij niet bewegen kan.

doordat ionen (zeer kleine geladen moleculen) adsorberen aan het deeltjesoppervlak. Deze oppervlaktelading leidt in de aangrenzende oplossing tot een gelijke hoeveelheid lading die tegengesteld van teken en meestal diffuus verdeeld is. De dikte van deze diffuse laag wordt aangeduid met κ^{-1}. In figuur 1a is als voorbeeld een rond kolloïdaal deeltje weergegeven met een negatieve oppervlaktelading en een positieve diffuse tegenlading. Beide ladingen tezamen vormen de *elektrische dubbellaag*. Als geheel is zo'n dubbellaag elektroneutraal. De aanwezigheid van lading op het oppervlak kan eenvoudig worden aangetoond door de deeltjes te onderwerpen aan een elektrisch veld. Zijn ze geladen dan gaan ze bewegen. Dit verschijnsel heet *elektroforese*. Uit de richting waarin ze zich verplaatsen volgt direct het ladingsteken van de oppervlaktelading. De snelheid informeert ons over de grootte van de oppervlaktelading.

Een deel van de kolloïden is van nature instabiel. De in het medium rondzwalkende deeltjes oefenen namelijk aantrekkende krachten op elkaar uit, de zogenaamde *Van der Waals krachten.* Wanneer deze krachten vrij spel hebben zullen de deeltjes gaan samenklitten en uiteindelijk grote klonten vormen. Het sol is dan instabiel en men noemt het uitgevlokt. De neiging tot vlokken wordt tegengewerkt door de elektrische lading op de deeltjes die zorgt voor onderling afstotende krachten (deeltjes met gelijke ladingen stoten elkaar af). Des te meer lading, des te sterker de afstoting tussen de deeltjes. De snelheid waarmee een sol uitvlokt wordt uiteindelijk bepaald door de balans tussen de aantrekkende van der Waals krachten en de afstotende elektrische krachten. Bevinden de kolloïdale deeltjes zich in een milieu met veel opgelost zout, dan wordt de deeltjeslading goed afgeschermd. De diffuse laag is dan dun (κ^{-1} is klein), de elektrische afstoting gering, en de deeltjes zijn eerder geneigd tot vlokken. Met daarentegen veel lading en

weinig zout kan de vloktijd enorm worden opgevoerd (van minuten naar tientallen jaren). In de praktijk is dit laatste vaak wenselijk. De houdbaarheid van verf in de pot, b.v., wordt volledig bepaald door de balans van afstotende krachten tussen pigmentdeeltjes en de altijd aanwezige attractieve Van der Waals krachten. In andere gevallen is vlokking juist wenselijk. In verf die eenmaal is aangebracht geven pigmentdeeltjes die aan elkaar vastklitten juist een hechte film.
Deze voorbeelden tonen het belang van methoden om de ladingstoestand van de deeltjes te achterhalen. Elektroforese is reeds genoemd. Een andere methode is het meten van de *elektrische geleidbaarheid* van een sol. Daarvoor wordt het sol in een (onveranderlijk) elektrisch veld gebracht. Omdat de diffuse laag bijdraagt aan de elektrische stroom door het sol is hiermee de elektrische lading van de deeltjes te achterhalen. Helaas valt deze bijdrage echter veelal in het niet ten opzichte van de elektrische stroom die buiten de deeltjes en de diffuse laag om door de oplossing loopt. Dit probleem kan worden ondervangen door aan zeer geconcentreerde solen te meten. Deze hebben relatief veel oppervlak en daarmee veel diffuse lading die bijdraagt aan de geleidingsstroom. Een zeer hoge concentratie aan deeltjes kan worden verkregen door het sol af te centrifugeren. Van de prop met deeltjes die men dan verkrijgt kan de geleidbaarheid worden bepaald. Proppen bieden ook andere mogelijkheden. Zo kan vloeistof door de poriën van de prop worden geperst. De vloeistofstroom neemt dan iets van de diffuse lading mee waardoor er een elektrisch potentiaalverschil over de prop ontstaat. Deze potentiaal wordt *stromingspotentiaal* genoemd en is wederom een maat voor de hoeveelheid lading op de deeltjes. Een deel van het onderzoek beschreven in dit proefschrift is verricht aan zulke proppen (waarin geleidbaarheden en stromingspotentialen zijn bepaald). Proppen hebben echter ook nadelen. De deeltjes in proppen zitten allemaal tegen elkaar. De overlap van de diffuse lagen van elkaar rakende deeltjes maakt de interpretatie van de meetgegevens lastig.
Wanneer een kolloïdaal deeltje wordt onderworpen aan een elektrisch veld, zoals bij elektroforese of bij het meten van de geleidbaarheid, zal de structuur van de diffuse laag zich aanpassen aan het opgelegde veld. Dit is schematisch weergegeven in figuur 1. De positieve diffuse lading wordt aangetrokken door de negatieve pool maar komt niet vrij van het negatieve deeltje. Dit resulteert in het compromis zoals weergegeven in figuur 1c. De diffuse laag is *gepolariseerd*. Deze toestand is er niet direct na het inschakelen van het elektrische veld, maar heeft korte tijd nodig om zich te ontwikkelen. Na het aanzetten van het veld gaan de positieve ionen bewegen en verandert de diffuse laag van ongepolariseerd (figuur 1a) via een beetje gepolariseerd (figuur 1b) naar uiteindelijk volledig gepolariseerd (figuur 1c). Dit gebeurt in de karakteristieke tijd τ die ionen nodig hebben om van de ene kant van het deeltje naar de andere kant te bewegen. Deze ionbeweging langs het oppervlak wordt *oppervlaktegeleiding* genoemd. De ladingsverschuiving is waarneembaar als een kort elektrisch stroompje direct na het inschakelen van het veld. In dit proefschrift is aandacht besteed aan het meten van deze zogenaamde polarisatiestroom in een sol. Daartoe is gebruik gemaakt van een elektrisch wisselveld. De diffuse laag is dan continu bezig dit

veld te volgen maar loopt altijd iets achter. Dit in tegenstelling tot de grote stroom die buitenom de deeltjes door de oplossing loopt. Deze reageert momentaan op het alsmaar wisselende veld. Door dit verschillend gedrag is de polarisatiestroom te scheiden van de grote stroom buitenom en wordt het eerder geschetste probleem verholpen: in een wisselveld is ook van een verdund sol de bijdrage van de diffuse laag aan de stroom te achterhalen. De grootte van de polarisatiestroom is een maat voor de hoeveelheid oppervlaktelading. De reactie van een sol op een wisselveld wordt aangeduid met de term *diëlektrische respons.*

Hierboven zijn de methoden geschetst die in dit proefschrift zijn gebruikt om de ladingstoestand van kolloïdale deeltjes te achterhalen. Voor de interpretatie van meetwaarden is het erg prettig dat alle deeltjes in het sol rond en even groot zijn. Daarom zijn de experimenten uitgevoerd aan *latex* en *silica* waarvoor dit realiseerbaar is. Het latex sol bestaat uit plastic bolletjes in water. Dit sol wordt o.a. gebruikt in de verfindustrie (latex verf). Het silica sol bestaat uit zeer kleine ronde zandkorreltjes in water. Bij de experimenten met deze solen bleek al spoedig bleek dat verschillende meetmethoden ook verschillende oppervlakteladingen opleveren. Zo is de oppervlaktelading berekend uit de geleidbaarheid van een prop enkele malen groter dan wanneer deze wordt berekend uit de stromingspotentiaal over de prop. Hieruit blijkt dat de opbouw van de dubbellaag zoals weergegeven in figuur 1a te primitief is voorgesteld. Door aan te nemen dat rondom het deeltje een dun waterlaagje aanwezig is dat stilstaat, maar waarin ionen wel kunnen bewegen, zijn de resultaten uit verschillende typen van experimenten met elkaar in overeenstemming te krijgen. De buitengrens van de stilstaande laag heet het *afschuifvlak.* Dit afschuifvlak is in figuur 1a aangegeven met een onderbroken lijn. De aanwezigheid van de stagnante waterlaag verklaart waarom er veel lading wordt gevonden in het geleidbaarheidsexperiment (alle positieve lading draagt bij aan de geleidbaarheid) en minder lading in het stromingspotentiaalexperiment (alleen de lading buiten het afschuifvlak wordt door de bewegende vloeistof meegenomen).

De stagnante laag valt te manipuleren. Hij kan dikker worden gemaakt door ongeladen polymeren te hechten aan het deeltjesoppervlak. Polymeren vormen dunne uitstekende haartjes en maken van het gladde kolloïdale deeltje een harig deeltje (van hockeybal naar tennisbal). De polymeerfilm houdt extra water vast waardoor het afschuifvlak verder naar buiten schuift. De aanwezigheid van deze film resulteert dan ook in een lagere stromingspotentiaal. De oppervlaktegeleiding neemt ook af. Hieruit valt te concluderen dat de ionen worden afgeremd in de harige polymeerlaag.

Het is prachtig dat door de introductie van het afschuifvlak met de resultaten van verschillende meetmethoden een consistent beeld is te vormen van de dynamische eigenschappen van de dubbellaag. Hiermee is nog niet benadrukt dat metingen van de diëlektrische respons een schat aan extra informatie bevatten. Door de frequentie van het wisselveld (het aantal keren per seconde dat we het veld laten omkeren) op te voeren zal op zeker moment de diffuse laag het veld niet meer kunnen bijhouden en verdwijnt de polarisatiestroom. Uit de frequentiekarakteristiek volgt τ, de tijd die de diffuse lading nodig heeft om te kunnen reageren op een verstoring van buitenaf. In figuur 1a is verondersteld dat de wandlading gefixeerd is. Er zijn echter vele situaties denkbaar waarbij deze lading kan bewegen door het hart of langs het oppervlak van het deeltje, danwel kan desorberen naar de oplossing. Via deze mechanismen zal ook de oppervlaktelading worden gepolariseerd (de negatieve wandlading in figuur 1c wordt dan juist hoger aan de kant waar positieve diffuse lading verdwijnt). Deze processen zijn te volgen met de diëlektrische spectrometer. Een theoretisch hoofdstuk in dit proefschrift is gewijd aan het vinden van de relatie tussen de diëlektrische respons en de parameters van de mechanismen die verantwoordelijk zijn voor de polarisatie van de (volledige) elektrische dubbellaag. De karakteristieke tijden van alle optredende polarisatieprocessen zijn hiermee toegankelijk via diëlektrische spectroscopie. Deze aspecten zijn interessant omdat tijdens wisselwerking tussen deeltjes in een vlokproces diffuse lagen overlappen en zich continu zo veel mogelijk aanpassen. Dit proces van aanpassing gaat ook op voor de oppervlaktelading. De deeltjes polariseren elkaar. De krachten die ze op elkaar uitoefenen, en daarmee de stabiliteit van het sol, zijn afhankelijk van de snelheid waarmee de aanpassing kan verlopen. Daarom is het laatste hoofdstuk van dit proefschrift gewijd aan het opstellen van de relatie tussen de solstabiliteit en de karakteristieke tijden van de verschillende polarisatieprocessen.

Het in dit proefschrift beschreven onderzoek behandelt niet-evenwichts elektrische eigenschappen van kolloïden op een zo hoog mogelijk niveau van integratie. De term *elektrodynamica* geeft dit aan. Daarom vindt u de titel "elektrodynamica van kolloïden" op de voorkant van dit proefschrift.

CURRICULUM VITAE

Marcel Minor werd op 21 juni 1968 geboren in Zevenaar. Na het behalen van de diploma's HAVO en Atheneum aan de Lorentz Scholengemeenschap te Arnhem begon hij in 1987 aan de studie Technische Natuurkunde aan de Universiteit Twente. In 1992 studeerde hij af bij de vakgroep Biofysische Techniek. Het doctoraalpakket omvatte voornamelijk optische vakken alsmede de oriëntatie Organische Materiaalkunde. Een bedrijfsstage werd vervuld bij de medische divisie van Delft Instruments in Delft. Van november 1992 tot januari 1997 werkte hij als Onderzoeker in Opleiding (OIO) in dienst van NWO (SON) bij de vakgroep Fysische en Kolloïdchemie van de Landbouwuniversiteit Wageningen. Hieruit is dit proefschrift voortgekomen. Vanaf 1 oktober 1997 is hij werkzaam bij Nutricia Corporate Research in Wageningen.

NAWOORD

Het proefschrift dat u zojuist heeft doorgelezen beschrijft een belangrijk deel van het wetenschappelijk werk dat ik de laatste vier jaar heb uitgevoerd in het laboratorium voor Fysische Chemie en Kolloïdkunde. Gelukkig zat ik er niet alleen! Dit is dan de geschikte plaats om enkele woorden van dank uit te spreken.

De intensieve samenwerking met Bert van der Wal zal ik niet snel vergeten. Eén Bert kan meer vragen dan tien Marcels kunnen beantwoorden. Bert, ik weet nog steeds niet of een elektroforenzende bacterie nu wel of geen stress ondervindt van 't veld. Het werk met Bert en zijn bacteriën heeft mij vroegtijdig gestimuleerd om op zoek te gaan naar het fysisch inzicht achter wiskundige formuleringen, iets waar ik nu nog profijt van heb.

Halverwege het onderzoek ontdekte ik de kelder. De tijd die ik er heb doorgebracht met Ab van der Linde is niet alleen erg plezierig geweest, maar heeft ook veel opgeleverd. De hoofdstukken 2, 5 en 6 zijn in deze periode ontstaan. Ab, ook nog bedankt voor het terugdraaien van mijn kano in de Weerribben toen ik er op de kop onderhing!

In de spoedcursus "polymeerstatistiek" die ik van Frans Leermakers kreeg, leerde ik dat een polymeer meer is dan alleen maar "een dun soort draadje". Zonder dit inzicht zou hoofdstuk 4 niet in de huidige vorm opgeschreven zijn.

Ik heb de grote speelruimte die ik van mijn promotor en co-promotor heb gekregen steeds als zeer prettig ervaren. Hans, je hebt altijd een grote interesse voor mijn werk getoond en het kritisch becommentarieerd. Bedankt hiervoor en veel succes met de (convergerende?) FICS-reeks. Houd hem draagbaar! Het overleg met Herman heeft een exponentiële groei gekend. Herman, het feit dat, op de vreemdste tijdstippen, Marten Toonder terstond terzijde werd gelegd wanneer ik met een stuk kwam aandraven, laat zien dat de elektrodynamica je na aan het hart ligt, en dat mijn figuurtjes mooi zijn. Veel van jullie bijdragen zijn terug te vinden in het proefschrift.

Ik heb in de luxe omstandigheid verkeerd dat ik in de grootste kamer van de vakgroep mocht wonen. Gelukkig niet alleen. Jeannette Wonders deelde geruime tijd de 50 m^2. Jeannette, bedankt voor de gezelligheid. Je hebt me vaak weggesleept vanachter de computer om de theorie van "relaxatie in een waterfase" in praktijk te brengen. Alle zwemmers in baan één, bedankt voor de gezonde competitie. Onze dierbare tijdelijke kamergenoot José Paulo hebben we helaas niet kunnen overhalen regelmatig mee te komen.

Luuk Koopal woonde bij ons op kamers. Van hem leerde ik mijn eerste woordjes grensvlakchemie. Deze werden later aangevuld door Arie de Keizer en kwamen goed van pas in hoofdstuk 5 over silica.

Ben Spee, bedankt voor het altijd kunnen vinden van de juiste potjes chemicaliën. Zonder deze zou niet veel meer dan het nawoord overblijven, en daar valt niet op te promoveren.

Marcel van Eijk heeft mij (te) vaak geholpen bij problemen met software. Het is jammer dat deze altijd worden meegeleverd.

I am indebted to many persons from beyond our department for stimulating discussions, initiating good ideas, or just spending a good time with. Some of them I want to mention personally: J. L. Anderson, S. S. Dukhin, C. S. Mangelsdorf, R. W. O'Brien, V. N. Shilov and N. Spanos.

U begrijpt het, ik heb het op de vakgroep goed naar mijn zin gehad. "Buitenlabse" activiteiten als labuitjes, fiets-, schaats- en kanotochten, wandelweekends en de maandagse volleybalwedstrijden hebben hieraan niet in het minst bijgedragen, evenals de stimulerende gesprekken in de wandelgangen, de koffiekamer en op het secretariaat.

Tot slot, met het gereedkomen van dit boekje stopt logischerwijs ook het praten in mijn slaap. Leonie, ik zal je vanaf vandaag niet meer wekken met kreten als "....we zijn de lading vergeten!"

Mensen, bedankt.

Marcel